



**THE EFFECT OF DIFFERENT WORKING FLUIDS AND INTERNAL
GEOMETRIES ON THE THERMAL PERFORMANCE OF HEAT PIPES IN
EVACUATED TUBE SOLAR COLLECTORS**

By

JEAN GAD MUBALA MUKUNA

Thesis submitted in fulfilment of the requirements

for the degree

Doctor of Engineering: Mechanical Engineering

In the

Faculty of Engineering

At the Cape Peninsula University of Technology

Supervisor: Prof. J. Gryzagoridis

Bellville 2021

CPUT copyright information

This thesis may not be published either in part (in scholarly, scientific or technical journals), or as a whole (as a monograph), unless permission has been obtained from the University.

DECLARATION

I, Jean Gad Mubala Mukuna, declare that the contents of this thesis represent my own unaided work, and that the thesis has not previously been submitted for academic examination towards any qualification. Furthermore, it represents my own opinions and not necessarily those of the Cape Peninsula University of Technology.



Signed

14/09/2021

Date

ABSTRACT

Evacuated tube heat pipe solar collectors produce hot water more efficiently than the flat plate type. It is observed from various studies that involve evacuated tube heat pipe solar collector that its thermal performance depends on various external and internal factors. The internal factors are primarily related to the performance of the heat pipe. It was assumed that the two elements that define the efficiency of the heat pipe are the working fluid and the internal geometry. No inclusive study exists that systematically investigated the combined effect of working fluid and internal geometry on the thermal performance of heat pipes in evacuated tube solar collectors.

This investigation consisted of the design and testing of an evacuated tube solar collector comprising new modified heat pipes. Heat pipes containing inserts with particular profiles were tested with different working fluids. A multivariate polynomial regression analysis was conducted to validate the assumption that the merit number of the working fluid and the insert's surface area affect the efficiency.

The regression analysis that resulted from the assumption that the merit number and the surface of the insert were the independent variables affecting the heat pipe's efficiency had to be rejected due to poor/unacceptably low coefficient of determination (R^2) result.

Based on a newly thought assumption, that the boiling point temperature of the working fluid could be an independent variable affecting the heat pipe's performance or efficiency, a new regression analysis produced very acceptable results.

The results have shown that the surface areas of the insert in the heat pipe had an impact on the efficiency of the solar collector. This is possibly because of the enhancing of the heat transfer by increased convection between the surfaces of the insert and the vapour of the working fluid moving from the evaporator to the condenser. For example, with distilled water as the working fluid, the experiment on the conventional circular heat pipe without an insert produced an efficiency of 53.3%, while results on the single insert and the S insert show efficiencies of 59.1% and 64.3% respectively.

A very good correlation with a $R^2 = 0.99$ was obtained when expressing the efficiency as a function of the boiling point of the working fluid for an evacuated tube heat pipe. It transpires from this correlation that the working fluid with a high boiling number has also a high thermal efficiency.

The comparison between the measured and the predicted results using the final multivariate polynomial regression (equation 5.2) exhibits excellent accuracy in the prediction of the performance of an evacuated heat pipe solar collector with $R^2 = 0.98$ and an average error of 1.1%. It may be of assistance in predicting the heat pipe's efficiency for any untested insert's profile, or working fluid's boiling temperature or a combination of both.

ACKNOWLEDGEMENTS

First, I would like to express my gratitude to my supervisor, Prof. Jasson Gryzagoridis, for providing guidance and feedback throughout this project. His insight and knowledge into the subject matter steered me through this research and contributed to the development of the skills necessary to undertake this research. In addition, his wisdom and experience helped me to accomplish this project, despite difficult moments and circumstances. I look for future opportunities to work together with him on projects and papers.

Equally, I wish to express my warm thanks and appreciation to the most supportive people at Mangosuthu University of Technology (MUT) without whom I would not have made it through my doctoral degree: my HOD, Prof. Ewa Zawilska; Research Director Dr Mienie; Research Coordinator Sfiso Qwabe; the industrial technician, Mr Mills; the lab assistant, Mr Memela; and all my colleagues in the Department of Mechanical Engineering.

For all the support and encouragement, for all the sacrifice, I would like to express my gratitude to my departed father, Medard Mpoyi Mwambi, and my mother, Charlotte Mpemba. I would also like to thank my wife, Nelly Mukuna, and my beautiful children for their patience and moral support during my doctoral studies.

Last, but not least, in acknowledgement to the Almighty God, my only statement is “El sal’i”.

DEDICATION

This thesis is dedicated to my entire family, for their constant love, endless support and incredible encouragement, particularly:

- My wife: Nelly Mukuna;
- My parents: Mpoyi Mwambi Kalala and Mpemba Nsengi Charlotte;
- My children: Gad Mukuna, Joice Mukuna, Blessing Mukuna and Sarah Mukuna; and
- My father and mother in-law: Mwilambwe Kabubu Augustin and Tshibwabwa Mbuyi Martine.

TABLE OF CONTENTS

DECLARATION	ii
ABSTRACT.....	iii
ACKNOWLEDGEMENTS	v
DEDICATION.....	vi
TABLE OF CONTENTS	vii
LIST OF FIGURES	xi
LIST OF TABLES.....	xiii
NOMENCLATURE	xiv
CHAPTER 1: INTRODUCTION.....	1
1.1 Background	1
1.1.1 Electricity demand	1
1.1.2 Diversifying energy sources	2
1.1.3 Household water heating	3
1.1.4 Solar energy in South Africa	4
1.1.5 Solar collectors	5
1.1.6 Principle of solar collectors	5
1.1.7 Regression	8
1.1.7.1 Polynomial regression.....	9
1.1.7.2 Multivariate polynomial regression	9
1.2 Statement of research problem.....	10
1.3 Motivation for research	10
1.4 Objectives of the research	11
1.5 Major contributions of the thesis.....	12
1.6 Research design and methodology.....	12
1.7 Outline of thesis	12
CHAPTER 2: SOLAR ENERGY AND SOLAR COLLECTORS.....	14
2.1 Introduction.....	14

2.2	Overview of solar energy	15
2.2.1	The sun.....	15
2.2.2	Solar energy	17
2.2.2.1	Solar energy measurement.....	17
2.2.2.2	Estimation of the monthly average daily global radiation.....	19
2.2.3	Solar thermal collectors	20
2.2.3.1	Description of an evacuated tube heat pipe solar collector.....	21
2.2.3.2	Research on the thermal performance of evacuated tube heat pipe solar collectors	22
CHAPTER 3: HEAT PIPES		24
3.1	Introduction.....	24
3.2	Historical background	25
3.3	Heat pipe components and materials.....	26
3.3.1	Description of a heat pipe	26
3.3.2	Working fluid.....	26
3.3.2.1	Classification of heat pipe based on working fluids	27
3.3.2.2	Working fluid and merit number	28
3.3.2.3	Working fluid inventory.....	29
3.3.2.4	Research on working fluids.....	30
3.3.3	Container	31
3.3.3.1	Material used in heat pipes	32
3.3.4	Wick capillary structure	32
3.4	Principle of operation of the heat pipe	33
3.4.1	Heat transfer limitations	35
3.5	Thermal performance.....	36
3.6	Heat pipe technologies	38
3.6.1	Conventional heat pipes	39
3.6.2	Loop and pulsating heat pipes	39

3.6.3	Concentric annular heat pipes	40
3.7	Multivariate polynomial regression analysis on the performance of the heat pipe	42
3.7.1	Modelling a heat pipe containing inserts	42
CHAPTER 4: EXPERIMENTAL SETUP		44
4.1	Description of the rig	44
4.1.1	The water tank	45
4.1.2	Solar simulator	47
4.1.3	Evacuated tube heat pipe	49
4.1.3.1	Specifications of the evacuated heat pipe	49
4.1.3.2	Preparation of the Heat pipe	50
4.1.3.3	Working fluid	53
4.2	Instrumentation	54
4.2.1	Data logger	54
4.2.2	Software and computer	55
4.2.3	Thermocouples	55
4.2.4	Power meter NanoVIP plus	58
4.2.5	Light meter	58
4.3	Experimental protocol	59
CHAPTER 5: RESULTS AND DISCUSSION		62
5.1	Tests with the heat pipe containing distilled water	62
5.2	Tests with the heat pipe containing methanol	63
5.3	Tests with the heat pipe containing acetone	64
5.4	Tests with the heat pipe containing toluene	65
5.5	Tests with the heat pipe containing ethanol	66
5.6	Tests with the heat pipe containing ethyl acetate	67
5.7	Ambient temperature	68

5.8	Comparison of the efficiency of the evacuated tube heat pipe on the basis of the contained fluid and geometry of the insert.....	69
5.9	Results of the Multivariate regression analysis.....	71
5.9.1	Efficiency of the evacuated heat pipe as a function of both the merit number and the surface area o the insert	71
5.9.2	Efficiency of the evacuated heat pipe as a function of the working fluid's boiling point and surface area of the insert.....	73
5.9.3	Final predictive equation of heat pipe efficiency	74
CHAPTER 6: CONCLUSION AND RECOMMENDATIONS		76
6.1	Conclusions	76
6.2	Recommendations for future work	77
REFERENCES		78
APPENDICES.....		85
APPENDIX A: Detailed description of equipment and measuring instruments.....		85
APPENDIX B: Data collected during the heat pipe tests for various internal geometries and working fluids		93
APPENDIX C: Properties of working fluid.....		106
APPENDIX D: Sample calculations		108
APPENDIX E: Regression analysis model		111

LIST OF FIGURES

Figure 1.1: Expected electricity demand forecast to 2050	2
Figure 1.2: Installed capacity mix by 2030.....	3
Figure 1.3: South African electricity consumption.....	4
Figure 1.4: South Africa annual solar radiation.....	5
Figure 1.5: Schematic of solar collector	6
Figure 1.6: Summary of the classification of solar collectors	6
Figure 2.1: Interior structure of the sun.....	16
Figure 2.2: Earth's solar energy budget	17
Figure 2.3: Solar zenith angle	18
Figure 2.4: Pyrheliometer.....	19
Figure 2.5: Pyranometer	19
Figure 2.6: Horace-Benedict de Saussure's hot box	20
Figure 2.7: Evacuated tube heat pipe solar collector.....	21
Figure 2.8: Detail of the evacuated tube heat pipe's condenser	22
Figure 3.1: Schematic diagram of the flow of fluid in a heat pipe.....	24
Figure 3.2: Components and sections of a heat pipe	26
Figure 3.3: Merit number of various working fluids (Byon, 2016).....	29
Figure 3.4: Heat pipe thermodynamic cycle	33
Figure 3.5: Movement of fluid and heat during a heat pipe's operation.....	34
Figure 3.6: Heat transfer limits on a heat pipe.....	36
Figure 3.7: Heat pipe thermal resistance network	37
Figure 3.8: Heat pipe technologies.....	40
Figure 3.9: Concentric annular heat pipe.....	41
Figure 3.10: Section of the heat pipe with an I profile insert	42
Figure 4.1: Schematic diagram of the testing rig.....	44
Figure 4.2: Schematic diagram of the water tank	45
Figure 4.3: Wells in the water tank	46
Figure 4.4: 15 mm pipe and valve	46
Figure 4.5: Heat pipe screwed into the water tank.....	47
Figure 4.6: BSP male thread welded on the heat pipe.....	47
Figure 4.7: Schematic diagram of the solar simulator.....	48
Figure 4.8: Variable transformers	48
Figure 4.9: Evacuated tube heat pipe.....	49
Figure 4.10: Insert manufacturing	50
Figure 4. 11: I insert	51

Figure 4.12: V insert.....	51
Figure 4.13: M6x1.0 mm screw attached to the heat pipe	52
Figure 4.14: Ethernet chassis cDAQ-9189	54
Figure 4.15: NI 9211 C series module.....	54
Figure 4.16: Temperature measurement bloc diagram.....	55
Figure 4.17: Calibration during DAQmx task building	56
Figure 4.18: calibration of the thermocouples.....	57
figure 4.19: temperature of the thermocouple to be calibrated against the reference temperature	58
Figure 4.20: Power meter NanoVIP plus	58
Figure 4.21: Working fluids	59
Figure 4.22: Thermocouples plunged in the water tank.....	60
Figure 4.23: Solar simulator over the rig.....	60
Figure 5.1: Efficiency of the evacuated tube heat pipe containing distilled water for each internal geometry	63
Figure 5.2: Efficiency of the evacuated tube heat pipe containing methanol for each internal geometry	64
Figure 5.3: Efficiency of the evacuated tube heat pipe containing acetone for each internal geometry.....	65
Figure 5.4: Efficiency of the evacuated tube heat pipe containing toluene for each internal geometry.....	66
Figure 5.5: Efficiency of the evacuated tube heat pipe containing ethanol for each internal geometry.....	67
Figure 5.6: Efficiency of the evacuated tube heat pipe containing ethyl acetate for each internal geometry	68
Figure 5.7: Maximum and minimum ambient temperatures during the tests for each working fluid.....	69
Figure 5.8: Comparison of the efficiency of the evacuated tube heat pipe as a function of its contained fluid and the geometry of its insert	70

LIST OF TABLES

Table 2.1: Comparison between renewable energy and conventional fossil fuel energy	14
Table 2.2: Characteristics of the sun	16
Table 3.1: Range of temperature of some working fluids used in heat pipes.....	28
Table 3.2: Compatibility between working fluid and container's material	32
Table 4.1: Components of the testing rig.....	45
Table 4.2: Evacuated tube heat pipe specifications.....	49
Table 4.3: Geometries of the insert in the heat pipe	52
Table 4.4: Thermophysical properties and the merit number of the chosen working fluids ..	53
Table 4.5: Various combinations between geometries and working fluids	61
Table 5.1: Heat pipe with distilled water.....	62
Table 5.2: Heat pipe with methanol	63
Table 5.3: Heat pipe with acetone	64
Table 5.4: Heat pipe with toluene	65
Table 5.5: Heat pipe with ethanol	66
Table 5.6: Heat pipe with ethyl acetate	67
Table 5.7: Surface area of the inserts as the first independent variable	71
Table 5.8: Merit number of the heat pipe as the second independent variable	71
Table 5.9: Results of the difference and percentage of error between experimental and predicted values of the evacuated tube heat pipe efficiency expressed as a function of the merit number and the surface number of the insert	72
Table 5.10: Boiling point temperature of the working fluid inside the actual heat pipes.....	73
Table 5.11: Results of the difference and percentage of error between experimental and predicted values of the evacuated tube heat pipe's efficiency expressed as a function of the temperature of the boiling point of the working fluid and the surface area of the insert.....	74

NOMENCLATURE

Symbol	Parameter	Units
A	Surface area	m ²
c	Velocity of the light	m/s
c_p	Specific heat capacity at constant pressure	J/kg.K
d	Diameter	m
E	Energy	J
h	Convective heat transfer coefficient	W/ m ² .K
I_R	Direct radiation from the solar simulator	W/ m ²
k	Thermal conductivity	W/m.K
L	Length	m
m	Mass	kg
N_1	Merit number	W/m ²
P	Pressure	Pa
Q	Heat transfer rate	W
r	Radius	m
R^2	Coefficient of determination	
R_{th}	Thermal resistance	K/W
T	Temperature	K
t	Time	s
u	Flow velocity	m/s
V	Volume	m ³
x	Independent variable	
y	Dependent variable	

Greek symbols

ε	Error	
ϵ	Porosity of the wick structure	
η	Efficiency	
κ	Permeability of the wick	
λ	Latent heat of the fluid	kJ/kg
μ	Dynamic viscosity of the fluid	Pa.s
ρ	Density of the fluid	kg/m ³
σ	Surface tension of the fluid	N/m

CHAPTER 1: INTRODUCTION

1.1 Background

Economic growth in developing countries like South Africa is based on energy production and supply. The growth in industry and the wellbeing of households are the motivations behind the development of various sectors of the economy (Aladejare, 2014).

South African's electricity provider (ESKOM) is in a difficult situation since 2008, as the supply of electricity has decreased, along with resource reserves (Khobai *et al.*, 2017).

The energy supply in South Africa depends largely (about 70%) on coal, which is the main method of energy production (Winkler, 2007). While trying to mitigate the shortage in energy supply, South Africa has increased its coal production, but at the beginning of 2019, the country encountered a series of power shortages, threatening the government's plans to revive the struggling economy. In addition, the increased usage of coal for the production of electricity has environmental considerations. The dependence on coal has resulted in carbon dioxide emissions reaching a level of 379 million tons per year (Winkler, 2007).

1.1.1 Electricity demand

Based on historical quantitative patterns, models designed by considering three different scenarios all show that the demand in energy will increase until 2050. Figure 1.1 depicts the total energy demand as contained in the demand forecast report but adjusted to reflect the lower actual value (2018) as a starting point (South Africa. Department of Mineral Resources and Energy, 2019).

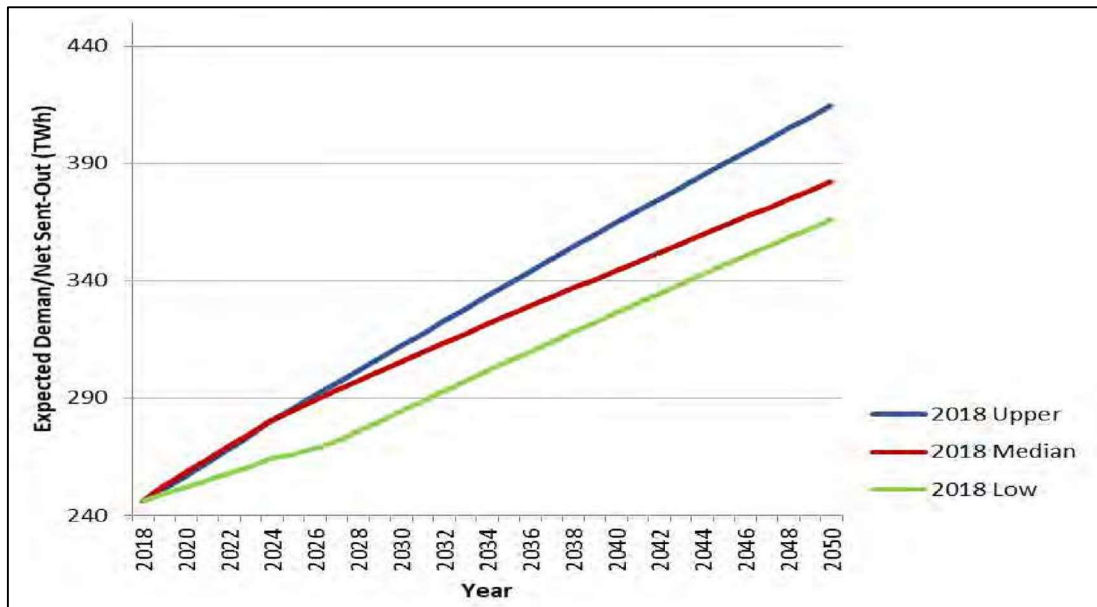


Figure 1.1: Expected electricity demand forecast to 2050

(South Africa, Department of Mineral Resources and Energy, 2019)

In the present context, Eskom will not have the capacity to supply sufficient energy without depleting the coal reserves and impacting negatively on the environment.

Due to economic inflation and limitation in power supply, the electricity tariff in South Africa has been increasing. Between 2008 and 2009 and 2016 and 2017, the price of electricity has increased by an average of 11.1% per year in real terms (Eskom, 2017).

To relieve the pressure of energy demand on the grid, Eskom proposed a demand-side management programme in 2006 with the objective of reducing the electricity demand by 3 000 MW by 2012, and a further 5 000 MW by 2025 by using renewable energy resources (Inglesi & Pouris, 2010).

1.1.2 Diversifying energy sources

Among solutions to the energy crisis in South Africa, the diversification of resources is one of the routes that has been seriously considered. The South African government drafted an energy master plan between 2010 and 2013, which includes the Renewable Energy Independent Power Producer Procurement Programme (REIPPP), as part of its approach to solve issues linked to the production and supply of energy. The main objective of the solution was to investigate the possibility of focusing on the diversification of the energy mix with an emphasis on solar, wind and hydro, as shown in Figure 1.2, without compromising the security of supply.

The motive behind the diversification of energy sources is not only industrialisation, but also the wellbeing of the population, whose basic needs require a continuous supply of electricity (South Africa. Department of Mineral Resources and Energy, 2019).

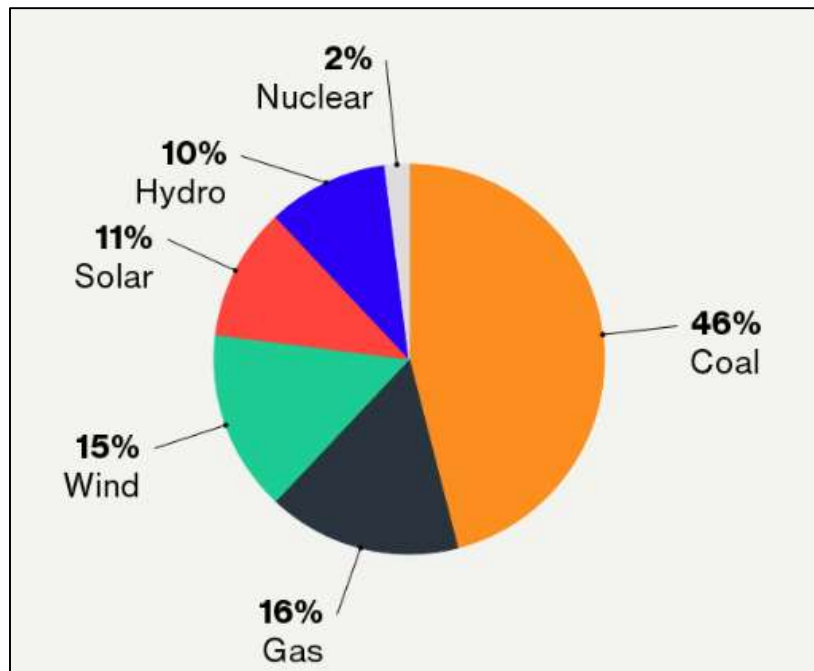


Figure 1.2: Installed capacity mix by 2030

(Source: <https://businesstech.co.za>)

1.1.3 Household water heating

Studies and surveys have shown that residential energy consumption stands at 23% (see Figure 1.3) of the total energy consumption in the country. Residential energy consumption comprises energy consumed by households for heating, cooling, lighting, and water heating (Eskom, 2016).

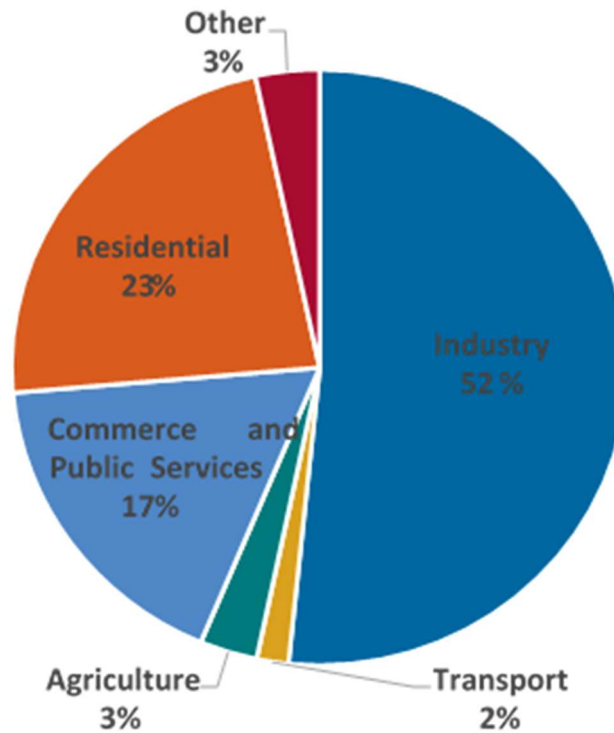


Figure 1.3: South African electricity consumption
(Eskom, 2016)

It is estimated that 40% of the electricity consumed in a household is used for water heating. Water heating can therefore be estimated as making up approximately 9.2% of national energy consumption.

It is estimated that a middle-class residential building may consume 11 797 kWh/year and the 40% allocated to water heating can be translated to 4718.18 kWh/year (Catherine *et al.*, 2012). Using alternative resources like solar energy for water heating in a household will reduce the demand for electricity and reduce the production of greenhouse gas emissions in South Africa (Veldman *et al.*, 2011).

1.1.4 Solar energy in South Africa

South Africa is among many countries in the world that receives a high concentration of solar radiation, as seen on the map in Figure 1.4. The provinces located on the west side of the country, like the Northern Cape Province, receive more radiation, i.e. about 9000 MJ/m² or 8 kWh/m² per day, while those located on the east side, like Mpumalanga and KwaZulu Natal receive an average of 6187.5 MJ/m² or 5.5 kWh/m² per day (Bokopane *et al.*, 2014). However, all areas receive enough solar radiation for the purpose of water heating.

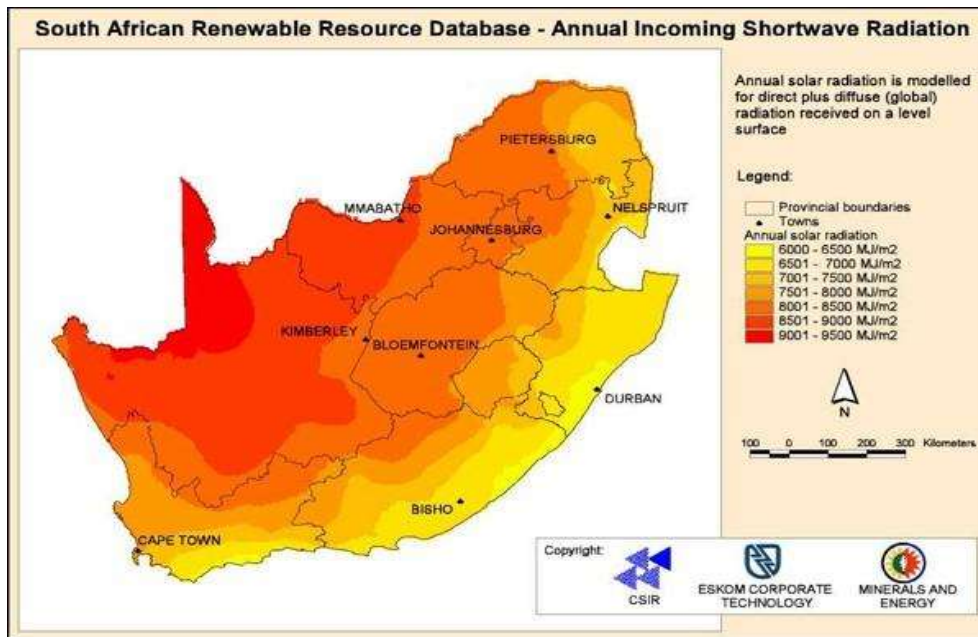


Figure 1.4: South Africa annual solar radiation
(Bokopane *et al.*, 2014)

1.1.5 Solar collectors

Technologies have been developed, tested, and used to harvest solar radiation for heating purposes. Devices used for the harnessing of radiation from the sun are known as solar collectors. These are used for domestic and industrial hot water and steam production, among other purposes. There are various types of solar water heaters, such as flat plate solar water heaters, concentrated solar water heaters and evacuated tube solar water heaters.

1.1.6 Principle of solar collectors

As shown in Figure 1.5, the radiation from the sun is collected by a black surface, called the absorber, which transfers the heat to a working fluid. Not all the absorbed radiation can be used, and there are always some losses due to reflection or heat transfer. Two factors determine the performance of a solar collector: the amount of energy reaching the absorber and the loss to the surroundings (Miloştean & Flori, 2017).

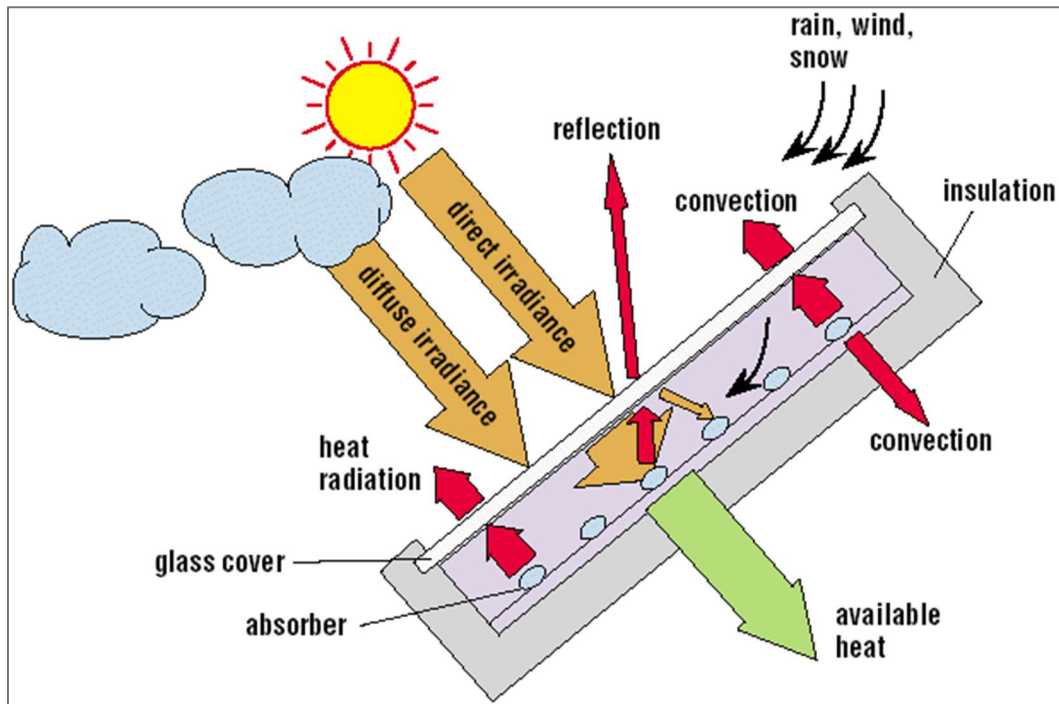


Figure 1.5: Schematic of solar collector

(Source: <http://www.solcoast.com>)

Various solar collectors are categorised according to their application, temperature ranges and their position in relation to the sun, as shown in Figure 1.6.

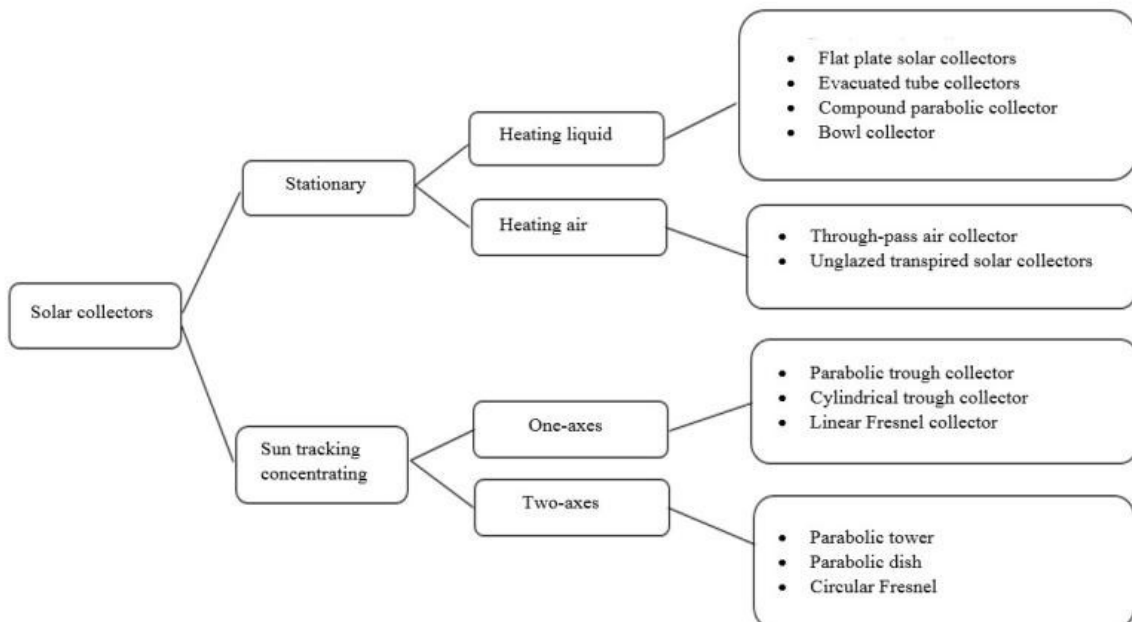


Figure 1.6: Summary of the classification of solar collectors

(Olia *et al.*, 2019)

A concentrated solar water heater is used for generating high temperature water or steam. For domestic household water heating, the temperature may vary from 20 to 90°C and the position of the collector in relation to the sun is fixed. For water heating, the flat plate, evacuated tube, and evacuated heat pipe solar collectors are used (Jesko, 2008).

The flat plate solar collector is the most common, due to its low maintenance cost and simple design. However, it has two major drawbacks:

- convection heat loss to the glass cover from the collector plate and to the environment thereafter by conduction, convection and radiation; and
- absence of sun tracking.

Evacuated tube heat pipe solar collectors overcome both these drawbacks due to the vacuum created between the inner and the outer tube, which eliminates heat transfer losses. Evacuated tube heat pipe solar collectors are suitable for bad climates and present high thermal performance, easy transportability and expedient installation.

Several authors have noted that evacuated tube heat pipe solar collectors have much greater efficiencies than the flat plate solar collectors, especially at low temperature and insolation (Chamoli, 2013; Ayompe *et al.*, 2011; Morrison *et al.*, 2004). For example, a study that compared the energy performance between flat-plate and evacuated tube heat pipe collectors for solar water heating systems (under Mediterranean climate conditions) concluded that the annual solar yield for the flat-plate collector was 664 kWh/m²year, whereas for the evacuated tube heat pipe collector, it was 885 kWh/m²year. The annual average collector efficiencies were thus 0.494 and 0.62, respectively (Maraj *et al.*, 2019).

Collecting solar radiation more efficiently and producing more usable heat, defined by the thermal efficiency of the evacuated tube heat pipe solar collector, has been at the centre of research and investigation recently. Many authors have studied different theoretical and experimental methods to improve the thermal performance of the evacuated tube heat pipe solar collectors.

Using a dry condenser and circular fin, a theoretical model of an evacuated tube heat pipe solar collector was evaluated, with the results for heat gain and efficiency obtained experimentally (Jafarkazemi & Abdi, 2012).

Kabeel *et al.* (2017) studied an evacuated tube solar collector comprising a modified coaxial heat pipe using air and a working fluid. The heat pipes were made up of two concentric copper tubes in such a way that the space between the tubes was filled with refrigerant. Two types of

refrigerant, R22 and R134a, were used for this investigation. In addition, air was also used at four different mass flow rates, 0.0051, 0.0062, 0.007 and 0.009 kg/s. They investigated the impact of the tilt angle, the filling ratio, and the refrigerant on the thermal performance of the evacuated tube heat pipe solar collector. They concluded that the efficiency of the evacuated tube with the modified heat pipe was superior to that of the collector with the conventional heat pipe.

Azad (2018) investigated the impact of the number of heat pipes on the thermal performance of the evacuated tube heat pipe solar collector. His results showed that collectors with a higher number of heat pipes presented higher thermal efficiency.

Alammar *et al.* (2016) developed a numerical study on the impact of the effect of inclination angle and fill ratio on the thermal performance of a thermosiphon heat pipe. They concluded that a fill ratio and inclination angle of 65% and 90° respectively provided an optimum thermal performance.

Brahim *et al.* (2014) developed a time-dependent theoretical model to study the effect of adding fin arrays to the heat pipe condenser with two types of working fluid (methanol and water). After comparing the results from the model to the experimental results, they concluded that the water system displayed better performance than that of the methanol, and that the addition of fins to the heat pipe condensing surface increased the system's overall efficiency.

1.1.7 Regression

Regression analysis is a modelling technique used to establish a relationship between a dependent variable and one or more independent variables in order to find a best fit that can be used as the prediction equation. This method is used to evaluate a relationship derived from collected data to depict the model of the data set (Sinha, 2013).

Various methods of regression can be found in the literature: simple linear regression, multivariate linear regression, polynomial regression and multivariate polynomial regression.

Equations describing a phenomena in the heat pipe involve numerous variables and a curvilinear relationship between dependent and independent variables (Ahmed *et al.*, 2011), hence a polynomial regression and multivariate polynomial regression have to be considered for this study.

1.1.7.1 Polynomial regression

The general form of the equation for polynomial regression is:

$$y = \beta_0 + \beta_1x + \beta_2x^2 + \beta_3x^3 + \dots + \beta_kx^k + \varepsilon \quad (1.1)$$

Where

y is the dependent variable

x is the independent variable

β_0 is the initial intercept

β_i is the partial regression coefficients for variable x^i

ε : is the error.

1.1.7.2 Multivariate polynomial regression

When the polynomial regression is established between one dependent variable and various independent variables, the model is then denoted as multivariate polynomial regression.

The general form of the equation for multivariate polynomial regression is:

$$y = \beta_0 + \beta_1x_1 + \beta_2x_2 + \beta_{11}x_1^2 + \beta_{22}x_2^2 + \beta_{12}x_1x_2 + \dots + \varepsilon \quad (1.2)$$

Where

y is the dependent variable

x is the independent variable

β_0 is the initial intercept

ε is the error

β_1, β_2 are designated as linear effect parameters

β_{11}, β_{22} are designated as quadratic effect parameters

β_{12} is designated as interaction effect parameter.

To estimate how well the regression model fits the measured or observed data, the coefficient of determination (R^2) should be calculated. R-squared is a statistical measure of the proportion of variance in the dependent variable that can be described by the independent variable in a regression analysis. To draw a valid conclusion on the accuracy of a regression model, the R-squared should be used. Taking values between 0 and 1, the coefficient of determination can be estimated using the formula:

$$R^2 = 1 - \frac{\sum(y_i - \hat{y}_i)^2}{\sum(y_i - \bar{y})^2} \quad (1.3)$$

Where

R^2 is the coefficient of determination

y_i is the measured or observed variable

\hat{y}_i is the estimated variable

\bar{y} is the average value of the measured values.

1.2 Statement of research problem

No comprehensive study exists which systematically investigates the combined effect of working fluids and parameters of the internal geometry on the thermal performance of heat pipes.

The project will consist of the design and testing of an evacuated tube solar collector comprising modified heat pipes. Each heat pipe will contain an insert with a particular profile, and will be tested with different working fluids. Using the experimental data, a multivariate polynomial regression analysis will be conducted to validate the assumptions that the thermal performance of a heat pipe depends on the working fluid and the surface area of the insert. The regression model may be used to predict the probable efficiency of a heat pipe.

1.3 Motivation for research

The desire to reduce energy demand has motivated researchers and industry to work on improving the thermal performance of the evacuated tube heat pipe solar collector. The research has been focused on improvement of the heat transfer parameters in the heat pipe. For example, an increase in the heat flux increases the heat transfer coefficient at the evaporator and an increase in the inclination angle decreases the thermal resistance of the

heat pipe (Peyghambarzadeh *et al.*, 2013). The choice of the working fluid, the filling ratio and the thermophysical properties of the working fluid have an impact on the thermal resistance and the heat transfer capability of the heat pipe (Manimaran *et al.*, 2012).

Experiments on heat pipes with and without working fluids were undertaken to assess the impact a variation of the working fluids had on the thermal resistance and overall heat transfer coefficient (Mozumder *et al.*, 2010). In addition to an analysis on the improvement of the heat pipe thermal performance by analysing the parameters linked to the working fluid, another analysis of the enhancement in heat transfer to the working fluid was considered. This led to the design and testing of a novel type of heat pipe known as a concentric annular heat pipe. It consists of two concentric tubes that create an annular space by closing and sealing both ends, with the space inside the inner tube exposed to the environment. Conventional circular heat pipes present high thermal conductivities of 5000-20000 W/mK, compared to 250-1500 W/mK for materials that are good conductors of heat, like copper, aluminium and graphite (Dunn & Ready, 2016). Research on concentric annular heat pipes has shown an enhancement in thermal performance when compared to the conventional circular heat pipe, as a result of the increase in the heat transfer capability (Faghri & Thomas, 1989).

The present study attempts to combine the impact of the thermophysical properties of the working fluid and the internal geometry in predicating improvements in the efficiency of the heat pipe, and hence the evacuated tube solar heat pipe collector.

1.4 Objectives of the research

The primary objectives of the present research are as follows:

- Undertake experimental measurements of the performance of heat pipes in evacuated tube heat pipe solar collectors for different working fluids using the various parameters of the internal geometry;
- Perform a multivariate polynomial regression analysis in order to validate the assumptions of the working fluids and the variation in the geometry of an insert (perhaps a mechanism of capillary forces) on the thermal performance and,
- Produce a database that would play a role in improving or corroborating the performance predictions of the evacuated heat pipe solar collector.

1.5 Major contributions of the thesis

The following are the major contributions of this research:

- A New type of evacuated tube heat pipe solar collector containing a modified internal geometry was developed.
- Various working fluids were tested in the heat pipes.
- The usage of a multivariate polynomial regression analysis in validating the assumption that the performance of the heat pipe depends on the merit number and the surface area of the insert.
- The analysis concluded that the merit number cannot be taken as an independent variable in the prediction of the thermal efficiency of the evacuated tube heat pipe but rather indicates its operating temperature range.
- Combining the surface area of the insert and the boiling point of the working fluid can give a relationship that can be used to predict the efficiency of the heat pipe.

1.6 Research design and methodology

In this study, the design and manufacture of an evacuated tube solar collector with a heat pipe made of various internal geometries will be attempted.

To perform the experimental part of this study, gravity-assisted heat pipes will be used for water heating applications with working temperature ranges from 200 K to 500 K.

A solar simulator (with four floodlights) will be used to simulate the sun and provide heat at the evaporator.

A small geyser made of an inner cylinder and outer insulation shell will be used. One evacuated tube containing the heat pipe will be attached directly to the geyser.

The results from the experiments will be used to verify or validate the assumption that the performance of the heat pipe depends on the merit number of the working fluid and the area of the insert, using a polynomial multivariate-regression analysis.

1.7 Outline of thesis

This thesis is presented in six chapters.

Chapter 1 presents a general introduction and background information about water heating, solar potential in South Africa and the regression method used in developing the mathematical

model. It also provides the motivation, the research question, the objectives, the major contributions and design and methodology of this research. This chapter, in addition, gives the outline of the thesis.

Chapter 2 provides information on solar energy and solar collectors.

Chapter 3 gives background information on heat pipes. It includes heat pipe components and materials, working principles and governing equations leading to the heat pipe's thermal performance.

Chapter 4 describes the design of the prototype or the experimental rig with various modifications implemented to the heat pipes of the solar collector, the components and materials, the testing protocol and the instrumentation used.

Chapter 5 presents the results from the various tests that were performed with different working fluids and the effect of the total surface area of the geometry of various inserts placed in the heat pipes on the thermal performance of the evacuated tube heat pipe solar collectors. This chapter is concluded with the validation of the assumptions from the regression analysis to predict the performance of the evacuated tube heat pipe solar collector.

Chapter 6, the final chapter, presents conclusions and recommendations for future work.

CHAPTER 2: SOLAR ENERGY AND SOLAR COLLECTORS

2.1 Introduction

Energy is one of the fundamental human needs, and the economic development of any society depends on it. As populations have increased and technology has become ubiquitous, a rise in the demand for energy has occurred. As a result of the depletion of conventional energy and the battle against pollution, academics and industry have decided to explore new types of energy sources, particularly renewables (Kocer *et al.*, 2015). The concept of “renewable energy” includes types of energy that can be replenished by a natural process at a faster rate than that required by normal human consumption (Bilgili *et al.*, 2015), and encompasses such sources as solar energy, wind energy, hydropower, geothermal heat, tidal energy and wave energy. Renewable energy is used in areas such as electricity generation, water heating or cooling, fuel production and energy usage in rural areas (Omer, 2008). Table 2.1 displays a comparison between conventional and renewable energy.

Table 2.1: Comparison between renewable energy and conventional fossil fuel energy

Conventional energy	Renewable energy
Process pollutes the environment because of carbon dioxide and other products of combustion.	The energy from the renewable source is natural and doesn't pollute the environment.
Affects the environment by creating problems such as the greenhouse effect and global warming.	Renewable energy does not produce any detrimental effect on the environment.
Combustion of fossil fuel produces more energy.	Renewable energy technologies have limited efficiency and produce less energy than fossil fuel sources.
When consumed, there is a depletion of the energy source with time	After consumption, there is no depletion because the source is renewed.

The benefit of using solar energy and a solar collector, instead of conventional energy, has been proven by (Weiss & Spörk-Dür, 2018) who stated that if 1m² of a solar collector is used, in one year, there will be a reduction in the consumption of coal of 250 kg, which would result in the reduction of 25 kg of unwanted emission, 6 kg of sulphur dioxide and 2 kg of nitrogen dioxide.

Due to the fact that the present investigation involves heat pipe internal geometries and working fluids as factors influencing the thermal efficiency of the evacuated tube heat pipe solar collectors, this chapter will focus on solar energy in water heating.

2.2 Overview of solar energy

Various sources of energy that are classified as renewable energy, like wind energy, geothermal heat, rain, tidal energy, wave energy, are directly or indirectly linked to solar energy (Manton, 2015). Solar energy is available, abundant and it can touch every point on the surface of the earth every day. Because it is also freely available, clean, and environmentally safe, solar power has been the subject of investigation for decades (Yogi Goswami, 1998). Though intermittent and affected by our planet's natural and climatic conditions, solar energy remains one of the biggest potential sources of renewable energy for the future (Sukhatme & Nayak, 2017). Presently, solar energy is used in industrial and domestic processes such as refrigeration and air conditioning, electricity production using photovoltaic panels, steam power plants, water heating and cooling (Sukhatme & Nayak, 2017). The harnessing of solar energy is possible because of the development of technologies aimed to optimise its collection by increasingly efficient means (Lewis *et al.*, 2005).

2.2.1 The sun

The sun is the star of our planetary system, which can be observed and studied in detail. It defines the days and brings light and heat to our planet (Jäger *et al.*, 2016). Figure 2.1 is a schematic diagram depicting the different zones of matter that make up the sun. The fusion reaction, where hydrogen gas is 'squeezed' to produce helium, takes place in the core. It is during this process that heat and light are formed (Magurean *et al.*, 2019). The helium stays in the core.

Radiation takes place in the form of gamma rays, which gradually lose their energy as they travel out from the core, emerging as visible light. The total energy produced in the core is transported by protons and enters the radiation zone, allowing energy to move outwards from the sun in the form of photons. The convection zone is the outer layer of the sun which allows energy to be transported by convection. The photosphere, chromosphere and transition zone are layers that help the radiation to escape from the sun (Sayigh, 2012).

- The energy produced by the sun can be determined using Einstein's equation:

$$E = mc^2 \tag{2.1}$$

$m = 4 \times 10^9$ kg is the mass of the residual hydrogen that is converted into energy while $c = 3 \times 10^8$ m/s is the speed of light.

The total power emitted by the sun is calculated by multiplying the power density by the surface area of the sun. Giving a surface area of the sun of $6.07 \times 10^{18} \text{ m}^2$, the total power output of the sun is equal to 3.9×10^{26} watts. (Magurean *et al.*, 2019).

- As measured outside of the atmosphere, the sun delivers radiation to the earth at the value of 1367 W/m^2 on the area which is perpendicular to the direction of the radiation. This value is referred to as the solar constant (Sayigh, 2012). More characteristics of the sun are given in Table 2.2.

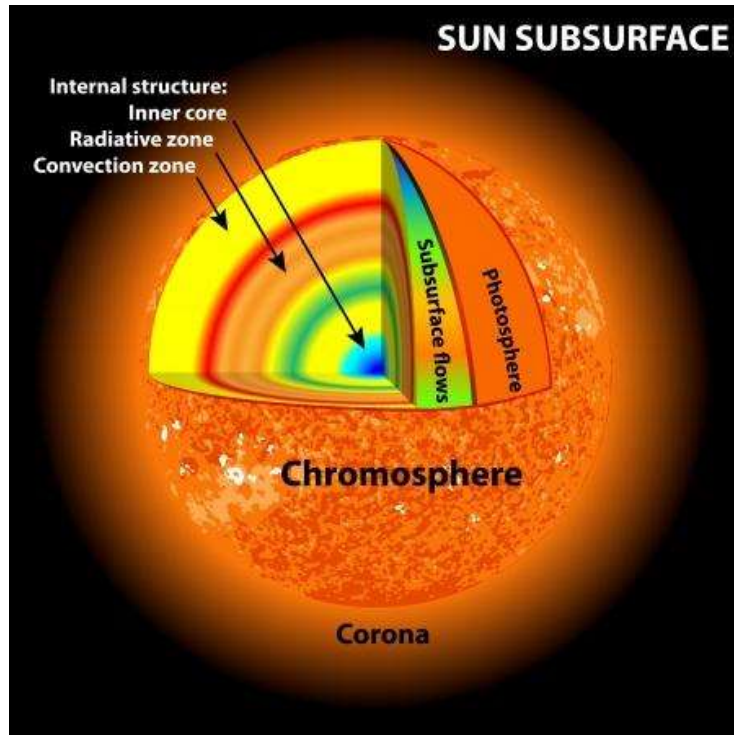


Figure 2.1: Interior structure of the sun
(Source: <https://observa-dome.com>)

Table 2.2: Characteristics of the sun

Mean distance from the earth	149 600 000 km
Diameter	1 392 000 km
Volume	1 300 000 x that of the earth
Mass	$1.993 \times 10^{27} \text{ kg}$
Density (at the centre)	10^5 kg/ m^3
Pressure (at the centre)	$101.325 \times 10^{12} \text{ kPa}$
Temperature (at the centre)	15 000 000 K
Temperature (at the surface)	6000 K
Power or radiant flux	$3.8 \times 10^{26} \text{ W}$
Power received on earth	$1.7 \times 10^{17} \text{ W}$

The sun has enough hydrogen left to continue fusion for about another 5 billion years (Sayigh, 2012).

2.2.2 Solar energy

Solar energy is made up of the heat and the light obtained from the sun. Electricity generation, water heating and cooling, solar architecture and artificial photosynthesis are some of the primary applications that use solar energy (Tian & Zhao, 2013). Presently, the usage of solar energy has been extended to such domestic and industrial applications as refrigeration, cooking, drying and chemical processes.

The sun produces an incredible amount of radiation, but, as illustrated in Figure 2.2 below, out of 100% of solar energy reaching Earth, 6% is reflected by the atmosphere, 20% is reflected by the clouds, and 4% reflected from the surface (Falayi & Rabi, 2012)).

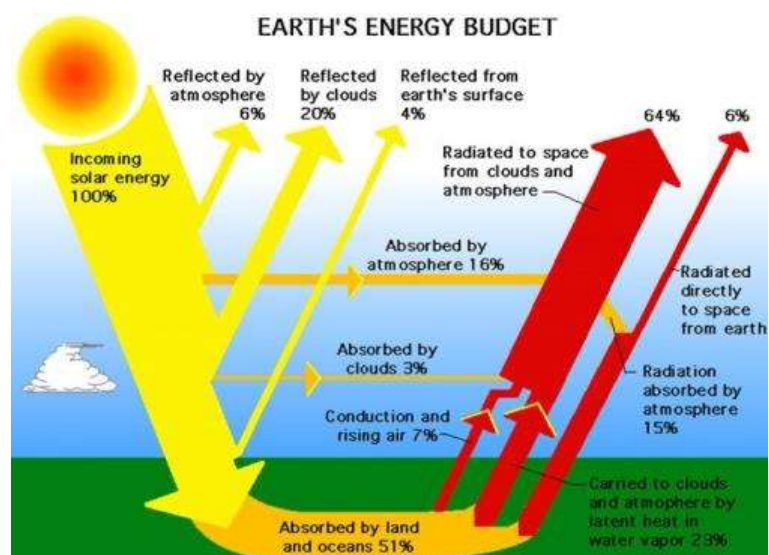


Figure 2.2: Earth's solar energy budget

(Falayi & Rabi, 2012)

2.2.2.1 Solar energy measurement

The component of the solar radiation that touches the earth without change of direction is referred as the direct normal irradiance (DNI), whereas the scattered component which reaches the earth from the sky is known as the diffuse horizontal irradiance (DHI). The sum of these two irradiances is known as the global horizontal irradiance (GHI) (Tian & Zhao, 2013).

$$GHI = DHI + DNI \tag{2.2}$$

In the case where the direct irradiance reaches the surface of the earth obliquely, the global horizontal irradiance will be the sum of the diffuse horizontal irradiance and the vertical component of the direct normal irradiance (Lysko, 2006).

$$\text{GHI} = \text{DHI} + \text{DNI} \cdot \cos(\theta) \quad (2.3)$$

where θ is the solar zenith angle as seen in Figure 2.3 (vertically above the location is 0° , horizontal is 90°).

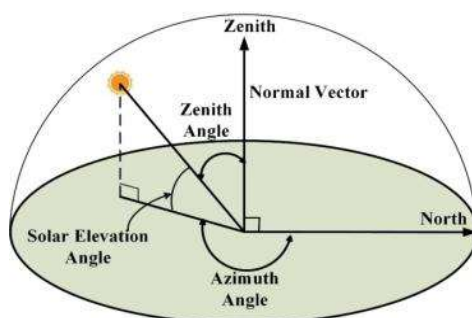


Figure 2.3: Solar zenith angle

(Cheng *et al.*, 2019)

For proper utilisation of solar energy, there is a need to measure the intensity of the radiation coming from the sun. Ground-based measurements are usually carried out by collecting daily values using radiometers with flat spectral response over a large bandwidth. Solar radiation is captured by a thermocouple with a black absorber. The received radiation may be converted to heat (Lysko, 2006).

GHI is measured by a horizontally-installed pyranometer that can be mounted on a solar tracker. This instrument is made of a thermopile detector protected by one or two glass domes, and has is used in meteorological and climatological stations.

DNI is measured using a pyrhelimeter. This device, usually mounted on an automatic sun tracker, is a thermopile type radiometer with a 5° field of view and a flat window. Unlike the GHI, the DNI can be measured on a horizontal surface (Lysko, 2006).



Figure 2.4: Pyrheliometer

(Source: <https://www.hukseflux.com>)

DHI may also be measured by using a second pyranometer placed on top of the sun tracker and comprising a shading assembly that moves together with the tracker to always stop the direct beam radiation from reaching the pyranometer (Lysko, 2006).



Figure 2.5: Pyranometer

(Source: <https://www.atmos-meteo.com>)

2.2.2.2 Estimation of the monthly average daily global radiation

Though Figure 2.2 describes the Earth's solar energy budget, the level of intensity, with which the extra-terrestrial radiation can touch the surface of the earth, depends on the local climatic conditions. Hence, data collection over a long period using different locations can yield an average global radiation in a specific area (for example, collecting data in different locations for 30 years). The average global radiation in any location is estimated by the actual sunshine hours and the maximum possible hours per day at a specific site. In some developing countries, estimation of the solar radiation is an issue because of lack of available data. One solution is the use of estimation of the monthly average daily global radiation models (Falayi & Rabi, 2012).

2.2.3 Solar thermal collectors

A solar collector is a device that is used to capture, collect, and convert solar radiation into useful thermal energy that can be stored or used in various applications (Sabiha *et al.*, 2015). Attempts to harness solar energy can be dated to the seventh century BC. It was mainly used for making fire and drying. But it is only in 1767 that Horace-Benedict de Saussure designed and manufactured a “hot box” plate collector known as the first solar collector (Szabó, 2017) as depicted in Figure 2.6.

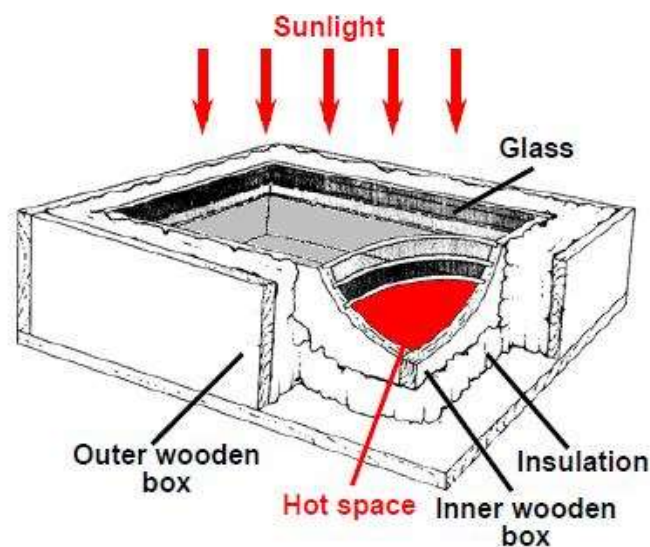


Figure 2.6: Horace-Benedict de Saussure's hot box

(Szabó, 2017)

The revolution in harnessing solar energy was boosted by Einstein's publication on the photoelectric effect, along with his paper on the theory of relativity in 1905 (Meinel & Meinel, 1977).

The oil crisis created by the 1973 war in the Middle East created a perceived need for research and usage of solar energy in various countries for the production of electricity and water heating. Since 1980, the United States of America, Japan, Denmark, Germany, and China have considered the expansion of solar energy technologies as priorities for their socio-economic development. Presently, China has become a major producer of solar photovoltaic panels and solar collectors (Energy & Wind, 2014).

The relevant literature presents different types of solar collectors, which can be classified into two categories: tracking and stationary solar collectors. For domestic water heating, stationary

solar collectors are used. In this category, three different solar collectors can be distinguished: flat plate, evacuated tube, and compound parabolic concentrating. This study was focussed on the evacuated tube (containing a heat pipe) solar collector.

2.2.3.1 Description of an evacuated tube heat pipe solar collector

Evacuated tube heat pipe solar collectors consist of a number of evacuated tubes, as shown in Figure 2.7. Each cylindrical tube is made up of annealed glass containing an absorber. The cylindrical shape of the tubes allows the sunlight to always strike the collector perpendicularly, permitting the collector to be efficient even early in the morning or late in the afternoon, or when shaded by clouds. Each evacuated tube comprises two tubes. The outer tube is transparent, to allow the solar irradiance to enter the collector, whereas the inner tube, covered with a selective coating, absorbs radiation, and keeps the heat inside the evacuated tube. The vacuum created between the two tubes creates an insulation that allows the radiation to enter and be absorbed by the collector without any losses. The heat is kept inside the tube to be transferred to the heat pipe, which contains a working fluid that transmits the heat to the water tank via its condenser (see detail in Figure 2.8) (Parmar & Bhojak, 2016). An evacuated tube heat pipe solar collector, unlike a flat plate solar collector, can work under any weather conditions with acceptable heat efficiency. Evacuated tube collectors are particularly useful in areas with cold, cloudy wintry weather (Parmar & Bhojak, 2016).



Figure 2.7: Evacuated tube heat pipe solar collector

(Source: <https://www.indiamart.com>)

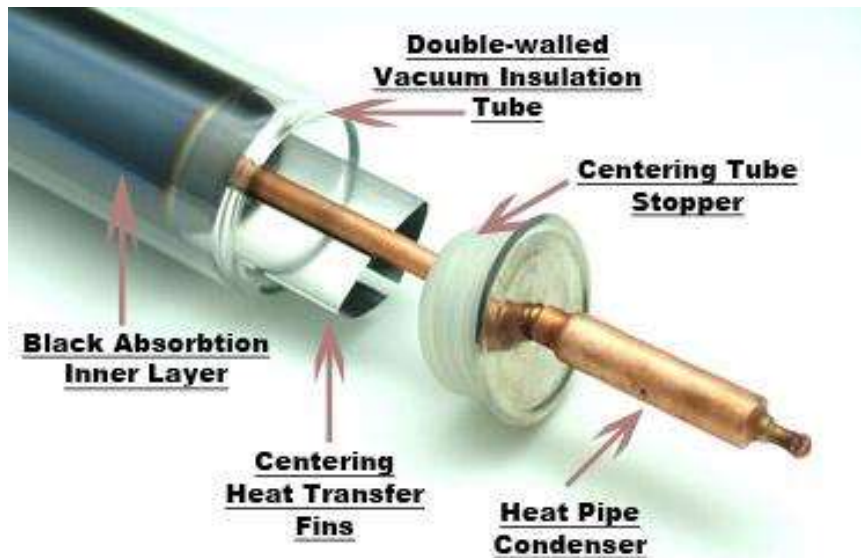


Figure 2.8: Detail of the evacuated tube heat pipe's condenser

(Source: <http://www.solarpanelsplus.com>)

The evacuated tube heat pipe solar collector has a high response to heat transfer, does not have any moving parts and does not produce noise. It can produce high temperatures because of the usage of the latent heat of the working fluid contained within the heat pipe. As the absorber is not exposed to the influence of the atmosphere, factors such as humidity and corrosion, which can alter the thermal performance of the solar collector, are radically reduced, leading to a longevity of approximately 15 years.

2.2.3.2 Research on the thermal performance of evacuated tube heat pipe solar collectors

Numerous researchers have worked on the impact of various parameters with a view to improving the efficiency of evacuated tube heat pipe solar collectors.

Ayompe and Duffy, 2013 investigated the energy performance of a heat pipe solar collector for water heating. They found that, for a mean daily collection of 20.4 MJ, the solar fraction and the system efficiency were 33.8% and 52.0%, respectively. A similar study was performed in Spain with the objective of evaluating the performance based on the extracted hot water

from the solar storage tank. The results revealed a direct relation between the system's efficiency and the required water temperature (Ayompe & Duffy, 2013).

A platform for the heat pipe solar collector was developed to investigate the instantaneous efficiency and its correlations with the receiver and absorber areas, the effective heat capacity, the incidence angle modifier, and the pressure drop. The model was found stable, reliable, and worthy for use in other models (Du *et al.*, 2013).

A theoretical and experimental study on the evacuated tube heat pipe solar collector both yielded a detailed method for energy and exergy analysis on the collector. It reported that the inlet water temperature, mass flow rate, the transmittance of tubes, and absorptance of the surface directly affects the energy and exergy efficiency of the evacuated tube heat pipe solar collector. It concludes that if the temperature of the water at the inlet increases, the heat transfer rate between the heat pipe's condenser and the water decreases (Jafarkazemi *et al.*, 2016).

More research on the effect of other parameters on the thermal performance of the evacuated tube heat pipe solar collector has been reported. These include using different working fluids in the heat pipe (Abd-Elhady *et al.*, 2018; Mujawar & Shaikh, 2016; Ersöz, 2016; Harikrishnan & Kotebavi, 2016); the impact of the heat pipe on the efficiency of the solar collector by considering the collector with and without heat pipe (Chopra *et al.*, 2018); studying the behaviour of the evacuated tube heat pipes solar collector in various weather conditions (Siuta-Olcha *et al.*, 2020; Redpath, 2012; Shafieian *et al.*, 2019); and adding a concentrator device or a reflector (Chamsa-ard *et al.*, 2014; Alhabeeb *et al.*, 2020).

It is deduced, from the various studies that involve the evacuated tube heat pipe solar collector that its thermal performance depends on various external and internal factors. The internal factors are mainly linked to the performance of the heat pipe. Enhancing the efficiency of the heat pipe should improve the efficiency of the collector.

CHAPTER 3: HEAT PIPES

3.1 Introduction

Reducing losses in heat transmission has been a challenge for scientists and industry for many years. Heat pipe technology is a notable accomplishment of engineering, providing the ability to transfer heat more efficiently.

A heat pipe is an innovative device that works on the principle of a two-phase heat transfer through comparatively small cross-sectional areas. As shown in Figure 3.1, high heat fluxes are transmitted by means of latent heat of vaporisation from a heat source known as an evaporator to a heat sink, known as a condenser (Liu, 2016). Classified as a passive device, a heat pipe works without external pumping power to help the recirculation of the working fluid. In many heat pipe designs, a capillary two-phase system is used to regulate the flow of the fluid. The heat pipe has no moving parts, making it a vibration-free device. With a thermal conductivity as high as 10 000 times that of copper, a heat pipe possesses an elevated heat transfer capacity. It can be used as a temperature control, a thermal diode device, for heat flux amplification in heating and heat flux diminution in cooling (Dunn & Reay, 2016)

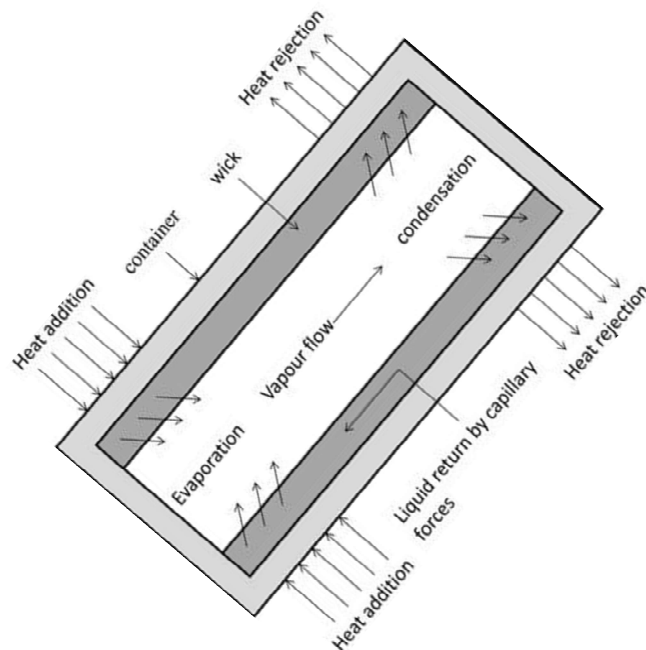


Figure 3.1: Schematic diagram of the flow of fluid in a heat pipe

(Sureshkumar *et al.*, 2013)

Heat pipes have been the subject of numerous scientific publications in international journals, reinforcing their importance in thermal technology. Heat recovery systems, electronic equipment, water heating, air conditioning systems, cooling and heat storage, and space apparatus are all areas of application of heat pipes (Shafieian *et al.*, 2018).

Nonetheless, regardless of the quantity of studies published for five decades, improving the thermal performance of heat pipes remains a serious challenge to researchers and industry. In view of this, there is still considerable work to be carried out regarding the usage of heat pipes in some applications, such as solar renewable energy, transportation systems, engines, automotive industry and cutting tools (Groll, 2014; Yang *et al.*, 2003).

This chapter will briefly cover background information on heat pipes, particularly:

- areas of heat pipe applications;
- heat pipe components and materials;
- working principles and governing equations;
- thermal performance of heat pipes;
- types of heat pipes; and
- multivariate polynomial regression analysis of the performance of heat pipes.

3.2 Historical background

To improve the performance of boilers and other steam engines, Jacob Perkins developed a closed tube capable of heating by means of evaporating fluids in 1836. Considered as the precursor of the heat pipe, numerous wickless tubes, developed by the Perkins family, were patented between 1800 and 1910 (Perkins, 1838).

Since 1970, research on heat pipes in the scientific and industrial world began increasing, as evidenced by publications of papers in journals and conference proceedings. Studies on the understanding of the principles of wick capillary structures, operational limitations, heat transfer and working fluid flow processes were performed and published. More applications in electronic equipment, commercial and domestic usage utilizing heat pipes were developed (Zohuri, 2019).

Reviews in the literature show a tremendous increase of interest in heat pipe technology. In their review, Riffat and Ma (2007) presented the development of heat pipe technology between 2000 and 2005. New working fluids and new capillary wick structures have been investigated for conventional heat pipes. They also provide an overview of the development of new types of heat pipes and micro heat pipes. New applications as solar collectors, air conditioning and

heat pipes integrated in turbines were reported. It is also during this period that various mathematical and thermal models of heat pipes were developed (Riffat & Ma, 2007).

3.3 Heat pipe components and materials

A conventional heat pipe consists of three main sections, as displayed in Figure 3.2. The section receiving the thermal energy from the heat source is known as an evaporator, while the section rejecting heat is called the condenser. With reference to the application, an adiabatic section can be created between the evaporator and the condenser (Reay *et al.*, 2013).

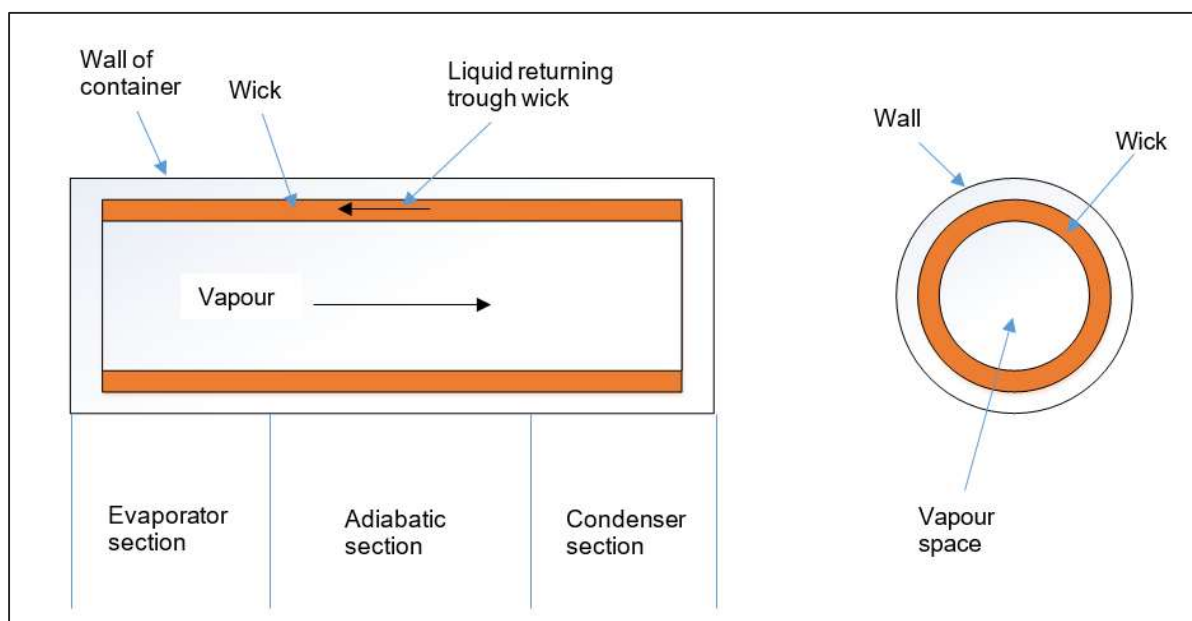


Figure 3.2: Components and sections of a heat pipe

3.3.1 Description of a heat pipe

Physically, a heat pipe consists of an envelope or container, a working fluid and often a capillary wick structure. It is through the vaporous working fluid that heat is transferred from the evaporator to the condenser. But inside the envelope's wall, usually but not always, a capillary wick structure is constructed to allow the return of the liquid working fluid from the condenser to the evaporator (Seshan & Vijayalakshmi, 1986). When no wick structure is provided, the liquid working fluid flows back to the evaporator aided by gravity.

3.3.2 Working fluid

The first parameter to consider in the selection of the working fluid is the operating temperature range, which depends on the type of application the heat pipe is used for. Within a chosen

range of temperatures, various working fluids are available, but their thermophysical properties must be scrutinised to select the working fluid that suits the specific application (Reay *et al.*, 2013).

For the selection of the working fluid, the following thermophysical properties must be considered:

- compatibility with wick and wall materials;
- good thermal stability;
- wettability of wick and wall materials;
- vapour pressure not too high or low over the operating temperature range;
- high latent heat;
- high thermal conductivity;
- low liquid and vapour viscosities;
- high surface tension; and
- acceptable freezing or pour (loss of flow characteristics) point.

The above properties define the thermodynamic aspects which act on the various limitations to the flow taking place within the heat pipe. A high value of surface tension is preferred, because it allows the heat pipe to work against gravity and to produce a high capillary driving force. A high vapour pressure is needed to avoid high velocities, which might create a high temperature gradient. Nonetheless, the vapour pressure must not be too high, as this requires a thick-walled container (Manimaran *et al.*, 2012).

It is also important to report that for maximum heat transfer by the heat pipe, a high latent heat of vaporization is preferable, and a low-pressure difference between the evaporator and the condenser. The working fluid should also have a high thermal conductivity in order to reduce the radial temperature gradient, which can increase the nucleate boiling at the wall interface (Jouhara *et al.*, 2017).

3.3.2.1 Classification of heat pipe based on working fluids

The classification of heat pipes based on the working fluid utilised can be carried out considering the useful range of temperatures attached to the applications (Nemec *et al.*, 2011).

- Working fluids used in cryogenic heat pipes for the temperature range from 1 to 200 K include helium, argon, neon, nitrogen, and oxygen. Due to their low latent heat, these fluids transmit small amounts of heat.

- Working fluids used in low-temperature heat pipes for the range of temperature from 200 K to 500 K include methanol, ethanol, ammonia, acetone, toluene, and water.
- Working fluids for medium-temperature heat pipes for the range of temperature from 500 K to 700 K include mercury and sulphur.
- The working fluids used in heat pipes for temperatures higher than 700 K are mostly liquid metals such as potassium, sodium, and silver.

Table 3.1 gives the boiling or melting point and the useful range of temperatures of some working fluids used in heat pipes.

Table 3.1: Range of temperature of some working fluids used in heat pipes

Medium	Melting point (K)	Boiling point (K)	Useful range (K)
Helium	2	12	2 to 4
Nitrogen	63	77	70 to 113
Ammonia	195	240	213 to 373
Pentane	143	301	253 to 393
Acetone	178	330	273 to 393
Methanol	175	337	283 to 403
Ethanol	161	351	273 to 403
Heptane	183	371	273 to 423
Water	273	373	303 to 473
Toluene	178	383	323 to 473
Mercury	234	634	523 to 923
Caesium	302	943	723 to 1173
Potassium	335	1047	773 to 1273
Sodium	371	1165	873 to 1473
Lithium	452	1613	1273 to 2073
Silver	1233	2485	2073 to 2573

3.3.2.2 Working fluid and merit number

For the selection of the most efficient working fluid, Chi (1976) derived a parameter known as the merit number, or transport factor, using thermophysical properties. The merit number compares the ability of the fluid to carry heat during the entire operating temperature range (Chi, 1976). For a cylindrical heat pipe, the transport factor or merit number is given by:

$$N_1 = \frac{\lambda \sigma \rho_l}{\mu_l} \quad (3.1)$$

- N_1 Merit number
 ρ_l Liquid density
 σ Surface tension

- λ Latent heat
- μ_l Liquid dynamic viscosity

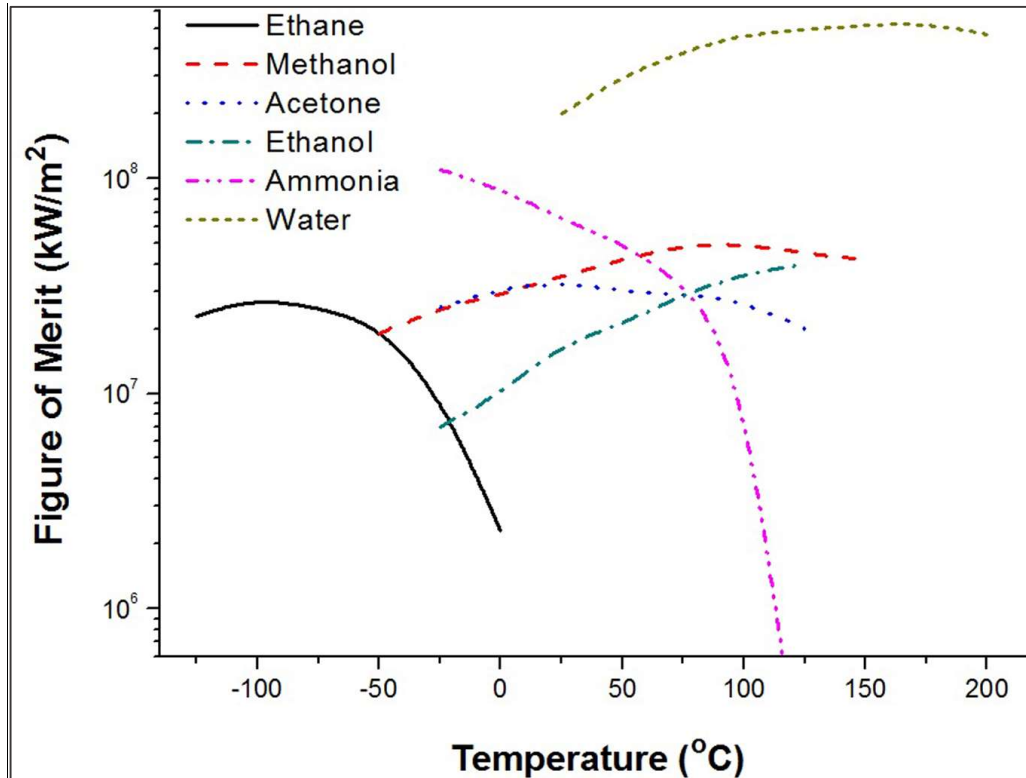


Figure 3.3: Merit number of various working fluids (Byon, 2016)

Figure 3.3 illustrates the merit number as a function of temperature of various working fluids used in heat pipe applications. For a given working fluid, the merit number is a temperature dependent parameter which loses its significance at or near the critical temperature. Another parameter considered to express an influence on the efficiency of a heat pipe is the boiling point of the working fluid. In an investigation performed to analyse the performance of different working fluids for use in organic Rankine cycles, it was concluded that the boiling point of the working fluid has an impact of the efficiency of the system (Mago et. Al., 2007).

3.3.2.3 Working fluid inventory

The amount of working fluid in the heat pipe is important in order to avoid drying out, if insufficient, or the reduction in the heat transfer, if excessive. Below is a procedure to determine the correct amount of fluid in a heat pipe. The space volume of the wick V_{wick} is expressed as:

$$V_{wick} = \pi(r_o^2 - r_i^2)L_{eff} \cdot \epsilon \quad (3.2)$$

With

V_{wick} : the space volume of the wick

r_o : Outer radius of the heat pipe

r_i : Inner radius of the heat pipe

L_{eff} : Effective length of the heat pipe

ϵ : Porosity of the wick structure

The effective length of the heat pipe is expressed as:

$$L_{eff} = \left(\frac{L_{evap} + L_{cond}}{2} \right) + L_{ad} \quad (3.3)$$

With

L_{evap} : Evaporator length

L_{cond} : Condenser length

L_{ad} : Adiabatic region length

The total volume (V_{tot}) of the heat pipe is given by:

$$V_{tot} = \pi r_i^2 L_{eff} + V_{wick} \quad (3.4)$$

In practical conditions, the volume corresponding to the desirable amount of working fluid V_f in the heat pipe should be slightly greater than V_{wick} and less than the total volume of the heat pipe (Lin *et al.*, 2011).

$$V_{wick} < V_f < V_{tot} \quad (3.5)$$

The maximum amount of working fluid in the heat pipe should be 25% of the total volume V_{tot} (Banovčan *et al.*, 2018).

3.3.2.4 Research on working fluids

Research on working fluids can be divided into two main groups:

- Some works have focussed on understanding the behaviour of the working fluid during the heat transmission process, the vapour and liquid flow in the heat pipe and its impact on

the thermal performance of the heat pipe (Mozumder *et al.*, 2010; Peyghambarzadeh *et al.*, 2013; Arab & Abbas, 2014; Savino & Paterna, 2006).

- The other group of studies was on discovering new working fluids (including nanofluids) that could be compatible with cheap, light and more ductile container materials and could also provide high heat pipe thermal performance (Riffat & Ma, 2007; Pachghare & Mahalle, 2013; Di Paola, 2010; Sonawane *et al.*, 2016; Andrzejczyk, 2019).

3.3.3 Container

The container serves as an envelope between the inside of the heat pipe and the surroundings and has to maintain a vacuum inside the heat pipe. For an efficient heat transfer between the heat source and the working fluid, the material used for the container should have a good thermal conductivity. To ensure enough capillary pressure to return the fluid to the condenser, the container should be hermetically sealed. The factors listed below are considered during selection of the material for the container (Reay *et al.*, 2013):

- The working life of the heat pipe is defined mainly by the compatibility between the working fluid and the container. Chemical reactions between the material used for the container and the working fluid can result in corrosion and production of uncondensable material/fluid, which can limit the performance and the life of the heat pipe.
- The strength-to-weight ratio intervenes in some applications, such as in spacecraft, where the weight of the heat pipe matters and the container material must be selected accordingly.
- To optimise the heat transmission in the heat pipe, the temperature drop between the evaporator and the wick capillary structure must be reduced to its lowest value by selecting a container material with good thermal conductivity.
- The container of the heat pipe can be of any shape and the capillary wick of any type according to the applications, but the material of the container must allow ease of fabrication, including welding, machineability, and ductility.
- Diffusion of gas is not desirable into the heat pipe, because it affects the thermal performance, which is porosity and wettability are important factors.

3.3.3.1 Material used in heat pipes

Due to its good thermal conductivity, availability on the market, cost, and compatibility for a majority of the working fluids, copper is the most widely used material in the manufacturing of heat pipes, especially for applications in the low and medium temperature ranges.

The need to reduce the weight of the heat pipe for spacecraft applications has led researchers to look for lightweight materials. The best-known lightweight material is aluminium, which is associated with a corrosion when using common working fluids (Kuroda *et al.*, 2014). Specific treatments, consisting of covering aluminium alloys, titanium alloys and magnesium alloys with a protective layer, have been performed to correct the incompatibility with working fluids like water. Also, the use of fibre in the manufacturing of the wick capillary structure has been adopted to reduce the weight of the heat pipe (Babu & Kamath, 2015).

Due to their mechanical strength and high thermal conductivity, stainless steel containers are also preferred for heat pipes. It is also important to note that stainless steel containers are not used with water, because of the reaction between the steel walls and water creating hydrogen, resulting in a cold plug of gas in the condenser. This fact reduces the total effective length of the heat pipe and limits its performance (Jouhara *et al.*, 2017). Table 3.2 illustrates the compatibility between some working fluids and common materials used in heat pipes.

Table 3.2: Compatibility between working fluid and container's material

Working Fluid	Compatible Material	Incompatible Material
Water	Stainless steel, aluminium, brass, copper	Aluminium
Methanol	Stainless steel, iron, copper, brass, silica, nickel	Aluminium
Acetone	Aluminium, stainless steel, copper, brass, silica	
Toluene	Stainless steel, aluminium, brass, copper	
Ethanol	Stainless steel, aluminium, brass, copper	
Ethyl Acetate	Stainless steel, brass, copper	Aluminium

3.3.4 Wick capillary structure

The wick capillary is a porous structure inside the wall of the container of the heat pipe in order to produce enough pressure to pump the liquid to the evaporator. The wick structure also has the important role of distributing the working fluid around any area of the evaporator that is likely to receive heat. It is usually made of material like copper, aluminium or nickel, provided that it is compatible with the working fluid and presents a low resistance to the transfer of heat (Mwaba *et al.*, 2006).

An enormous amount of material is available in literature about the characteristics of a wick (Faghri, 2014), and the main categories of capillary wick structures (Nemec, 2017; Dunn & Reay, 2016; Franchi & Huang, 2008; Jouhara *et al.*, 2018).

In this work, the heat pipes used are conventional and flow of the working fluid is assisted by gravity.

3.4 Principle of operation of the heat pipe

The working principle of the heat pipe can be explained by reference to the temperature – entropy diagram presented in Figure 3.4

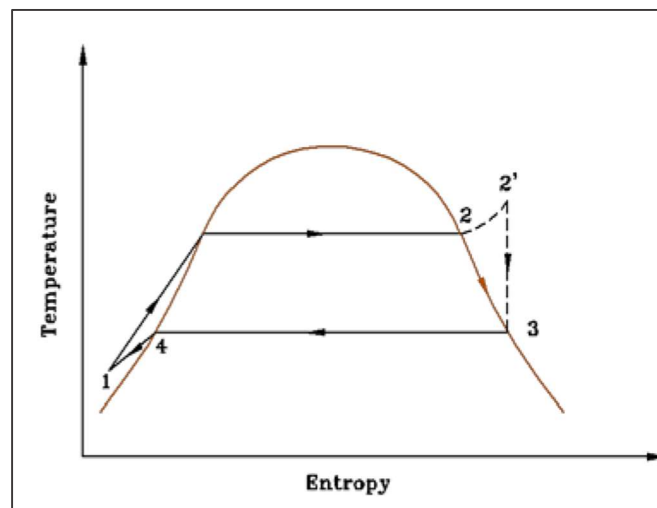


Figure 3.4: Heat pipe thermodynamic cycle

(Faghri, 2014)

The cycle describing the principle of operation of the heat pipe is made up of four processes:

- *Process 1-2*: This illustrates what happens in the evaporator once the thermal energy is absorbed by the working fluid. From an initial low pressure (vacuum), the temperature of the working fluid increases quickly to reach the saturation temperature, where the evaporation process starts. The phase change from liquid to vapour takes place at constant temperature and constant pressure. The state of vapour leaving the evaporator can be saturated (point 2) or superheated (2') depending on the amount of heat added.
- *Process 2-3*: The saturated or superheated vapour, produced at the evaporator at high temperature and high pressure, moves to the condenser through the adiabatic region, where it experiences a pressure and temperature drop.

- *Process 3-4*: Once the vapour reaches the condenser, latent heat is rejected to the sink, provoking a change of phase from vapour to liquid at constant pressure and constant temperature.
- *Process 4-1*: By capillary action against or with the aid of the gravitational field, the condensed liquid in the condenser is pumped back to the evaporator to restart the cycle.

Various movements of heat transfer and fluid flow during the operation of a heat pipe are presented in Figure 3.5.

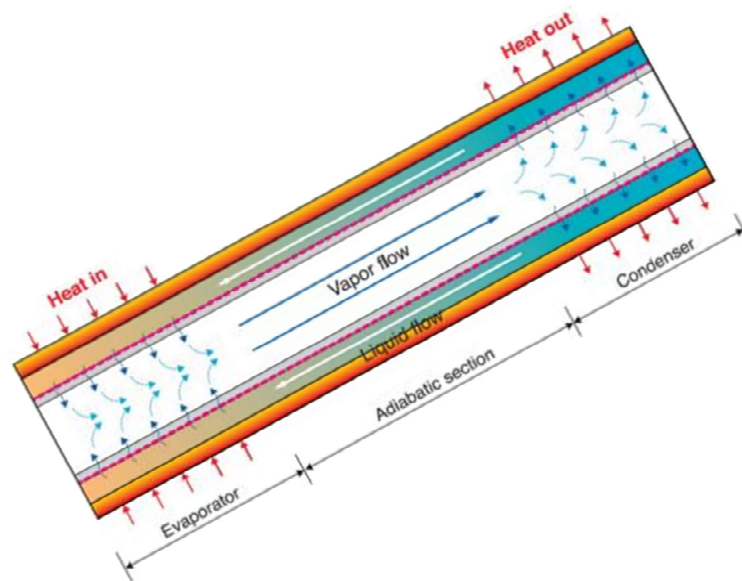


Figure 3.5: Movement of fluid and heat during a heat pipe's operation
(Byon, 2016)

For a heat pipe to function, the maximum capillary pressure must be greater than the total pressure drop in the heat pipe, which is made up of the pressure needed to create a flow of the vapour from the evaporator to the condenser, the pressure necessary to bring back the liquid from the condenser to the evaporator and if it happens to act against it, the force due to gravity. The latter (force of gravity) may be nonapplicable, positive, or negative, according to the inclination of the heat pipe, or it could be zero if in space (Zuo & Faghri, 1998).

$$\Delta P_{\text{cap,max}} \geq \Delta P_{\text{liq}} + \Delta P_{\text{vap}} + \Delta P_{\text{grav}} \quad (3.6)$$

Where,

$\Delta P_{\text{cap,max}}$: Maximum capillary pressure

ΔP_{liq} : The pressure drop required to move back the liquid from the condenser to the evaporator

ΔP_{vap} : The pressure increase required for the vapour to flow from the evaporator to the condenser

ΔP_{grav} : The equivalent pressure due to the gravitational force

3.4.1 Heat transfer limitations

During its operation, a heat pipe is subjected to limitations and constraints due to a number of aspects, which can be physical or operational. Those limitations affect the heat transferred and the thermal performance of the heat pipe. The shape of the heat pipe, the working fluid, the wick capillary structure and the operational temperature are the factors intervening directly in the heat transfer limitations. Below are the physical singularities attached to each heat transfer limitation (Margaris *et al.*, 2007). Figure 3.6 presents various heat transfer limits, as described below.

Capillary limit

This limit is also called hydrodynamic limitation, and occurs when the pressure drop between the evaporator and the condenser is greater than the capillary pressure available to pump enough liquid back to the evaporator for the restart of the cycle. A dry-out may be caused when there is any attempt to increase the heat transfer.

Sonic limit

This limit is based on the principle used in a convergent divergent nozzle, where the velocity at the throat cannot exceed the local velocity of the sound. In a heat pipe, the velocity flow between the evaporator and the condenser cannot exceed local velocity of the sound at the end of the evaporator. This limitation is usually coupled with liquid-metal heat pipes, due to high vapour velocities and low densities.

Boiling limit

If the radial heat in the evaporator increases excessively, the working fluid in the evaporator region wick will boil and bubbles can be produced, preventing the walls being wetted. That causes hotspots. This limitation is known as the boiling limit.

Entrainment limit

The entrainment limit is considered to occur when high shear forces can take place as the vapour is flowing to the condenser in the counterflow direction to the liquid moving to the evaporator. The shear forces can entrain the liquid back to the condenser, creating insufficient liquid flow in the wick structure.

Viscous limit (vapour pressure limit)

The viscous limit is considered to occur when the heat pipe is working in low temperatures, where the saturation pressure of the vapour can be the same order of intensity of the pressure drop needed to the vapour to flow to the condenser. No flow will happen in the heat pipe.

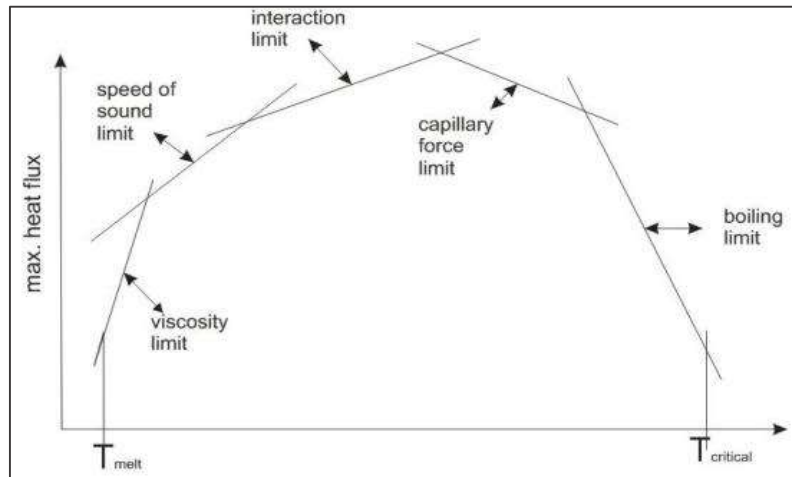


Figure 3.6: Heat transfer limits on a heat pipe

(Korn, 2008)

3.5 Thermal performance

The thermal performance of a heat pipe expresses and measures its ability to transfer heat from the evaporator to the condenser. Measurements of the input and output parameters as temperature and heat fluxes are useful in the determination of the performance of a heat pipe (Zohuri, 2019).

Literature presents the overall thermal resistance of the heat pipe as the primary means of measuring its thermal performance (Nemec *et al.*, 2011). The overall thermal conductivity of the heat pipe is given by the Fourier heat conduction equation:

$$k_{hp} = Q \frac{L_{eff}}{A \Delta T} \quad (3.7)$$

Where

Q is the heat transfer rate

A is the heat pipe's surface area

ΔT is the temperature difference between the evaporator and condenser

L_{eff} is the effective length of the heat pipe, as defined by Equation 3.3.

The overall thermal resistance of the heat pipe is a preferred methodology of determining the performance, because it illustrates the impact of different parameters. It is given by the equation:

$$R_{th, hp} = \frac{T_{hot} - T_{cold}}{Q} \quad (3.8)$$

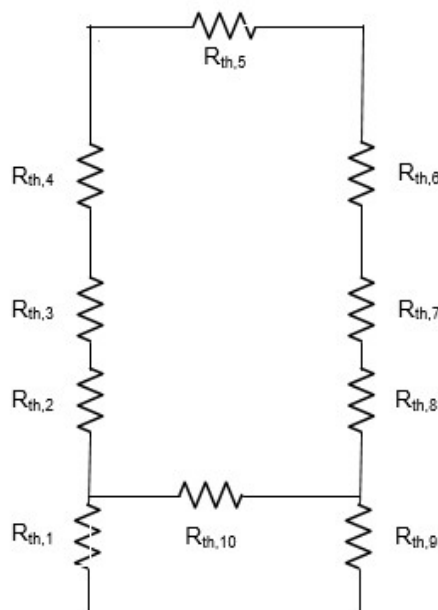
Where

T_{hot} : Temperature at the evaporator

T_{cold} : Temperature at the condenser

Q : Heat transfer rate

This total resistance is the sum of the different thermal resistances engaged in the operation of the heat pipe when considering the thermal network.



**Figure 3.7: Heat pipe thermal resistance network
(EI-Nasr & EI-Haggar, 1996)**

Where

$R_{th,1}$: Heat source - the evaporator resistance

$R_{th,2}$: Evaporator wall radial resistance

$R_{th,3}$: Evaporator wall-wick radial resistance

$R_{th,4}$: Evaporator liquid-vapour interface resistance

$R_{th,5}$: Vapour flow resistance

$R_{th,6}$: Condenser liquid-vapour interface resistance

$R_{th,7}$: Condenser wall-wick radial resistance

$R_{th,8}$: Condenser wall radial resistance

$R_{th,9}$: Condenser-heat sink resistance

$R_{th,10}$: Wall and wick (axial resistance) at the evaporator and condenser

The above resistances show that the thermal performance of a heat pipe is based on different heat transfer mechanisms occurring between the heat source and the heat sink, which are: radiation, conduction, and convection. Numerous studies of different parameters have shown that the following factors have an influence on the thermal performance of the heat pipe (El-Nasr & El-Haggar, 1996).

- Material used for the container
- Properties of the working fluid used
- Type of wick structure
- Dimensional variation
- Source and sink temperature
- Power input at the evaporator section
- Orientation of the heat pipe

3.6 Heat pipe technologies

Various heat pipe technologies have been developed with the purpose of increasing the thermal efficiency and in response to specific applications. The main factors used to classify the different technologies are the vapour flow from the evaporator to the condenser and the mechanisms applied to return the liquid back to the evaporator (Reay *et al.*, 2013).

Two categories can be distinguished:

- Conventional heat pipes
- Loop and pulsating heat pipes

Each of the above-mentioned categories, can be divided into the following subcategories:

- Gravity-assisted heat pipes,
- Capillary heat pipes
- Other heat pipes.

Figure 3.8 illustrates the various heat pipe technologies.

3.6.1 Conventional heat pipes

In the conventional category of heat pipes, the liquid and vapour are flowing in the same pipe because of the difference in pressure between the evaporator and the condenser. If the liquid flows back to the evaporator by gravity, the heat pipe is labelled a gravity-assisted heat pipe, whereas when the liquid flows back to the evaporator due to the capillary force or a centrifugal force, it is called a capillary heat pipe. The group of conventional heat pipes comprises thermosiphons, cylindrical heat pipes, flat plate heat pipes and rotating heat pipes (Riffat & Ma, 2007).

3.6.2 Loop and pulsating heat pipes

In the loop heat pipes, the liquid and the vapour flow in different pipes. When the pressure drop in these heat pipes is compensated by gravity, the loop heat pipe is known as a loop thermosiphon. In the loop heat pipes and the capillary pumped loop, the frictional pressure drop is compensated for by the capillary forces created in the capillary situated in the evaporator. The difference between a capillary pumped loop and the loop heat pipe is determined by the location of the reservoir, which plays an important role in the operation of the heat pipe (Rahman *et al.*, 2015).

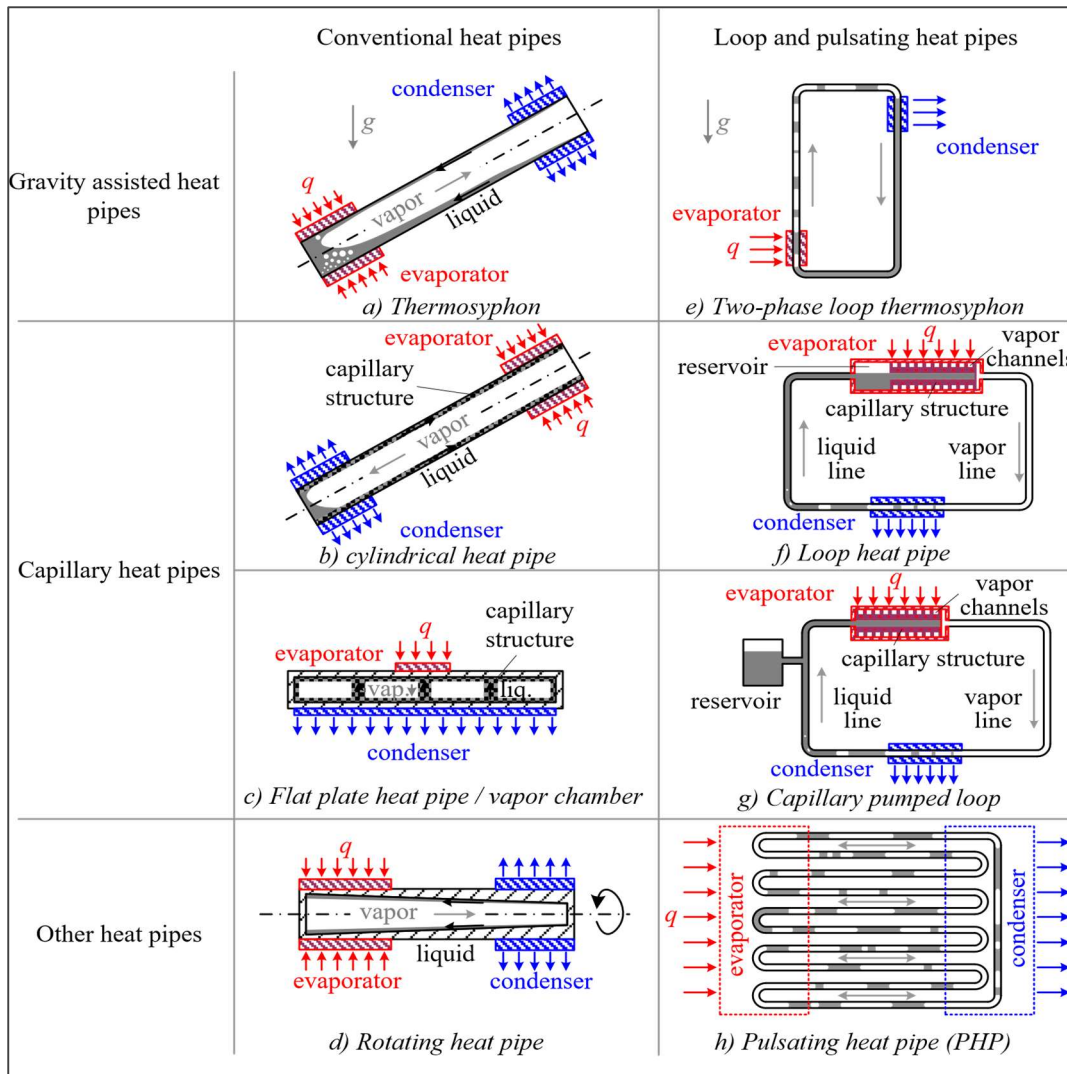


Figure 3.8: Heat pipe technologies

(Lips et al., 2016)

3.6.3 Concentric annular heat pipes

The need to further improve thermal performance and to respond to certain applications prompted industry and researchers to conduct theoretical and experimental work on newer types of heat pipes. For example, heat pipe cross-sections with polygonal shapes, such as micro/miniature heat pipes, or cross sections that vary along the length of the heat pipe and concentric annular heat pipes (Faghri, 2014).

The concentric annular heat pipe consists of two concentric pipes making an annular space with wick structures in the gap between them. The space in the inner tube is exposed to the environment, as shown in Figure 3.9.

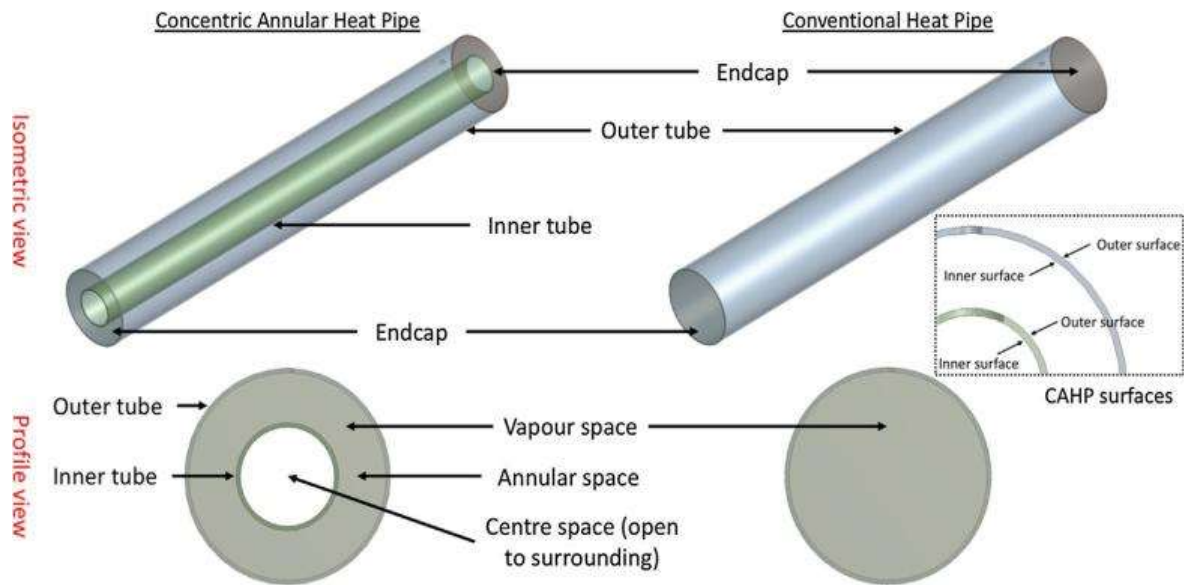


Figure 3.9: Concentric annular heat pipe
(Mustaffar *et al.*, 2019)

Research conducted on the concentric annular heat pipe has shown an improvement in thermal performance, probably as a result of the increase in heat transfer area (Faghri & Thomas, 1989; Nouri-Borujerdi & Layeghi, 2005).

Boo *et al.* (2005) investigated the thermal characteristics of concentric annular heat pipes by manufacturing three heat pipes with different diameters. They covered the inner surface of the heat pipe with screen mesh wicks connected by four bridges to allow the return of the working fluid. The diameter ratio varied from 2.31 to 4.23, while conserving the same outer diameter. They concluded that higher thermal performance was obtained for the larger inner diameter.

Vijra *et al.* (2015) compared a concentric annular and a conventional heat pipe by conducting experiments to investigate the effect of the variation of the heat input and inclination angle. Using a concentric annular heat pipe, where the inner surface of the outer pipe was covered with single layer of screen mesh wick, temperatures were recorded for various heat inputs and inclination angles. They concluded that for all inclination angles, the temperature difference between the evaporator and the condenser increases with an increase of the heat input for the concentric annular heat pipes. Due to the improvement in nucleate boiling activity, there is a decrease in thermal resistance, with a possible enhancement of the input heat transfer.

Inspired by the design and various studies on the improvement of the thermal performance of concentric annular heat pipe, it was decided in this work to modify the internal geometry of a conventional (gravity-assisted) heat pipe, by inserting in it different profiles, in addition to

different working fluids, in order to investigate their effect on the performance of an evacuated tube heat pipe solar collector.

Few studies have been conducted to analyse the effect of an insert in a heat pipe's thermal performance.

An investigation was conducted on a normal pipe, having no internal fins, and three other pipe types with 3, 4, and 6 rectangular and straight fins soldered longitudinally to the inner surface of the pipes. The finned pipes were shown to enhance heat transfer to the flowing water inside the pipes, with the 4-fins pipe showing the best results in terms of fastest response time and highest temperature rise (Shehadi, 2019).

A study on the effect of a fin as an insert, on the performance characteristics of an open loop pulsing heat pipe showed that its performance in all circumstances were better (Rahman, et al., 2015).

3.7 Multivariate polynomial regression analysis on the performance of the heat pipe

3.7.1 Modelling a heat pipe containing inserts

In this study, with regard to the heat transfer around the insert, there is a combination of conduction and perhaps radiation heat coming from the cylindrical pipe (casing) and convection between the working fluid and the insert's surface.

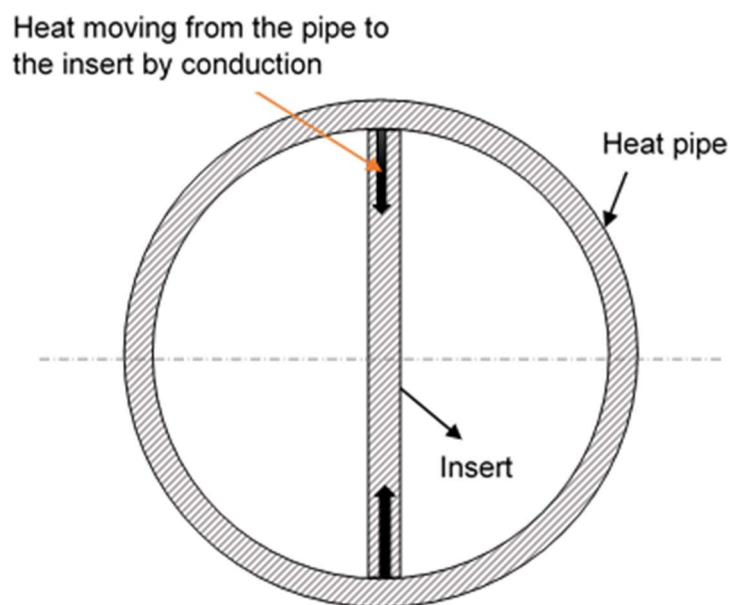


Figure 3.10: Section of the heat pipe with an I profile insert

As shown in Figure 3.10, there is heat being transferred by conduction from the cylindrical pipe to the insert. For any insert, the transmitted heat by conduction will depend on the surface area of contact between the pipe and the insert.

As the working fluid is flowing from the evaporator to the condenser, there is heat transfer by convection from the insert's surfaces exposed to the working fluid.

No attempt was made to model the various modes of heat transfer between the heat pipe's casing inner surface and the insert's surfaces and from the insert's surfaces to the working fluid.

Instead, it was decided to test the assumption that the independent variables, such as the working fluid and the internal geometry affected the thermal performance of the heat pipe, using a multivariate polynomial regression analysis. The analysis consists of a relationship between the efficiency of the heat pipe, as dependent on the thermophysical properties of the working fluid (represented by the fluid's merit number) and the surface area of the insert.

CHAPTER 4: EXPERIMENTAL SETUP

The experimental rig, the components and materials, the testing protocol and the instrumentation used in this investigation are described in this chapter. The components used in the building of the experimental apparatus were assembled by qualified personnel in the workshop at the Mangosuthu University of Technology. Different fluids compatible with copper heat pipes were obtained from the laboratory of the Department of Chemistry.

4.1 Description of the rig

To measure the thermal performance of the heat pipe using various working fluids and different geometries of the internal insert, a rig was made comprising of a mobile frame, an insulated container (storage tank), an evacuated tube containing a heat pipe and a solar simulator. The experimental apparatus, as depicted in the schematic diagram (Figure 4.1), and itemised in Table 4.1, was designed in such way that the condenser of the heat pipe could be screwed into the tank containing four litres of water. The solar simulator was made of halogen floodlights attached to the mobile frame to provide thermal energy to the heat pipe through the evacuated glass tube.

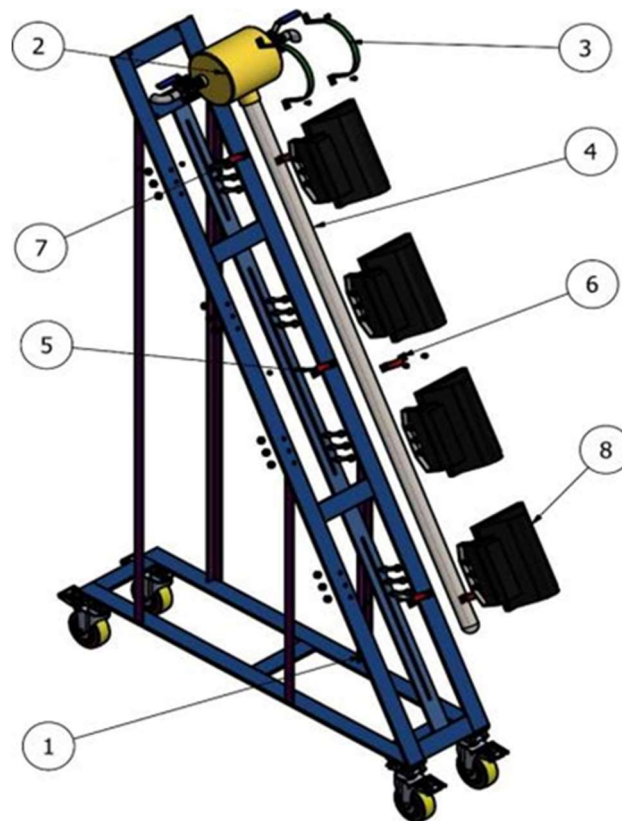


Figure 4.1: Schematic diagram of the testing rig

Table 4.1: Components of the testing rig

Item N°	Description	Quantity
1	Mobile frame	1
2	Water tank	1
3	Water tank clamp	2
4	Evacuated tube heat glass	1
5	Glass tube support	3
6	Evacuated tube clamp	3
7	M10 screw with nuts	12
8	Flood lights (solar simulator)	4

4.1.1 The water tank

A stainless-steel reservoir (storage tank), measuring 180 mm in inner diameter and 200 mm in length, was used as a geyser.

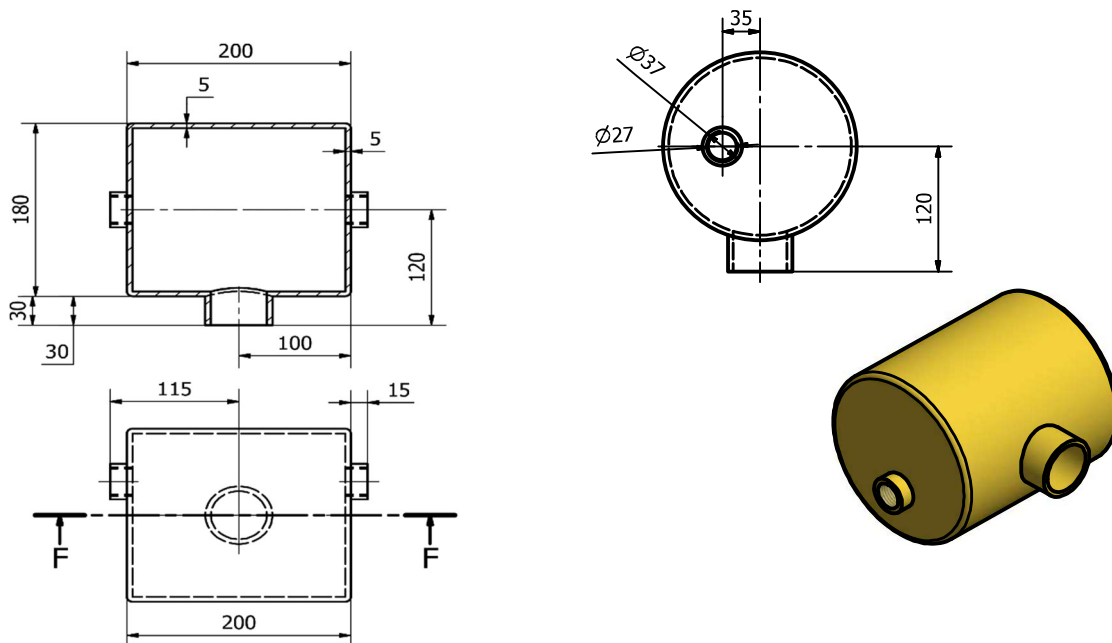


Figure 4.2: Schematic diagram of the water tank

As shown on Figure 4.3, two wells were made on top of the container to accommodate thermocouples, in order to measure the temperature of the water at top and bottom of the container. To fill and to drain the container, a 15 mm pipe and a valve, indicated on Figure 4.4, were placed at the top and bottom of the tank, respectively. To minimise the heat loss, a 50 mm fibre wire in forced lagging was placed on the container.

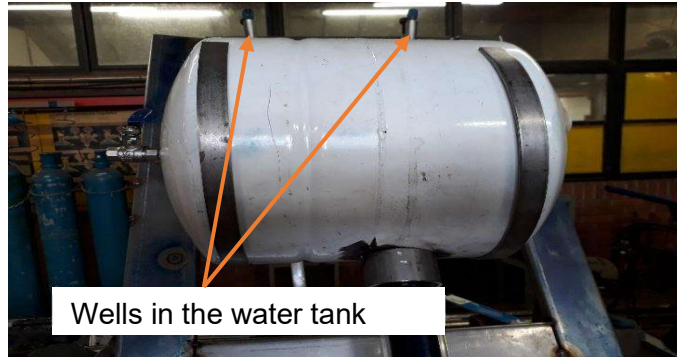


Figure 4.3: Wells in the water tank



Figure 4.4: 15 mm pipe and valve

As shown on Figure 4.5, the heat pipe was screwed into the water tank using a set of tapered British standard pipe (BSP) threads. The female thread of 19.1 mm was welded in the opening prepared in the water tank, while a male thread of 20.8 mm was welded on the heat pipe, as shown in Figure 4.7.



Figure 4.5: Heat pipe screwed into the water tank



Figure 4.6: BSP male thread welded on the heat pipe

4.1.2 Solar simulator

As described in figure 4.7, the rig was equipped with a solar simulator made of four halogen floodlights, each producing 400 W. Separated by a distance of 173 mm, the lights were placed

over the entire length of the evacuated tube heat pipe. The total irradiance of the solar simulator was set to a constant average value of 700 W per square meter. Variable transformers were used to control the voltage powering the lights.

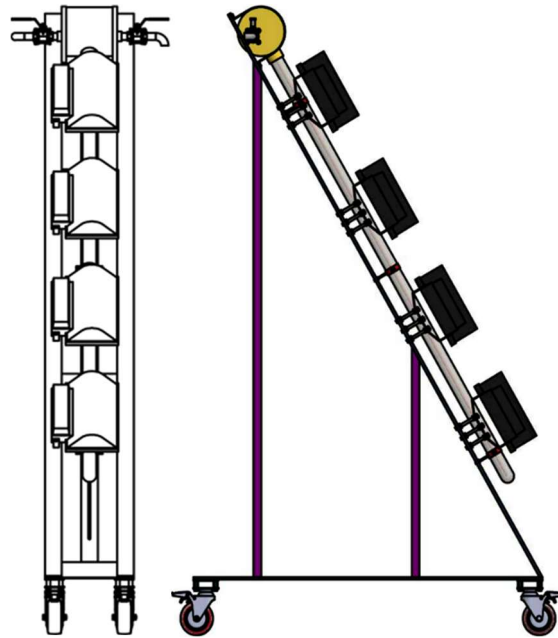


Figure 4.7: Schematic diagram of the solar simulator

To adjust the irradiance of the solar simulator, each floodlight was connected to the outlet of a variable transformer, which controlled the voltage powering the lights as shown in figure 4.8.



Figure 4.8: Variable transformers

4.1.3 Evacuated tube heat pipe

A copper pipe with both ends closed with end covers was used for this study. One end cover incorporated the filling tube for charging the working fluid. In order to reduce the impact of the ambient temperature on the thermal performance of the heat pipe (minimise the heat loss between the heat pipe and the environment), an evacuated glass tube made of two concentric tubes with vacuum between them encased the heat pipe.

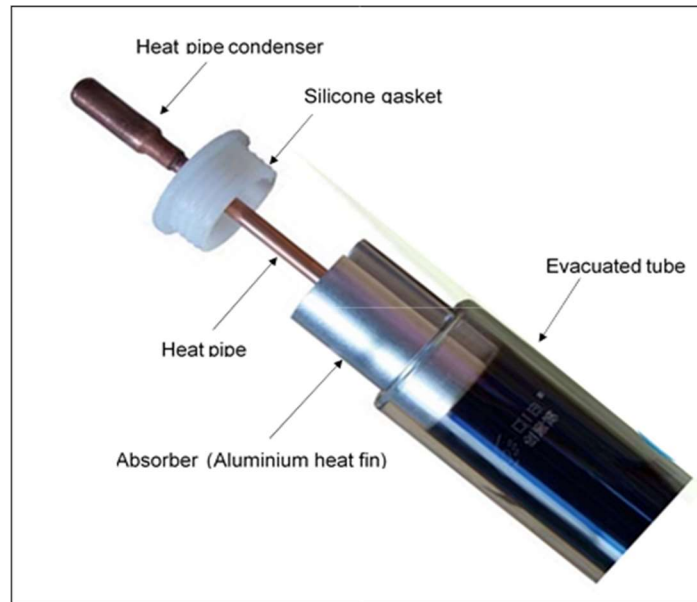


Figure 4.9: Evacuated tube heat pipe

<https://www.zenplumb.com/solar-hot-water>

4.1.3.1 Specifications of the evacuated heat pipe

The selection of the heat pipe was determined by availability on the market.

The evacuated tube and heat pipe were bought from Plumblink, a reseller of KWIKOT products in Durban.

Table 4.2: Evacuated tube heat pipe specifications

Evacuated Tube	
Parameter	Value
Material	Borosilicate Glass 3.3
Glass tube length	1.8 m
Outer tube outside diameter	0.058 m
Inner tube outside diameter	0.049 m
Inner tube inner diameter	0.047 m
Glass thickness	0.0016 m
Net weight	2.02 kg
Absorptance	0.9
Gross area	3.93 m ²

Emittance	0.08
Heat loss	0.8 W/m ² °C
Heat Pipe	
Parameter	Value
Material	Red copper
Evaporator outside diameter	0.008 m
Evaporator inside diameter	0.0065 m
Evaporator thickness	0.00075 m
Evaporator length	1.72 m
Condenser outside diameter	0.014 m
Condenser length	0.0645 m
Wick structure	Gravity-assisted
Absorber Plate	
Material	Aluminium / SS/ Cu
Emission coefficient	0.065
Absorption coefficient	0.93

4.1.3.2 Preparation of the Heat pipe

The geometries considered in this investigation were created by inserting the profiles described in Table 4.3 into the heat pipes. The inserts were made from a copper sheet purchased from Copalcor Trading – a Durban metals distributor. The copper sheet was 1800 mm long, 600 mm width and 0.7 mm thick. It was cut using a cutting machine, according to the dimensions displayed in the Table 4.3 below.



Figure 4.10: Insert manufacturing

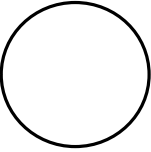
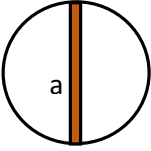
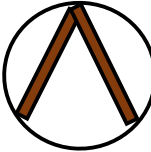

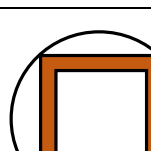


Figure 4. 11: I insert



Figure 4.12: V insert

Table 4.3: Geometries of the insert in the heat pipe

Geometry	Insert (label)	Dimensions [mm]
	No insert [NI]	Length= 1720 Outer diameter = 8 Thickness = 0.7
	I insert [II]	Length = 1720 Thickness = 0.7 a = 6.5
	V insert [VI] (a & b are the sides of the V)	Length = 1720 Thickness = 0.7 a = b = 6.2
	T insert [TI] (a, b & c are the sides of the triangle)	Length = 1720 Thickness = 0.7 a = b = c = 5.6
	S insert [SI] (a, b, c & d are the sides of the square)	Length = 1720 Thickness = 0.7 a = b = c = d = 4.6

An M6x1.0 mm m/s set screw with copper and fibre washers was fitted at the end of the heat pipe as a screw valve to allow for ease in changing the working fluid.



Figure 4.13: M6x1.0 mm screw attached to the heat pipe

4.1.3.3 Working fluid

A. Selection of the working fluid

The selection of the working fluid was based on the temperature range needed for the heat pipe to operate, given a specific application. Therefore, the application being limited to domestic water heating, with the temperature range being 200 K to 500 K, the working fluids to be considered in this investigation were: acetone, ethanol, ethyl acetate, methanol, toluene, and distilled water. For each working fluid selected in this range of temperature, the thermophysical properties were taken into account and its merit number calculated, as indicated in Table 4.4.

For this application (as the range of temperatures extends from 200 K to 500 K), an average temperature of 353.15 K (80° C) was considered to calculate the merit numbers, which represent the ability of each working fluid to transport heat.

Table 4.4: Thermophysical properties and the merit number of the chosen working fluids

Working fluid	Liq. density [kg/m ³]	Liq. viscosity [Pa-S] x10 ⁻³	Surface tension [N/m] x10 ⁻²	Latent heat [J/kg] x10 ³	Merit number [W/m ²] x10 ⁹
Acetone	719	0.192	1.62	495	30.02
Ethanol	734.1	0.44	2.105	845.2	29.69
Ethyl acetate	825.6	0.248	1.637	460.6	25.10
Methanol	735.3	0.286	1.755	1060	47.82
Toluene	779.6	0.247	1.8	370.5	21.04
Water	972	0.36	6.26	2309	390.26

According to Lin *et al.* (2011), for practical purposes, the volume corresponding to the desirable amount of working fluid V_f in the heat pipe should be greater than V_{wick} and less than the total volume of the heat pipe,

$$V_{wick} < V_f < V_{tot} \quad (4.1)$$

After calculation, the required amount of the working fluid for the heat pipe used in this study was revealed to be between 8.69 ml and 14.48 ml. An average amount of 10 ml was selected for all tests.

4.2 Instrumentation

4.2.1 Data logger

Various thermocouples were connected to the National Instruments temperature input module which transmitted the information to the primary computer by means of Ethernet. For this study, a National Instruments data acquisition (DAQ) eight-slot Ethernet chassis cDAQ-9189 was used. The eight-slot chassis controls the timing, the synchronisation and the transfer data between the input/output modules and the computer.



Figure 4.14: Ethernet chassis cDAQ-9189

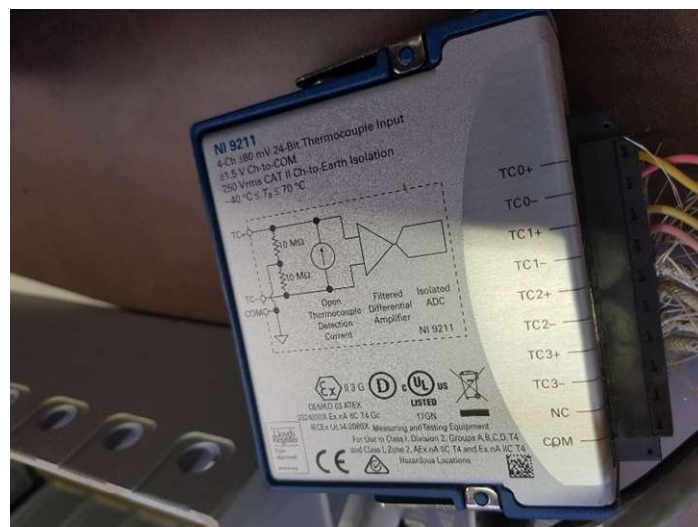


Figure 4.15: NI 9211 C series module

4.2.2 Software and computer

The compact DAQ chassis was used with LabVIEW to visualise, analyse, and manage the acquired data. In this work, LabVIEW 2015 was used. For the measurement of temperature, LabVIEW was configured using the bloc diagram below.

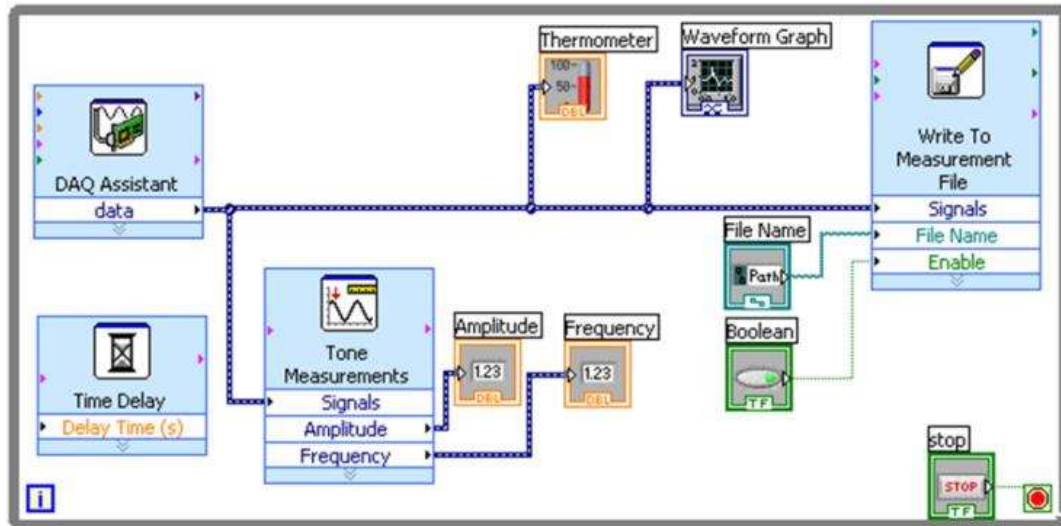


Figure 4.16: Temperature measurement bloc diagram

4.2.3 Thermocouples

Four K-type thermocouples were connected to the input/output module NI 9211, monitored with a NI-DAQ chassis to measure the temperatures at various locations in the system. Two of the four thermocouples were placed in the tank to measure the temperatures of water at two different levels: bottom, and top. The two remaining thermocouples were used to measure the ambient temperature.

4.2.3.1 Calibration of thermocouples

In various settings, thermocouple wires are likely to lose their accuracy over time because of a concert of factors such as chemical exposure, mechanical damage and continuous temperature changes. The lack of homogeneity alters the voltage generated by the thermocouple wires leading to an overall error in measurement. Therefore, thermocouples require regular calibration to ensure accurate temperature measurements.

In this investigation, using Labview, the calibration was performed while building the temperature measurement diagram bloc. As displayed in figure 4.17, each thermocouple used in this investigation was calibrated while creating a DAQmx task for the temperature measurement. Each channel was calibrated within the task.

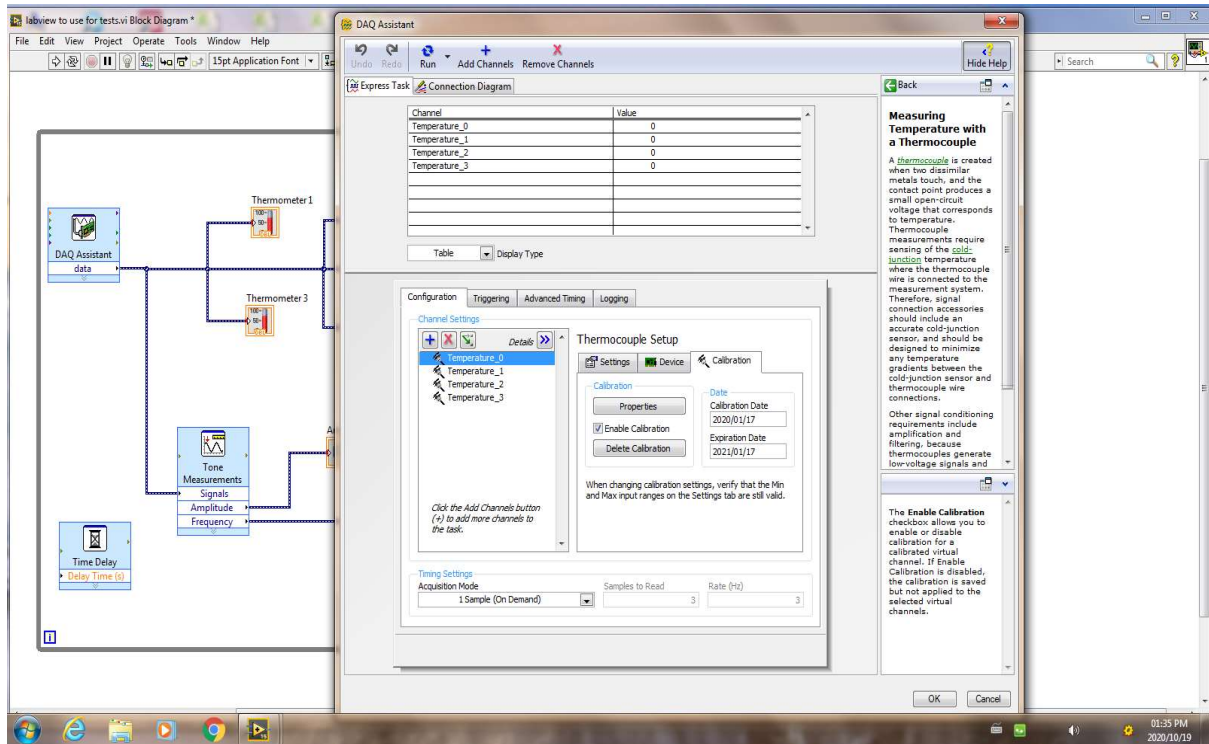


Figure 4.17: Calibration during DAQmx task building

A. Procedure

As shown in the figure 4.18, the experiment was performed by pouring 800 ML of water at 0 °C, in a 1 litre beaker, where the thermocouple to be calibrated and a thermometer (reference) were placed. The two devices were positioned close to each other and maintained at same depth during the experiment. The beaker was warmed on an electrical thermal plate until the water reached its boiling point.

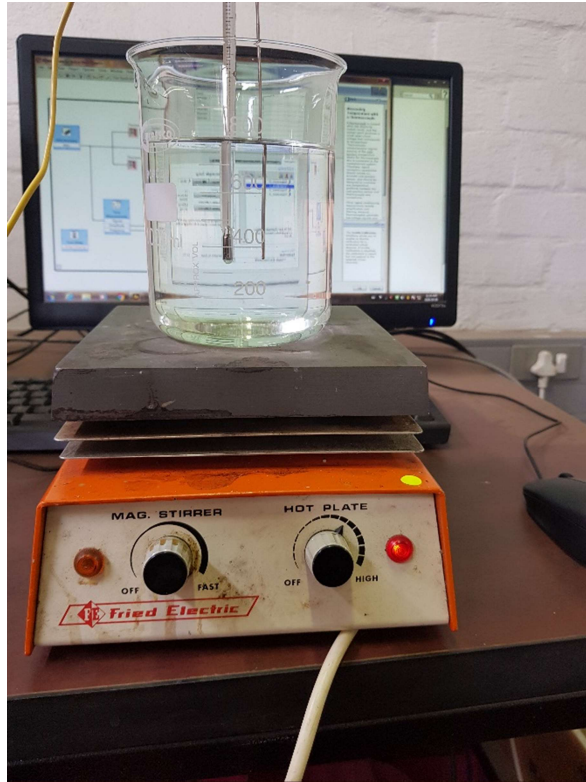
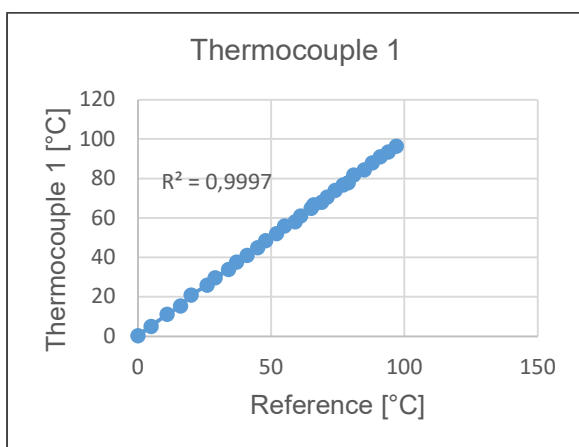


Figure 4.18: calibration of the thermocouples

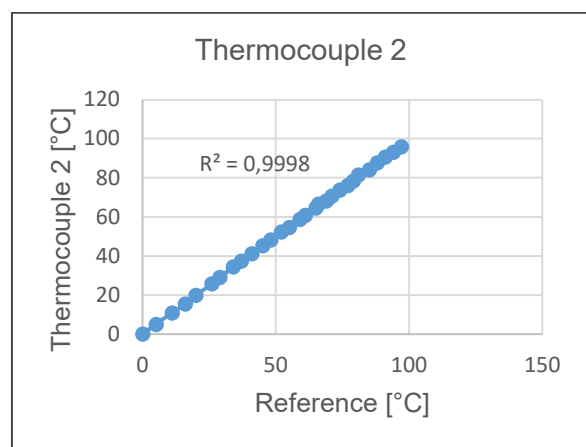
B. Results

Approximately 28 minutes were sufficient for the water to reach its boiling point. Reports were generated from Labview providing the reference and the uncalibrated temperatures as well as the difference between them for each channel (see Appendix A3).

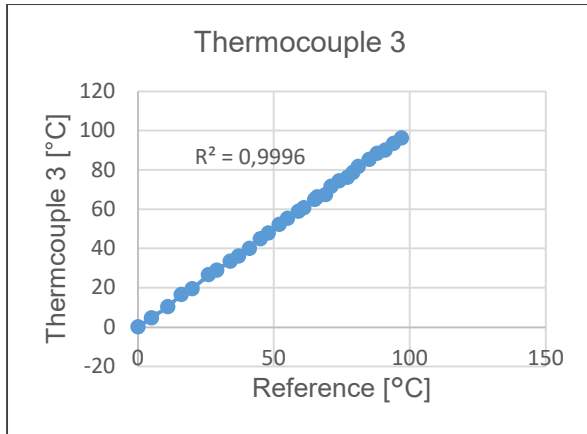
Figure 4.19 shows the temperature of the thermocouple to be calibrated against the reference temperature in order to find the value of R^2 between two measurements for the performed experiments.



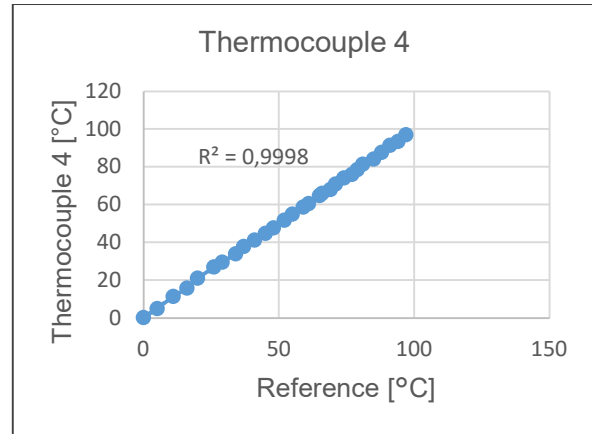
(a)



(b)



(c)



(d)

figure 4.19: temperature of the thermocouple to be calibrated against the reference temperature

Maximum difference of 1.1 °C with a minimum R^2 of 0.9996 were observed between the two values. According to the standard ASTM E220 - 19, a difference of up to 2.2 °C is allowed for K type thermocouples. The obtained results show that the value of R^2 in all cases was very close to unity making these thermocouples reliable for the measurements.

4.2.4 Power meter NanoVIP plus

The NanoVIP provides accurate measurements in the 7 W to 150 KW power range with a 200 A/1 V current clamp; and from 35 W to 750 kW in single-phase connection with a 1000 A/1 V current clamp (1.299 MW in three phase connection). It has a system that automatically recognises the type of current clamp, and switches between the two types of current clamps, making its operation extremely simple.



Figure 4.20: Power meter NanoVIP plus

4.2.5 Light meter

An MT 942 light meter was used to measure the global irradiance from the solar simulator. It measures light from visible luminaries equipped with white light LED fluorescent, metal halide, high pressure sodium and incandescent sources. Measurements were carried out in lux and then converted to W/m^2 . The MT 942 light meter has a measurement range from 0 to 400000 lux ($3160 W/m^2$).

4.3 Experimental protocol



Figure 4.21: Working fluids

1. The heat pipe with a specific geometry insert was filled with 10 ml of the working fluid.
2. A vacuum pump was used to remove the air from inside the heat pipe. During the experiments, the lowest pressure that could be obtained when preparing the heat pipes was 2.3 KPa.
3. Once the vacuum state was reached, the M6x1.0 mm screws with copper and fibre washers were used to close the heat pipe's evaporator. To avoid leakage, Loctite was used each time a specific working fluid was loaded into the pipe.
4. The water tank was filled with four litres of water before screwing in the heat pipe. To prevent a leak between the heat pipe and the water tank, a thread tape was wrapped around the 20.8 mm brass BSP male thread welded on the heat pipe. The water tank was then placed in the clamps welded on the top part of the frame. The heat pipe was slid into the evacuated tube, which was fixed on the tank and attached to the three middle C sections of the frame using two supports.
5. The thermocouples submerged in the tank measured the water temperature, while the other two were placed at different locations in the room to measure the ambient temperature.

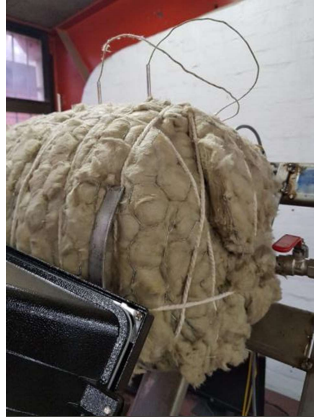


Figure 4.22: Thermocouples plunged in the water tank

6. The computer and the LabVIEW software were switched on. The DAQ assistant was tested and the amplitudes and frequencies of the output signal, displayed as a waveform graph, were adjusted. The software was set to record the data at 5-minute intervals.
7. The halogen floodlights were switched on to provide the necessary irradiance to the evacuated tube heat pipe. The average irradiance of the solar simulator was set to a value of 700 watts per square meter, similar to the average global horizontal irradiance in KwaZulu-Natal as the investigation was conducted in Durban-KZN (Zawilska & Brooks, 2011).

A value of 700 W/m^2 was read using the light meter and a NanoVIP power meter obtained by a voltage of 195 V at the outlet of the variable transformer connected to the light.

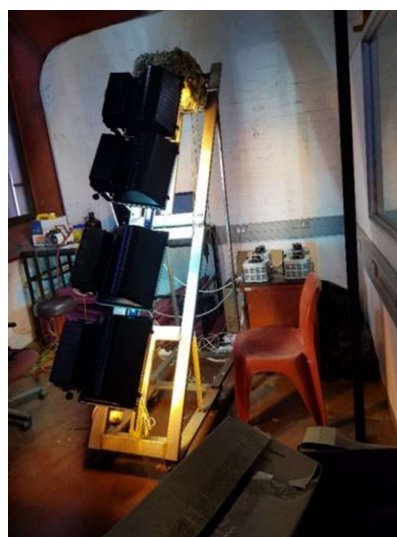


Figure 4.23: Solar simulator over the rig

8. During each experiment, the raw data comprising the temperatures of the water in the tank, the ambient temperatures and irradiance from the solar simulator were recorded. The test was run for seven hours, at the end of which the software was switched off and the values were stored in a folder in an Excel spreadsheet for analysis. In the beginning of the experiments tests were repeated a couple of times with almost identical results, hence there was no need to repeat the tests.
9. The halogen floodlights were also switched off, together with the variable transformers.
10. The water tank was then brought down from the frame and the evacuated tube and the heat pipe were removed from the water tank. The heat pipe was emptied from its working fluid and refilled with another one.
11. The rig was ready for another test i.e. the repetition of all the steps from seven to 10.

In summary, the tests on the evacuated heat pipe were conducted for each insert (geometry described in Table 4.5) and the pipe filled with different working fluids: five geometries and six working fluids, resulting in 30 tests.

Table 4.5: Various combinations between geometries and working fluids

Working fluids	Geometries	N insert [NI]	I insert [II]	V insert [VI]	T insert [TI]	S insert [SI]
Distilled water		1	2	3	4	5
Methanol		6	7	8	9	10
Acetone		11	12	13	14	15
Toluene		16	17	18	19	20
Ethanol		21	22	23	24	25
Ethyl acetate		26	27	28	29	30

CHAPTER 5: RESULTS AND DISCUSSION

The experimental results concerning the effect of different working fluids and internal geometries on the thermal performance of a heat pipe in an evacuated tube solar collector are presented in this chapter.

Based on the Faghri and Thomas's (1989) work, different profiles of inserts and working fluids were used in the circular heat pipes in this study, in order to investigate their impact on the performance of an evacuated tube heat pipe solar collector.

Altogether, 30 experiments were performed to test the various configurations of the evacuated tube heat pipe in the solar collector. For the different combinations, a list of the various tests is presented in Table 4.5.

5.1 Tests with the heat pipe containing distilled water

Table 5.1 presents the results obtained from tests 1 to 5 on the evacuated tube with the heat pipe containing distilled water as the working fluid.

Table 5.1: Heat pipe with distilled water

Test N°	Ambient temperature [°C]	Water tank temperature difference [°C]	Evacuated tube heat pipe efficiency η [%]
1	29.1	45.4	53.3
2	28.5	50.4	59.1
3	28.8	51.6	60.6
4	31	51.9	61
5	30.9	54.7	64.3

Figure 5.1 depicts the increase in efficiency of the evacuated tube heat pipe containing distilled water as a working fluid. The increase in efficiency appears to correspond to the geometrical complexity of the insert.

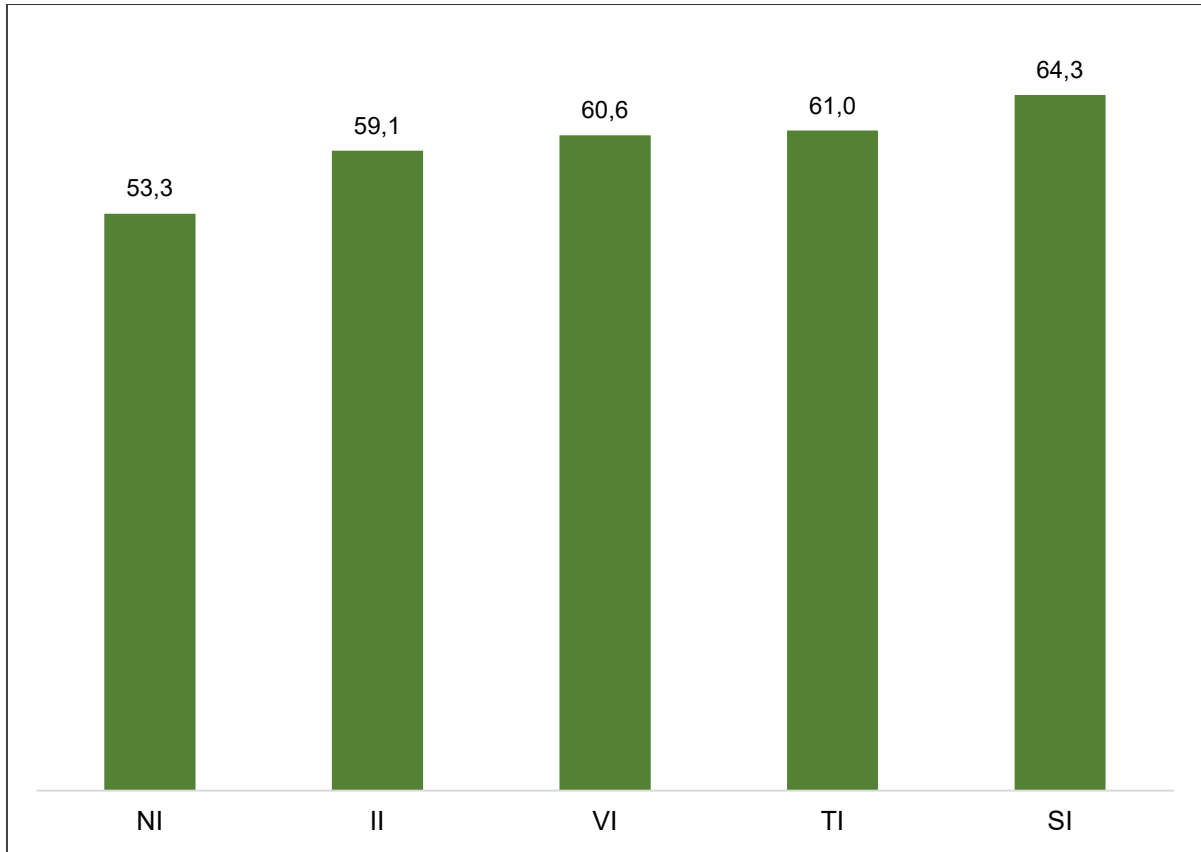


Figure 5.1: Efficiency of the evacuated tube heat pipe containing distilled water for each internal geometry

5.2 Tests with the heat pipe containing methanol

Table 5.2 presents the results obtained during tests 6 to 10 performed on the evacuated tube heat pipe containing methanol.

Table 5.2: Heat pipe with methanol

Test N°	Ambient temperature [°C]	Water tank temperature difference [°C]	Evacuated tube heat pipe efficiency η [%]
6	29.1	44.6	52.4
7	29.4	47.8	56.1
8	28	50	58.7
9	31.1	51.2	60.1
10	30.7	53	62.3

The efficiency for the evacuated tube with the heat pipe containing methanol, for each internal geometry, is illustrated in Figure 5.2. The trend of the efficiency increasing with greater complexity of internal geometry persists.

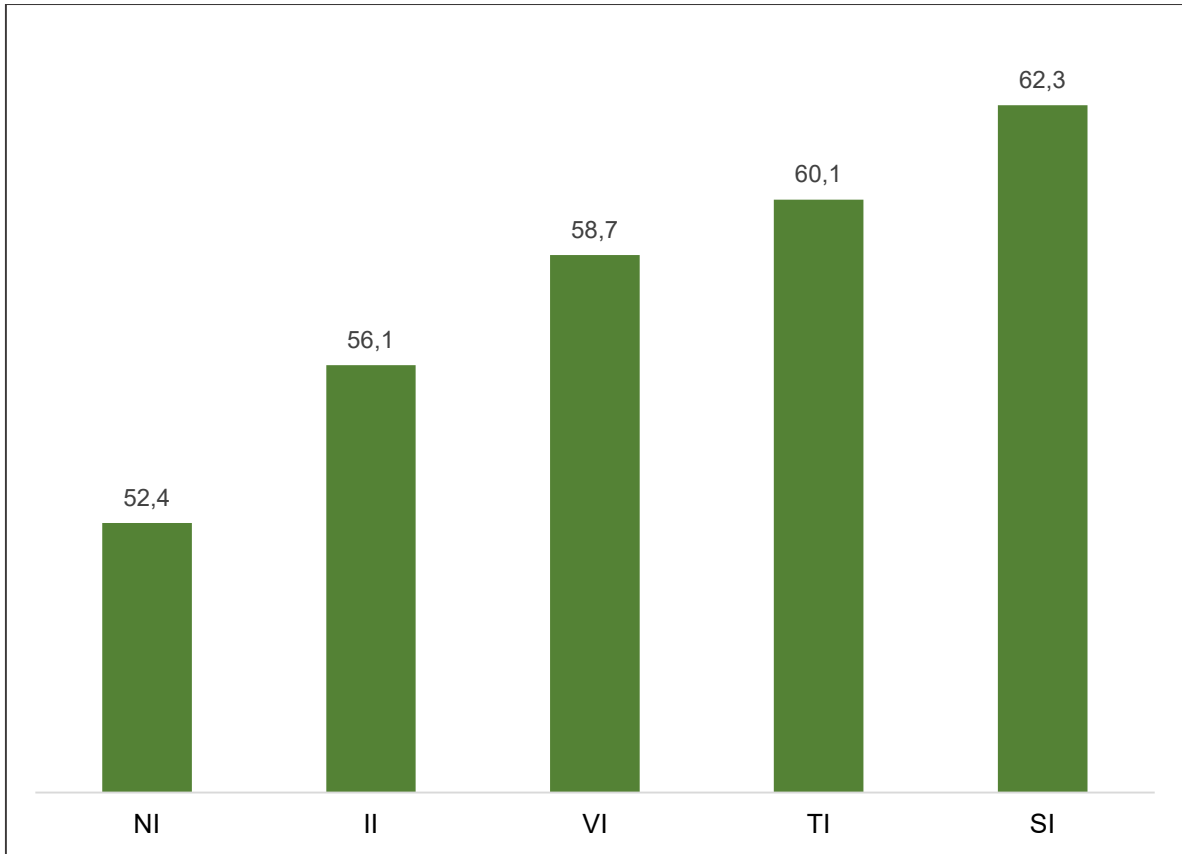


Figure 5.2: Efficiency of the evacuated tube heat pipe containing methanol for each internal geometry

5.3 Tests with the heat pipe containing acetone

Results obtained on the evacuated tube with the heat pipe containing acetone are presented in Table 5.3.

Table 5.3: Heat pipe with acetone

Test N°	Ambient temperature [°C]	Water tank temperature difference [°C]	Evacuated tube heat pipe efficiency η [%]
11	30.4	44.3	52.1
12	30	47.1	55.3
13	31.4	49.2	57.8
14	31.2	50.1	58.9
15	32	52.5	61.7

The efficiency for tests 11 to 15 on an evacuated heat pipe containing acetone is displayed in Figure 5.3. The same tendency of efficiency increase with complex geometries is observed.

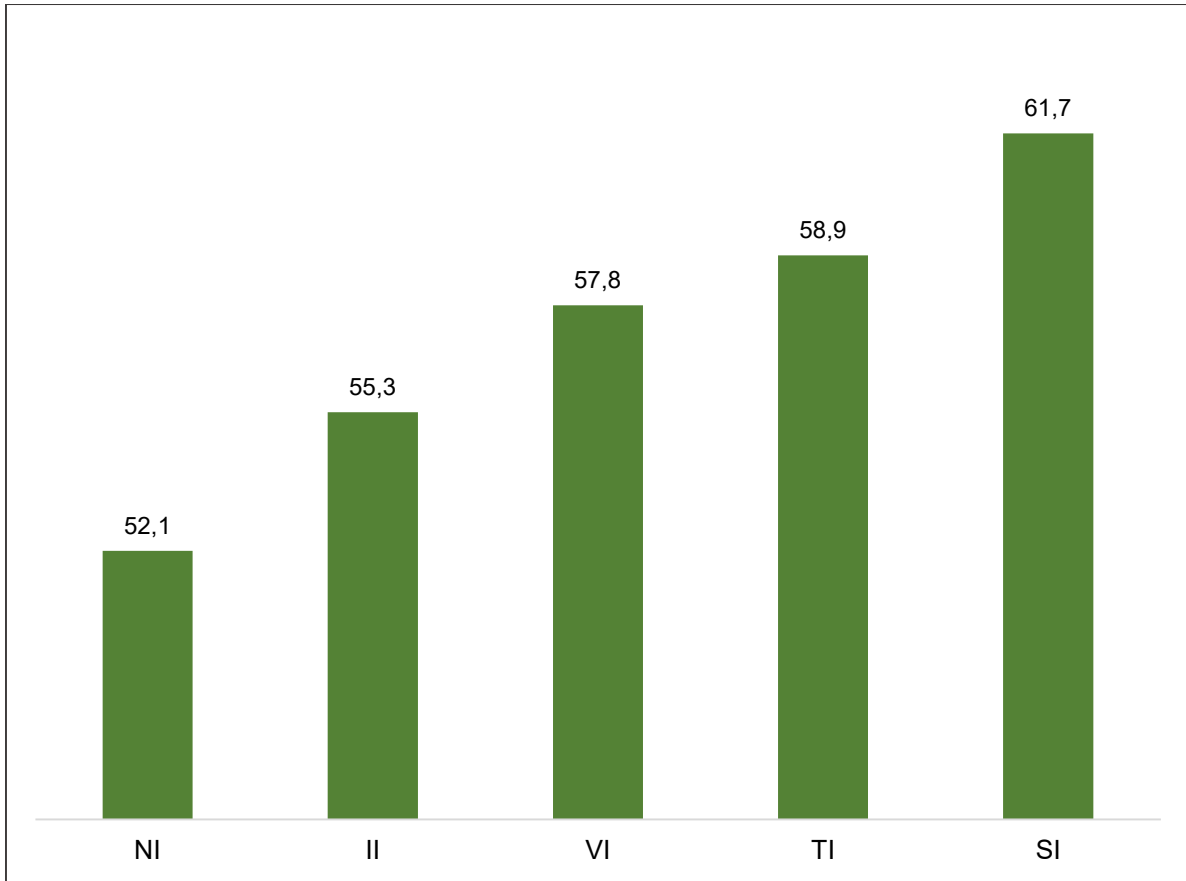


Figure 5.3: Efficiency of the evacuated tube heat pipe containing acetone for each internal geometry

5.4 Tests with the heat pipe containing toluene

Table 5.4 displays the results obtained on the evacuated tube with the heat pipe containing toluene.

Table 5.4: Heat pipe with toluene

Test N°	Ambient temperature [°C]	Water tank temperature difference [°C]	Evacuated tube heat pipe efficiency η [%]
16	30.8	43.3	50.9
17	30.8	46.7	54.9
18	30.4	48.9	57.4
19	27.9	49.9	58.6
20	27.1	51.9	60.9

The efficiency of the evacuated tube with the heat pipe containing toluene, for each internal geometry, is illustrated in Figure 5.4. In a similar manner to the results from the distilled water, acetone and methanol, the efficiency also increased with complexity of internal geometry.

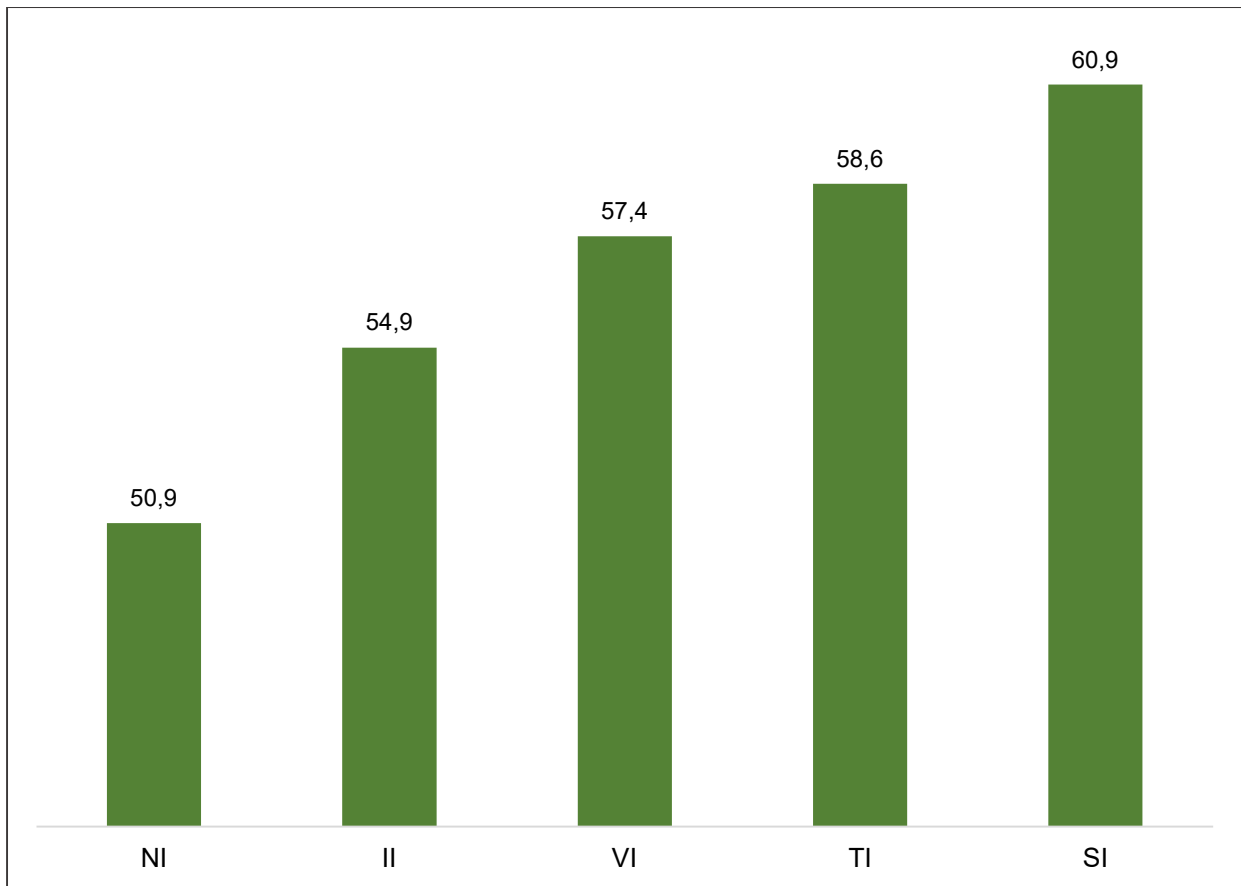


Figure 5.4: Efficiency of the evacuated tube heat pipe containing toluene for each internal geometry

5.5 Tests with the heat pipe containing ethanol

Results obtained on tests 21 to 25 conducted on the heat pipe containing ethanol are presented in Table 5.5.

Table 5.5: Heat pipe with ethanol

Test N°	Ambient temperature [°C]	Water tank temperature difference [°C]	Evacuated tube heat pipe efficiency η [%]
21	30.5	36.8	43.2
22	28.6	39.7	46.6
23	30.3	41.2	48.4
24	30.4	42.5	49.9
25	29.1	42.7	50.2

As illustrated in Figure 5.5, the efficiency of an evacuated tube heat pipe containing ethanol also increased with the complexity of the insert's geometry.

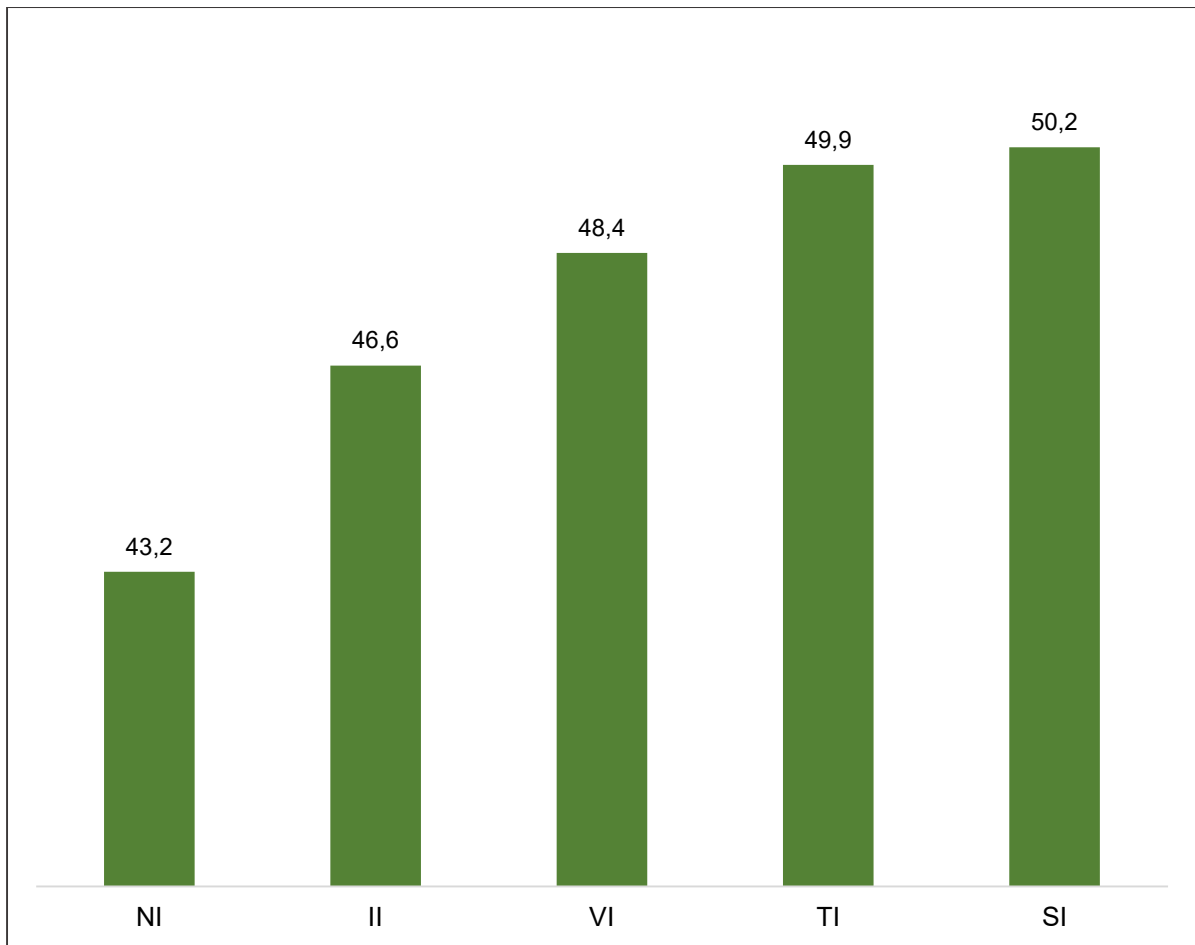


Figure 5.5: Efficiency of the evacuated tube heat pipe containing ethanol for each internal geometry

5.6 Tests with the heat pipe containing ethyl acetate

The results obtained during the tests on the evacuated tube with a heat pipe containing ethyl acetate are displayed in Table 5.6.

Table 5.6: Heat pipe with ethyl acetate

Test N°	Ambient temperature [°C]	Water tank temperature difference [°C]	Evacuated tube heat pipe efficiency η [%]
26	27.7	36.3	42.7
27	30.2	38.1	44.8
28	27.1	41.2	47.6
29	28.2	40.5	48.3
30	29.5	42.5	49.3

The efficiency for the evacuated tube with a heat pipe containing acetate is displayed in Figure 5.6.

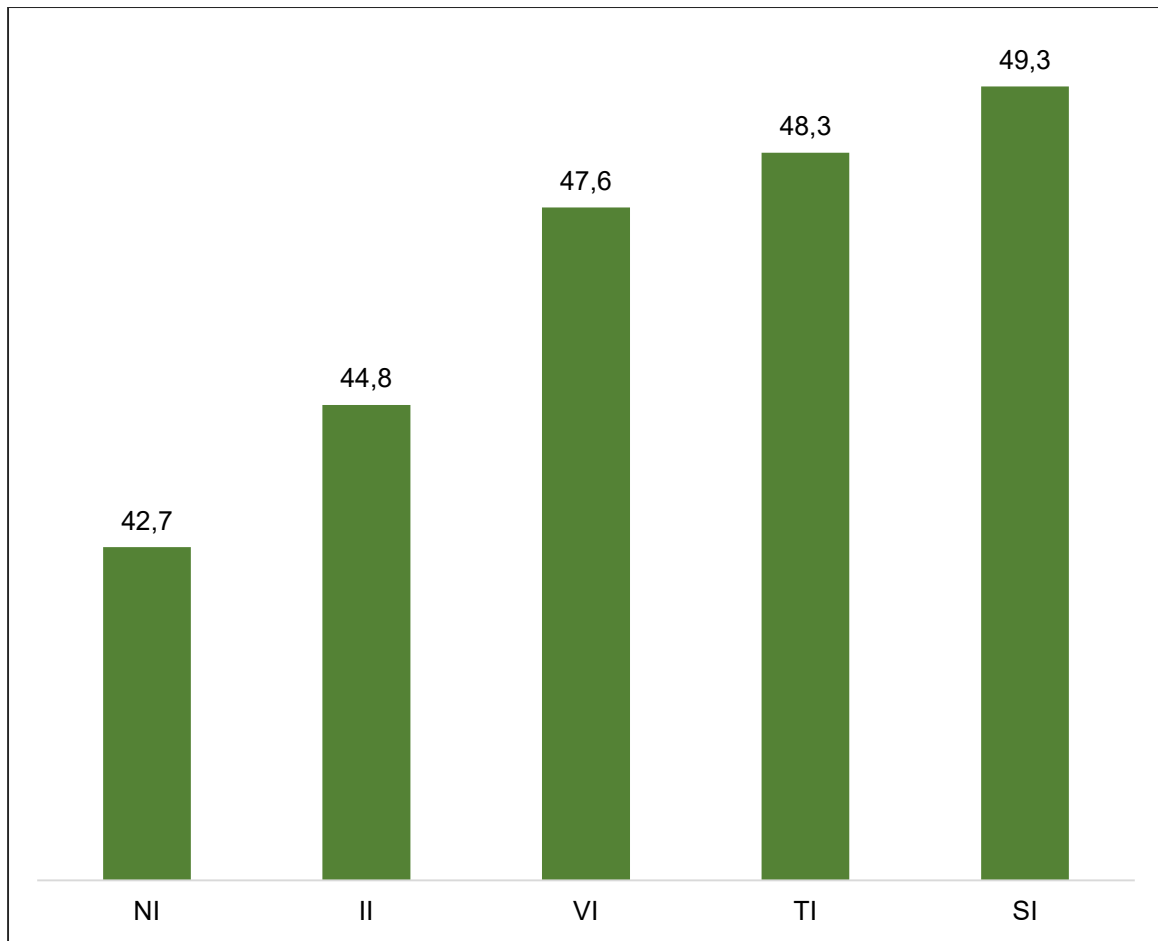


Figure 5.6: Efficiency of the evacuated tube heat pipe containing ethyl acetate for each internal geometry

5.7 Ambient temperature

The ambient temperature was measured because it is an important parameter which could affect the heat loss from the tank to the environment. A low ambient temperature could lower the tank's water temperature difference, which would reflect on the efficiency of the evacuated heat pipe. However, the heat loss from the tank is a function of the surface temperature of the insulation. The heat loss from the tank to the environment happens by radiation and free convection. Losses by radiation depend on the shape factor, material emissivity, and the ambient and tank surface temperatures.

Heat loss by free convection is a function of the convective heat transfer coefficient between the surface of the insulation of the tank and the ambient air, and depends on the Nusselt number. The determination of the Nusselt number is based on the Prandtl and Grashof numbers that involve properties of the ambient air, such as the specific heat capacity, the dynamic viscosity, the thermal conductivity, the density and volumetric expansion, all evaluated at the film temperature, which is the average of the tank's surface temperature and

the ambient air temperature. Figure 5.7 represents the maximum and minimum ambient temperature recorded during the thirty tests. Variations of ambient temperatures are small, and reach a maximum value of 3.7°C. The change in the average temperature between the environment and the tank's surface is smaller, and can be estimated as a maximum of 2°C, hence the impact of the change in the film temperature on the various properties in the Nusselt, Prandtl and Grashof numbers should be insignificant. Therefore, the temperature changes in the ambient air, depicted in Figure 5.7 that were recorded during the testing of the evacuated tube heat pipe with the various inserts were relatively small, and should not have had any considerable impact on the efficiency of the evacuated tube heat pipe solar collector.

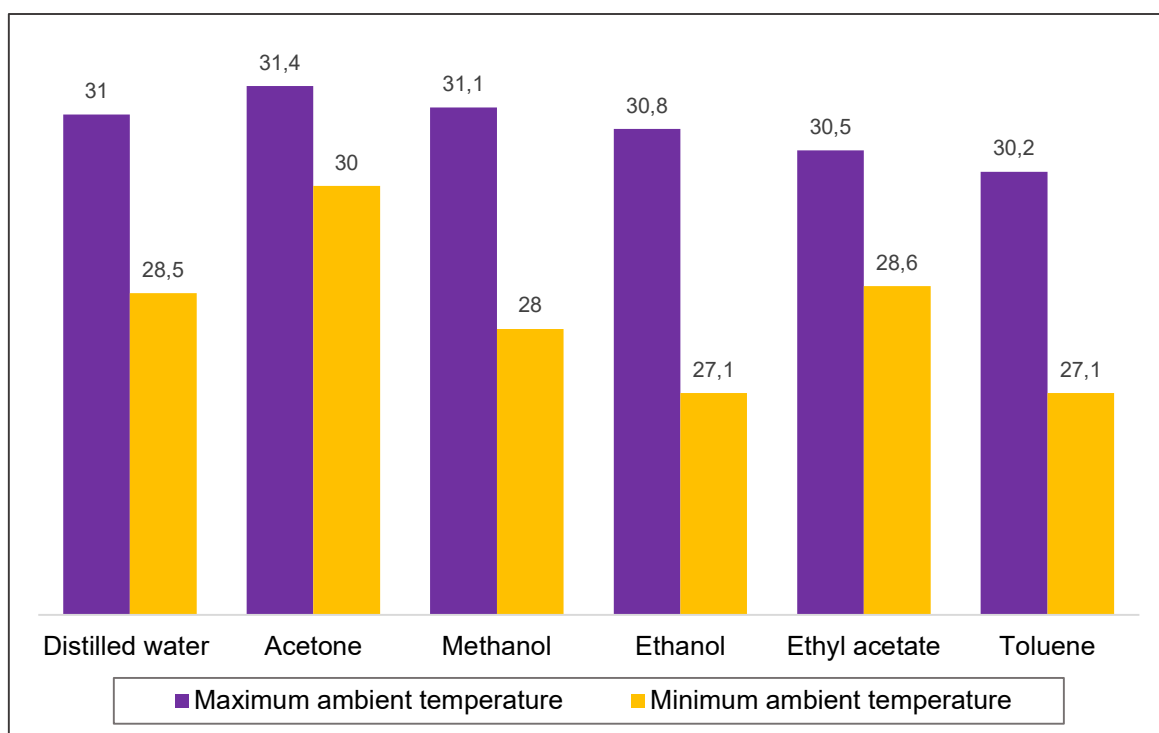


Figure 5.7: Maximum and minimum ambient temperatures during the tests for each working fluid

5.8 Comparison of the efficiency of the evacuated tube heat pipe on the basis of the contained fluid and geometry of the insert

The comparison of the efficiency of the evacuated tube heat pipe (benchmarked on the configuration without an insert) per working fluid and insert geometry is presented in Figure 5.8. It is observed that there is a strong dependence on the working fluid contained in the heat pipe. However, for a heat pipe containing a particular working fluid, thermal efficiency may be enhanced by the geometry of the insert. As explained previously, for the evacuated tube with a heat pipe, the increase in the efficiency was possibly due to the rise in the mass of the heat

pipe and more probably the heat transfer by conduction occasioned by the larger contact area between the insert and circular pipe. However, a point of contact with the circular pipe implies a surface emanating from it, which will transfer heat by convection to the working fluid. More points of contact (hence more insert surface area) produce an increase in the efficiency. For example, for tests 1 to 5, the “no insert” run produced an efficiency of 53.3%, the single insert 59.1% and the S insert (which has a greater mass and four points of contact), 64.3%. This trend of increasing efficiency is noticed with all heat pipes.

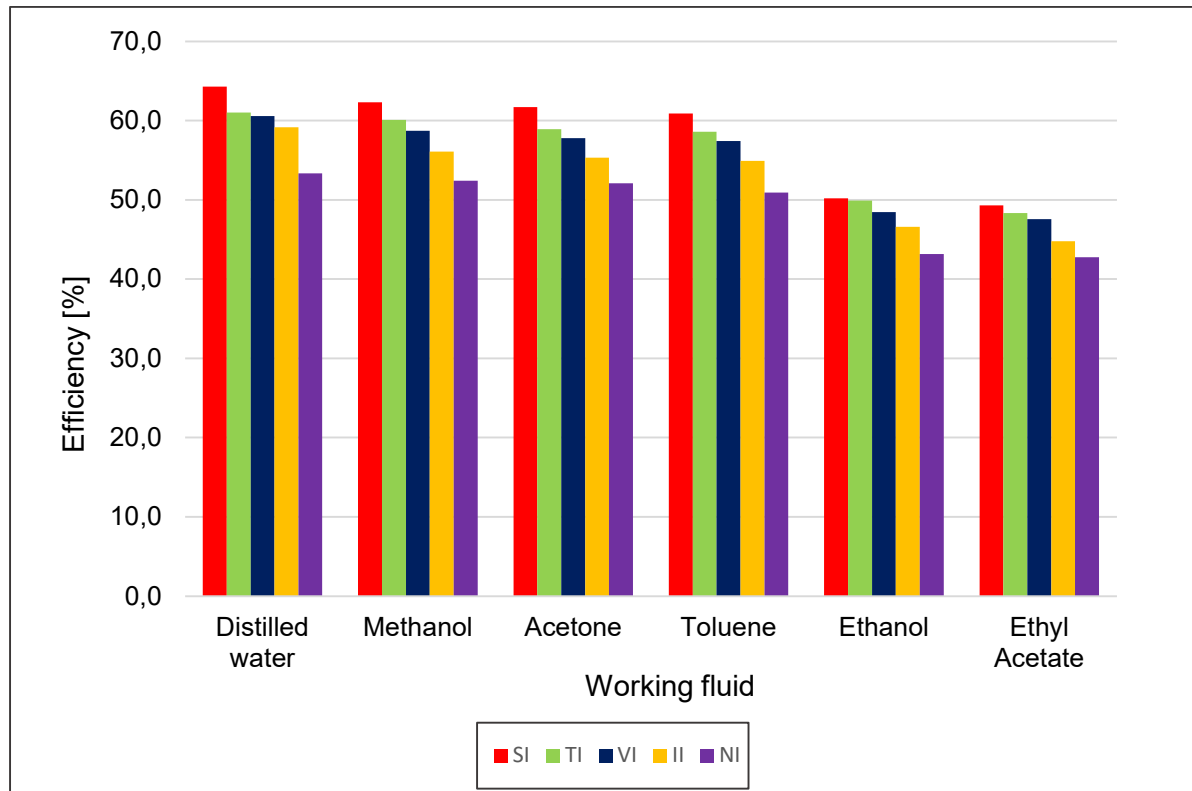


Figure 5.8: Comparison of the efficiency of the evacuated tube heat pipe as a function of its contained fluid and the geometry of its insert

The difference in the levels of efficiency attained by the evacuated tube heat pipe are attributable to the difference in each fluid’s ability to transmit heat, and is related to its merit number, described in detail in Section 3.3.2.2, Chapter 3. The merit number of each working fluid used in this study is displayed in Table 5.7. When compared, the fluid with the maximum efficiency attained during testing is matched by the highest merit number.

The results expressing the efficiency of the evacuated tube heat pipe as a function of the geometry of its insert, correlates with the literature as pointed out in section 3.6.3 showing that the performance characteristics in all the circumstances are better for setup with fin and insert than the normal setup.

5.9 Results of the Multivariate regression analysis

In Section 3.7.1, a model was established for the prediction of the efficiency of the evacuated tube heat pipe as dependent variable, with the parameters relating to the surface area of the insert and the merit number of the working fluid as independent variables.

The impact of the parameter of the internal geometry as one of the independent variables, was the total surface area of the sides of the insert as indicated in table 5.7.

Table 5.7: Surface area of the inserts as the first independent variable

Insert	I insert	V insert	T insert	S insert
Surface area [m ²]	0.0224	0.0426	0.0577	0.0632

The second independent variable affecting the efficiency of the heat pipe was assumed to be the merit number of the working fluid as shown in table 5.8.

Table 5.8: Merit number of the heat pipe as the second independent variable

Working fluid	Merit Number [N/m ²]
Distilled water	3.48E+11
Methanol	4.27E+10
Acetone	3.04E+10
Toluene	2.90E+10
Ethanol	2.71E+10
Ethyl acetate	3.83E+09

Expressing the efficiency of the evacuated tube heat pipe as a function of an insert's surface areas and merit number of the working fluids separately (as detailed in Appendices E1 and E2) indicated that the surface areas of the insert is statistically significant as an independent variable with a $R^2 = 0.89$ and a probability value (p-value) of 0.01 below 0.05 defined as the significance level for the analysis. However, the use of the merit number yielded a regression with a $R^2 = 0.52$ with a p-value of 0.1 which makes the merit number statistically not significant for the thermal efficiency of the heat pipe.

5.9.1 Efficiency of the evacuated heat pipe as a function of both the merit number and the surface area of the insert

With y as dependent variable representing the evacuated tube heat pipe's efficiency, x_1 as the surface area of the insert's geometry and x_2 as the merit number of the working fluid, yielded the following equation:

$$y = 117.45x_1 + 3.006\ln x_2 - 22.5 \quad (5.1)$$

The multivariate regression analysis linking the efficiency with merit number and area of the insert (as detailed in Appendix E3) however indicated a very poor correlation with a low value of $R^2 = 0.59$, with a p-value for the merit number of 0.56 higher than the significance level of 0.05 making the merit number not statistically significant as an independent variable for the efficiency of the evacuated tube heat pipe. Also, the analysis presents high values of residuals reaching 12% as it displayed in table 5.9.

Table 5.9: Results of the difference and percentage of error between experimental and predicted values of the evacuated tube heat pipe efficiency expressed as a function of the merit number and the surface number of the insert

Insert	Working fluid	Measured Y	Predicted Y	Residuals	Error [%]
II	Ethyl Acetate	44.8	46.4	-1.6	-3.5
	Ethanol	46.6	52.3	-5.7	-10.9
	Toluene	54.9	51.4	3.5	6.9
	Acetone	55.3	52.6	2.7	5.1
	Methanol	56.1	53.6	2.5	4.6
	Distilled water	59.1	59.9	-0.8	-1.3
VI	Ethyl Acetate	47.6	48.8	-1.2	-2.5
	Ethanol	48.4	54.6	-6.2	-11.4
	Toluene	57.4	53.7	3.7	6.8
	Acetone	57.8	55.0	2.8	5.1
	Methanol	58.7	56.0	2.7	4.8
	Distilled water	60.6	62.3	-1.7	-2.8
TI	Ethyl Acetate	48.3	50.5	-2.2	-4.3
	Ethanol	49.9	56.4	-6.5	-11.6
	Toluene	58.6	55.5	3.1	5.6
	Acetone	58.9	56.8	2.1	3.8
	Methanol	60.1	57.8	2.3	4.0
	Distilled water	61.0	64.1	-3.1	-4.8
SI	Ethyl Acetate	49.3	51.2	-1.9	-3.7
	Ethanol	50.2	57.1	-6.9	-12.1
	Toluene	60.9	56.2	4.7	8.5
	Acetone	61.7	57.4	4.3	7.5
	Methanol	62.3	58.4	3.9	6.6
	Distilled water	64.3	64.7	-0.4	-0.7

In the literature about heat pipes, it is shown that the merit number may also be seen as an indicator of the temperature range that the heat pipe should operate (see figure 3.3 Byon, 2016). The heat pipes containing distilled water (the highest merit number) were exposed to irradiance high enough to vaporize the working fluid and transmit the heat to its destination. In heat pipes with lower merit number, the working fluid vaporized at lower temperature and perhaps some of the excessive heat available superheated the vapour. However lower heat must have been acquired from what was available at the source to be delivered to its

destination, which obviously affects adversely the thermal efficiency of the device when compared to one operating at a higher temperature range. The efficiency does not depend on the merit number directly but perhaps on a newly thought/assumed parameter such as the boiling point of the working fluid (Mago et. Al., 2007).

During the experiments, the lowest pressure that could be obtained when preparing the heat pipes was 2.3 KPa. Table 5.10 depicts each working fluid's absolute pressure at its triple point and the actual pressure used during the preparation of the heat pipes. The last column in table 5.10 indicates the corresponding boiling point of the working fluid based on the manufacturing pressure of the heat pipe.

Table 5.10: Boiling point temperature of the working fluid inside the actual heat pipes

Working fluid	Pressure (triple point) (absolute) [Pa]	Actual Pressure [KPa]	Boling point [K]
Water	611	2.3	289,2
Methanol	0.183	2.3	269,4
Acetone	2.32	2.3	264,3
Toluene	0.039	2.3	266,4
Ethanol	0.000 43	2.3	244,0
Ethyl Acetate	0.003	2.3	224,1

Example of the calculation of the boiling point for water using the Antoine's equation (De Nevers, 2012) is shown In Appendix D3.

The regression analysis expressing the efficiency of the evacuated tube heat pipe as a function of the boiling point only (as detailed in Appendix E4) indicates that the boiling point of the working fluid is statistically significant in the correlation with a $R^2 = 0.99$ and all the p-values below 0.05.

5.9.2 Efficiency of the evacuated heat pipe as a function of the working fluid's boiling point and surface area of the insert

In view of the very poor correlation that was indicated between the heat pipe's efficiency as the dependent variable, being influenced by the previously assumed independent variables namely the merit number of the working fluid and the surface area of the insert, a new multivariate regression analysis was performed. Replacing one of the independent variables namely the merit number, with the boiling point temperature for the working fluid.

A multivariate polynomial regression analysis (as detailed in Appendix E5) was performed which yielded the following equation:

$$y = 117.45x_1 - 0.00023x_2^3 + 0.179x_2^2 - 45.73x_2 + 3886.5844 \quad (5.2)$$

The regression equation 5.2 has a $R^2 = 0.98$. Considering a level of $R^2 = 0.95$ appropriate for regression analysis, equation 5.2 is accepted with confidence. The multivariate regression analysis indicates that the p-values for x_1 (surface area of the insert) is $3.94 \cdot 10^{-9}$, while the p-value for x_2 , x_2^2 and x_2^3 (boiling point) are $6.38 \cdot 10^{-8}$, $5.24 \cdot 10^{-8}$ and $5.022 \cdot 10^{-8}$ respectively. As p-values are below the significance level of 0.05, statistically all independent variables are significant for the model.

Using the regression equation and taking the results of the measured values of the efficiency for each working fluid as encountered in Figures 5.1 to 5.6, their differences and respective percentage errors are displayed in Table 5.11. The comparison between the measured and the predicted results yielded an average error of 1.1% (from equally mixed over and underestimated values).

Table 5.11: Results of the difference and percentage of error between experimental and predicted values of the evacuated tube heat pipe's efficiency expressed as a function of the temperature of the boiling point of the working fluid and the surface area of the insert

Insert	Working fluid	Measured Y	Predicted Y	Residuals	Error [%]
II	Ethyl Acetate	44.8	44,6	0,1	0,3
	Ethanol	46.6	46,1	0,5	1,1
	Toluene	54.9	55,6	-0,7	-1,3
	Acetone	55.3	54,8	0,6	1,0
	Methanol	56.1	56,7	-0,6	-1,1
	Distilled water	59.1	58,4	0,7	1,3
VI	Ethyl Acetate	47.6	47,0	0,6	1,2
	Ethanol	48.4	48,4	0,0	0,0
	Toluene	57.4	58,0	-0,6	-1,0
	Acetone	57.8	57,1	0,7	1,1
	Methanol	58.7	59,1	-0,4	-0,7
	Distilled water	60.6	60,8	-0,2	-0,3
TI	Ethyl Acetate	48.3	48,8	-0,4	-0,9
	Ethanol	49.9	50,2	-0,3	-0,6
	Toluene	58.6	59,8	-1,2	-2,0
	Acetone	58.9	58,9	0,0	0,0
	Methanol	60.1	60,9	-0,8	-1,3
	Distilled water	61.0	62,5	-1,5	-2,5
SI	Ethyl Acetate	49.3	49,4	-0,1	-0,3
	Ethanol	50.2	50,9	-0,7	-1,3
	Toluene	60.9	60,4	0,5	0,8
	Acetone	61.7	59,6	2,1	3,6
	Methanol	62.3	61,5	0,8	1,3
	Distilled water	64.3	63,2	1,1	1,8

5.9.3 Final predictive equation of heat pipe efficiency

By replacing the working fluid's merit number with its boiling point temperature, an acceptable regression equation 5.2, was obtained. Limitation in the increase of the efficiency could be due to numerous constraints to the heat transfer in a heat pipe such as capillary limit, sonic

limit, boiling limit, entrainment limit and viscous limit, briefly repeated here for convenience, but presented in more detail in Chapter 3, section 3.4.1.

CHAPTER 6: CONCLUSION AND RECOMMENDATIONS

Motivated by the global desire to reduce the usage of traditional energy resources, this investigation was performed with the aim of improving the thermal performance of the evacuated tube heat pipe solar collector. The work involved the analysis of the effect that different working fluids and inserts of different geometries have on the thermal performance of heat pipes in evacuated tube solar collectors. Broad conclusions and some recommendations are presented below.

6.1 Conclusions

Modified heat pipes containing inserts with a range of different geometrical profiles were designed and manufactured. They were used to determine the impact of the geometry of the inserts on the thermal performance of the evacuated tube solar collector. Various working fluids were selected based on varying merit numbers in order to investigate the impact of the thermophysical properties of each working fluid on the performance of the evacuated heat pipe solar collector.

The experimental measurements were performed by combining the internal geometry from five inserts and the use of six working fluids that were selected encompassing heat pipe operating temperature range between 200K and 500K.

Considering the effect of the thermophysical properties of the working fluid, as a parameter represented by the merit number, and the surface area of the insert as a second independent variable, the efficiency of the evacuated tube heat pipe solar collector was measured by a series of experiments.

A predictive multivariate polynomial regression equation was developed, using the results from the experiments.

The results obtained are summarised as follows:

- During the tests performed on the evacuated tube heat pipe with various inserts and each working fluid, the temperature changes in the ambient air were small and did not have any substantial impact on the efficiency of the evacuated tube heat pipe.
- The working fluid with the higher merit number has also the high thermal performance for all the inserts.
- The regression analysis that resulted from the assumption that the merit number and the surface of the insert were the independent variables affecting the heat pipe's

efficiency had to be rejected due poor/unacceptably low coefficient of determination (R^2) result.

- From the literature, it was evident that the merit number serves to indicate the suitable temperature range that a heat pipe should operate based, on its working fluid (see figure 3.3, Byon, 2016).
- The effect of the surface area of the insert was proven to impact on the efficiency of the evacuated heat pipe for each working fluid, enhancing the heat transfer by convection between the surfaces of the insert and the vapor moving from the evaporator to the condenser.
- Based on a newly thought assumption, that the boiling point temperature of the working fluid could be an independent variable affecting the heat pipe's performance or efficiency, a new regression analysis produced very acceptable results.
- The comparison between the measured and the predicted results using the multivariate polynomial regression which yielded equation 5.2 exhibits excellent accuracy in the prediction of the performance of an evacuated heat pipe solar collector. It may be of assistance in predicting the heat pipe's efficiency for any untested insert's profile or working fluid's boiling temperature or a combination of both.

6.2 Recommendations for future work

- To possibly enhance the liquid/vapour movement and hence the internal rate of heat transfer, an insert with wick structures on the surfaces could be considered.
- Different filling ratios of a chosen working fluid contained in the heat pipe may have an impact, together with the surface area of the insert, on the thermal performance of the evacuated tube heat pipe solar collector.

REFERENCES

- Abd-Elhady, M.S., Nasreldin, M. & Elsheikh, M.N. 2018. Improving the performance of evacuated tube heat pipe collectors using oil and foamed metals. *Ain Shams Engineering Journal*, 9(4):2683-2689.
- Ahmed, N.Z., Singh, P.K., Janajreh, I. & Shatilla, Y. 2011. January. Simulation of flow inside heat pipe: sensitivity study, conditions and configuration. In *Energy Sustainability* (Vol. 54686, pp. 1219-1228).
- Ahmed, N.Z., Singh, P.K., Janajreh, I. and Shatilla, Y., 2011, January. Simulation of flow inside heat pipe: sensitivity study, conditions and configuration. *Energy Sustainability*, 54686:1219-1228.
- Aladejare, S.A. 2014. Energy, growth and economic development: A case study of the Nigerian electricity sector. *American Journal of Business, Economics and Management*, 2(2):41-54.
- Alammar, A.A., Al-Dadah, R.K. & Mahmoud, S.M. 2016. Numerical investigation of effect of fill ratio and inclination angle on a thermosiphon heat pipe thermal performance. *Applied Thermal Engineering*, 108:1055-1065.
- Alhabeeb, B.A., Kadhim, T.J., Hashim, H.T. & Mohammed, H.N. 2020. Enhancement of the Thermal Efficiency of the Evacuated Tubes Solar Water Heater by Adding a Reflector. *International Energy Journal*, 20(1).
- Andrzejczyk, R. 2019. Experimental Investigation of the Thermal Performance of a Wickless Heat Pipe Operating with Different Fluids: Water, Ethanol, and SES36. Analysis of Influences of Instability Processes at Working Operation Parameters. *Energies*, 12(1):80.
- Arab, M. & Abbas, A. 2014. A model-based approach for analysis of working fluids in heat pipes. *Applied Thermal Engineering*, 73(1):751-763.
- Ayompe, L.M. & Duffy, A. 2013. Thermal performance analysis of a solar water heating system with heat pipe evacuated tube collector using data from a field trial. *Solar Energy*, 90:17-28.
- Ayompe, L.M., Duffy, A., Mc Keever, M., Conlon, M. & McCormack, S.J. 2011. Comparative field performance study of flat plate and heat pipe evacuated tube collectors (ETCs) for domestic water heating systems in a temperate climate. *Energy*, 36(5):3370-3378.
- Azad, E. 2018. Experimental analysis of thermal performance of solar collectors with different numbers of heat pipes versus a flow-through solar collector. *Renewable and Sustainable Energy Reviews*, 82:4320-4325.
- Babu, N.N. & Kamath, H. 2015. Materials used in Heat Pipe. *Materials Today: Proceedings*, 2(4-5):1469-1478.
- Banovčan, R., Novomestský, M., Vantúch, M., Kapjor, A. & Nemeč, P. 2018. Methods of filling the heat pipes. *MATEC Web of Conferences*, 168. EDP Sciences.
- Bilgili, M., Ozbek, A., Sahin, B. & Kahraman, A. 2015. An overview of renewable electric power capacity and progress in new technologies in the world. *Renewable and Sustainable Energy Reviews*, 49:323-334.

- Bokopane, L., Kusakana, K. & Vermaak, H.J. 2014. Hybrid System Configurations and Charging Strategies for Isolated Electric Tuk-Tuk Charging Station in South Africa. *International Journal of Electrical and Computer Engineering*, 8(11):1671-1676.
- Boo, J.H., Park, S.Y. & Kim, D.H. 2005. An experimental study on the thermal performance of a concentric annular heat pipe. *Journal of Mechanical Science and Technology*, 19(4):1036-1043.
- Brahim, T., Dhaou, M.H. & Jemni, A. 2014. Theoretical and experimental investigation of plate screen mesh heat pipe solar collector. *Energy Conversion and Management*, 87:428-438.
- businesstech.co.za. 2020. *South Africa drops nuclear energy plan*. [ONLINE] Available at: <https://businesstech.co.za/news/energy/267581/south-africa-drops-nuclear-energy-plan/>. [Accessed 18 June 2020].
- Byon, C. 2016. Heat pipe and phase change heat transfer technologies for electronics cooling. *Electronics Cooling*, p. 31.
- Catherine, Q., Wheeler, J., Wilkinson, R. & de Jager, G. 2012. Hot water usage profiling to improve geyser efficiency. *Journal of Energy in Southern Africa*, 23(1):39-45.
- Chamoli, S. 2013. Exergy analysis of a flat plate solar collector. *Journal of Energy in Southern Africa*, 24(3), pp.08-13.
- Chamsa-ard, W., Sukchai, S., Sonsaree, S. & Sirisamphanwong, C. 2014. Thermal performance testing of heat pipe evacuated tube with compound parabolic concentrating solar collector by ISO 9806-1. *Energy Procedia*, 56:237-246.
- Cheng, H.Y., Yu, C.C., Hsu, K.C., Chan, C.C., Tseng, M.H. & Lin, C.L. 2019. Estimating Solar Irradiance on Tilted Surface with Arbitrary Orientations and Tilt Angles. *Energies*, 12(8):1427.
- Chi, S.W. 1976. *Heat pipe theory and practice*. Washington, DC, Hemisphere Publishing Corp.; New York, McGraw-Hill Book Co.
- De Nevers, N., 2012. *Physical and chemical equilibrium for chemical engineers*. Hoboken, NJ: Wiley.
- Dhingra, D., 2014. Thermo-physical Property Models and Effect on Heat Pipe Modelling.
- Di Paola, R. 2010. *Research on non-conventional working fluids for space and terrestrial heat pipes* (Doctoral dissertation, Università degli studi di Napoli Federico II).
- Du, B., Hu, E. & Kolhe, M., 2013. An experimental platform for heat pipe solar collector testing. *Renewable and Sustainable Energy Reviews*, 17:119-125.
- Dunn, P. & Reay, D. 2016. *Heat pipes*. Elsevier.
- El-Nasr, A.A. & El-Haggar, S.M. 1996. Effective thermal conductivity of heat pipes. *Heat and Mass transfer*, 32(1-2):97-101.
- Energy, W., 2014. The Socio-economic Benefits of Solar and Wind Energy.
- Ersöz, M.A. 2016. Effects of different working fluid use on the energy and exergy performance for evacuated tube solar collector with thermosyphon heat pipe. *Renewable Energy*, 96:244-256.
- Eskom, S.O.C. 2017. Eskom Integrated Report. *Eskom*. Available online: http://www.eskom.co.za/IR2017/Documents/Eskom_integrated_report_2017.pdf [Accessed 12 April 2018].

- Eskom, S.O.C. (Ltd). 2016. Integrated Report. *Eskom*. Available online: http://www.eskom.co.za/IR2016/Documents/Eskom_integrated_report_2016.pdf [Accessed 12 April 2018].
- Faghri, A., 1989. Performance characteristics of a concentric annular heat pipe: Part 2-Vapor flow analysis. *Journal of Heat Transfer (Transactions of the ASME (American Society of Mechanical Engineers), Series C);(United States)*, 111(4).
- Faghri, A. 2014. Heat pipes: review, opportunities and challenges. *Frontiers in Heat Pipes (FHP)*, 5(1).
- Falayi, E. & Rabi, A. 2012. Solar Radiation Models and Information for Renewable Energy Applications. *Solar radiation*. Available at: [http://cdn.intechopen.com/pdfs/33347/InTech-Solar radiation models and information for renewable energy applications.pdf](http://cdn.intechopen.com/pdfs/33347/InTech-Solar_radiation_models_and_information_for_renewable_energy_applications.pdf).
- Franchi, G. & Huang, X. 2008. Development of composite wicks for heat pipe performance enhancement. *Heat Transfer Engineering*, 29(10):873-884.
- Gaugler, R.S. Motors Liquidation Co, 1944. *Heat transfer device*. U.S. Patent 2,350,348.
- Groll, M. 2014. Heat pipe science and technology: A historical review. *Heat Pipe Science and Technology, an International Journal*, 5(1-4).
- Grover, G., Cotter, T. & Erickson, G., 1964. Erratum: Structures of Very High Thermal Conductance. *Journal of Applied Physics*, 35(10), pp.3072-3072.
- Harikrishnan, S.S. & Kotebavi, V. 2016, September. Performance study of solar heat pipe with different working fluids and fill ratios. In *IOP Conference Series: Materials Science and Engineering*, 149(1):012224. IOP Publishing.
- Hukseflux.com. 2020. *Pyrheliometer*. [ONLINE] Available at: <https://www.hukseflux.com/applications/solar-energy-pv-system-performance-monitoring/what-is-a-pyrheliometer>. [Accessed 25 July 2020].
- Indiamart.com. 2020. Services-of-solar-water-heater. [ONLINE] Available at: <https://www.indiamart.com/proddetail/services-of-solar-water-heater-17572877888.html>. [Accessed 19 July 2020].
- Inglesi, R. & Pouris, A. 2010. Forecasting electricity demand in South Africa: A critique of Eskom's projections. *South African Journal of Science*, 106(1-2):50-53.
- Iqbal M. 1983. *An introduction to solar radiation*, 1st ed. Academic Press: New York.
- Jafarkazemi, F. & Abdi, H. 2012. Evacuated tube solar heat pipe collector model and associated tests. *Journal of Renewable and Sustainable Energy*, 4(2):023101.
- Jafarkazemi, F., Ahmadifard, E. & Abdi, H. 2016. Energy and exergy efficiency of heat pipe evacuated tube solar collectors *Thermal Science*, 20(1):327-335.
- Jäger, K.D., Isabella, O., Smets, A.H., van Swaaij, R.A. & Zeman, M. 2016. *Solar energy: fundamentals, technology and systems*. UIT Cambridge.
- Jasvanth, V.S., Ambirajan, A., Kumar, D. and Arakeri, J.H., 2013. Effect of heat pipe figure of merit on an evaporating thin film. *Journal of thermophysics and heat transfer*, 27(4):633-640.
- Jesko, Ž. 2008. Classification of solar collectors. *rN*, 1(21):21.
- Jouhara, H., Chauhan, A., Nannou, T., Almahmoud, S., Delpech, B. & Wrobel, L.C. 2017. Heat pipe-based systems-Advances and applications. *Energy*, 128:729-754.

- Jouhara, H., Khordehgah, N., Almahmoud, S., Delpech, B., Chauhan, A. & Tassou, S.A. 2018. Waste heat recovery technologies and applications. *Thermal Science and Engineering Progress*, 6:268-289.
- Kabeel, A.E., Dawood, M.M.K. & Shehata, A.I. 2017. Augmentation of thermal efficiency of the glass evacuated solar tube collector with coaxial heat pipe with different refrigerants and filling ratio. *Energy Conversion and Management*, 138, pp.286-298.
- Khobai, H., Mugano, G. & Le Roux, P. 2017. The impact of electricity price on economic growth in South Africa. *International Journal of Energy Economics and Policy*, 7(1):108-116.
- Kocer, A., Atmaca, I. & Ertekin, C. 2015. A comparison of flat plate and evacuated tube solar collectors with f-chart method. *Journal of Thermal Science and Technology*, 35(1):77-86.
- Korn, F. 2008. Heat pipes and its applications. *Heat and Mass Transport, Project Report*.
- Kuroda, M., Chang, J.Y., Gwin, P., Mongia, R., Kim, C.U., Cabusao, G.P., Goto, K. & Mochizuki, M. 2014. Development of aluminum-water heat pipes. *Heat Pipe Science and Technology, An International Journal*, 5(1-4).
- Lin, W.K., Chao, C.I., Tzou, Y.M., Hsu, G.H. & Chou, S.M. 2011. *Effect of the Vacuum Pressure and the Working Fluid Inventory to the Maximum Heat Loading (Q_{max}) of the Heat Pipe*.
- Lips, S., Sartre, V., Lefevre, F., Khandekar, S. and Bonjour, J. 2016. Overview of Heat Pipe Studies during the Period 2010–2015. *Interfacial Phenomena and Heat Transfer*, 4(1).
- Liu, Y. 2016, January. Principle, Application and Development of Heat Pipe Technology. *2016 International Conference on Civil, Transportation and Environment*. Atlantis Press.
- Lysko, M.D., 2006. *Measurement and models of solar irradiance*.
- Ma, J. & Koutsougeras, C. 2015. Effects of Design Parameters on the Fluid Flow and the Efficiency of Single Ended Evacuated Tubular Solar Thermal Collectors via FEM Modelling and Experimentation. *Engineering Journal*, 19(5):69-80.
- Mago, P.J., Chamra, L.M. and Somayaji, C., 2007. Performance analysis of different working fluids for use in organic Rankine cycles. Proceedings of the Institution of Mechanical Engineers, Part A: Journal of Power and Energy, 221(3), pp.255-263.
- Magurean, A.M., Pop, O.G., Pocola, A.G., Serban, A. & Balan, M.C. 2019. Einstein's Equation in Nuclear and Solar Energy. In *Thermodynamics and Energy Engineering*. IntechOpen.
- Mamimaran, R., Palaniradja, K., Alagumurthi, J., Wisnoe, W. & Hussain, J. 2012. Factors affecting the thermal performance of heat pipe a review. *Journal of Engineering Research and Studies*, 3(2): 20-24.
- Manton, A. 2015. Solar Energy: A Renewable Resource with Global Importance. *ESSAI*, 13(1):26.
- Maraj, A., Londo, A., Firat, C. & Gebremedhin, A. 2019. Comparison of the Energy Performance between Flat-plate and Heat Pipe Evacuated Tube Collectors for Solar Water Heating Systems under Mediterranean Climate Conditions. *Journal of Sustainable Development of Energy, Water and Environment Systems*, 7(1):87-100.

- Margaris, D.P., Diamantis, Z.G., Photeinos, D.I. & Tsahalis, D.T. 2007. Performance of heat pipes as capillary pumps: modelling and comparison with experimental results. *International Journal of Low-Carbon Technologies*, 2(2):149-161.
- Meinel, A.B. & Meinel, M.P. 1977. Applied solar energy: an introduction. *STIA*, 77:33445.
- Meteo. 2020. *Pyranometer*. [ONLINE] Available at: <https://www.atmos-meteo.com/sensors/pyranometer.html>. [Accessed 26 July 2020].
- Miloştean, D. & Flori, M. 2017. An overview on the flat-plate solar collectors and their thermal efficiency. *Annals of the Faculty of Engineering Hunedoara*, 15(4)123-128.
- Morrison, G.L., Budihardjo, I. & Behnia, M. 2004. Water-in-glass evacuated tube solar water heaters. *Solar energy*, 76(1-3):135-140.
- Mozumder, A.K., Akon, A.F., Chowdhury, M.S.H. & Banik, S.C. 2010. Performance of heat pipe for different working fluids and fill ratios. *Journal of Mechanical Engineering*, 41(2):96-102.
- Mujawar, N.H. & Shaikh, S.M. 2016. Thermal performance investigation of evacuated tube heat pipe solar collector with nanofluids. *Int. J. Eng. Sci. Res. Tech*, 5:824-837.
- Mustaffar, A., Phan, A.N., Reay, D. & Boodhoo, K. 2019. Concentric annular heat pipe characterisation analysis for a drying application. *Applied Thermal Engineering*, 149:275-286.
- Mwaba, M.G., Huang, X. & Gu, J. 2006. Influence of wick characteristics on heat pipe performance. *International Journal of Energy Research*, 30(7):489-499.
- Nemec, P., Caja, A. & Malcho, M. 2011. Thermal performance measurement of heat pipe. *Global Journal of Technology and Optimization*, 2(1).
- Nouri-Borujerdi, A. & Layeghi, M. 2005. A review of concentric annular heat pipes. *Heat Transfer Engineering*, 26(6):45-58.
- Observa-dome. 2020. *summer-heat-NASAs-mission-to-touch-the-sun*. [ONLINE] Available at: <https://observa-dome.com/summer-heat-nasas-mission-to-touch-the-sun/>. [Accessed 24 July 2020].
- Olia, H., Torabi, M., Bahiraei, M., Ahmadi, M.H., Goodarzi, M. & Safaei, M.R. 2019. Application of nanofluids in thermal performance enhancement of parabolic trough solar collector: state-of-the-art. *Applied Sciences*, 9(3):463.
- Omer, A.M. 2008. Energy, environment and sustainable development. *Renewable and Sustainable Energy Reviews*, 12(9):2265-2300.
- Pachghare, P. & Mahalle, A. 2013. Thermal performance of closed loop pulsating heat pipe using pure and binary working fluids. *Frontiers in heat pipes (FHP)*, 3(3).
- Parmar, R.B. & Bhojak, K. 2016. Performance of an evacuated tube collector with heat pipe technology. *International Journal of Engineering Research and General Science*, 4(3):71-89.
- Perkins, J. *Boilers of Locomotive and other steam engines*, 1838. Steam boiler water-tube. US Patent 1,034.
- Peyghambarzadeh, S.M., Shahpouri, S., Aslanzadeh, N. & Rahimnejad, M. 2013. Thermal performance of different working fluids in a dual diameter circular heat pipe. *Ain Shams Engineering Journal*, 4(4)855-861.

- Rahman, M.L., Sultan, R.A., Islam, T., Hasan, N.M. & Ali, M. 2015. An experimental investigation on the effect of fin in the performance of closed loop pulsating heat pipe (CLPHP). *Procedia Engineering*, 105:137-144.
- Reay, D., McGlen, R. & Kew, P. 2013. *Heat pipes: theory, design and applications*. Butterworth-Heinemann.
- Riffat, S. & Ma, X. 2007. Recent developments in heat pipe technology and applications: a review. *International Journal of Low-carbon Technologies*, 2(2):162-177.
- Sabiha, M.A., Saidur, R., Mekhilef, S. & Mahian, O. 2015. Progress and latest developments of evacuated tube solar collectors. *Renewable and Sustainable Energy Reviews*, 51:1038-1054.
- Savino, R. & Paterna, D. 2006. Marangoni effect and heat pipe dry-out. *Physics of Fluids*, 18(11):118103.
- Sayigh, A.A.M. ed. 2012. *Solar energy engineering*. Elsevier.
- Seshan, S. & Vijayalakshmi, D. 1986. Heat pipes—concepts, materials and applications. *Energy conversion and management*, 26(1):1-9.
- Shafieian, A., Khiadani, M. & Nosrati, A. 2018. A review of latest developments, progress, and applications of heat pipe solar collectors. *Renewable and Sustainable Energy Reviews*, 95:273-304.
- Shafieian, A., Khiadani, M. & Nosrati, A. 2019. Thermal performance of an evacuated tube heat pipe solar water heating system in cold season. *Applied Thermal Engineering*, 149:644-657.
- Shehadi, M., 2019. Experimental Investigation of Pipe Heating Enhancement using Different Number of Internal Fins.
- Sinha, P. 2013. Multivariate polynomial regression in data mining: methodology, problems and solutions. *International Journal of Scientific and Engineering Research*, 4(12):962-965.
- Siuta-Olcha, A., Cholewa, T. & Dopieralska-Howoruszko, K. 2020. Experimental Studies of Thermal Performance of An Evacuated Tube Heat Pipe Solar Collector in Polish Climatic Conditions. *Environmental Science and Pollution Research*, 1-10.
- Solarpanelsplus.com. 2020. *Evacuated-Tube-Collectors*. [ONLINE] Available at: <http://www.solarpanelsplus.com/evacuated-tube-collectors/>. [Accessed 14 July 2020].
- Solcoast.com. 2020. *Go-solar-by-november-8th-and-save-big*. [ONLINE] Available at: <http://www.solcoast.com/go-solar-by-november-8th-and-save-big/>. [Accessed 18 June 2020].
- Sonawane, P.M., Shende, M.D. & Baisane, V.P. 2016. Effect of nanofluids on heat pipe thermal performance: a review of the recent literature. *International Journal of Engineering and Applied Sciences*, 3(1).
- South Africa. Department of Mineral Resources and Energy. 2019. *Integrated Resource Plan*. Pretoria: Government Printer.
- Sukhatme, S.P. & Nayak, J.K. 2017. *Solar Energy*. McGraw-Hill Education.
- Sureshkumar, R., Mohideen, S.T. & Nethaji, N. 2013. Heat transfer characteristics of nanofluids in heat pipes: a review. *Renewable and Sustainable Energy Reviews*, 20:397-410.

- Szabó, L. 2017. The History of Using Solar Energy. Paper presented at the 7th International Conference, *Modern Power Systems* (MPS, 2017).
- Tian, Y. & Zhao, C.Y. 2013. A review of solar collectors and thermal energy storage in solar thermal applications. *Applied energy*, 104:538-553.
- Veldman, E., Gibescu, M., Slootweg, H. & Kling, W.L. 2011, June. Impact of electrification of residential heating on loading of distribution networks. In *2011 IEEE Trondheim PowerTech* (pp. 1-7). IEEE.
- Vijra, N. & Singh, T.P. 2015. An experimental study of thermal performance of concentric annular heat pipe. *American Int. J. Research in Sci, Tech, Eng, and Math*, 9:176-182.
- Weiss, W. & Spörk-Dür, M. 2018. Solar Heat Worldwide—Global Market Development and Trends in 2017—Detailed Market Figures 2016. *International Energy Agency Solar Heating and Cooling Programme [Verkköjulkaisu][Viitattu 18.6. 2018] Saatavissa: [http://www. iea-shc.Org/Data/Sites/1/publications/Solar-Heat-Worldwide-2018](http://www.iea-shc.Org/Data/Sites/1/publications/Solar-Heat-Worldwide-2018). Pdf.*
- Winkler, H. 2007. Energy policies for sustainable development in South Africa. *Energy for sustainable Development*, 11(1):26-34.
- Yang, F., Yuan, X. & Lin, G. 2003. Waste heat recovery using heat pipe heat exchanger for heating automobile using exhaust gas. *Applied Thermal Engineering*, 23(3):367-372.
- Yogi Goswami, D. 1998. Solar thermal power technology: present status and ideas for the future. *Energy Sources*, 20(2):137-145.
- Zawilska, E. & Brooks, M.J. 2011. An assessment of the solar resource for Durban, South Africa. *Renewable Energy*, 36(12):3433-3438.
- Zenplumb - Natural Plumbing Systems. 2021. *Zenplumb - Natural Plumbing Systems-Solar Hot Water*. [online] Available at: <<https://www.zenplumb.com/solar-hot-water>> [Accessed 11 June 2021].
- Zohuri, B. 2019. Basic Principles of Heat Pipes and History. In *Heat Pipe Applications in Fission Driven Nuclear Power Plants* (pp. 161-202). Springer, Cham.
- Zuo, Z.J. & Faghri, A. 1998. A network thermodynamic analysis of the heat pipe. *International Journal of Heat and Mass Transfer*, 41(11):1473-1484.

APPENDICES

APPENDIX A: Detailed description of equipment and measuring instruments

1. 8-Slot, TSN-Enabled Ethernet Compact DAQ Chassis

The 8-slot Ethernet Compact DAQ chassis, shown in Figure A.1, was used with LabVIEW as data logger for the collection of data during the experiments. It has the following specifications:

Precise synchronised timing over the network with TSN, providing tightly synchronised measurements for accurate analysis.

Easily scale systems with an integrated network switch for simple daisy-chaining.

Supports more than 60 sensor-specific I/O modules with integrated signal conditioning.

Four general-purpose 32-bit counter/timers built into chassis.

Run up to 7 hardware-timed analogue I/O, digital I/O, or counter/timer operations simultaneously.

Built-in SMB connection for external clocks and triggers (up to 1 MHz).

Reliable operation in harsh environments with -40 °C to 70 °C operating temperature range, shock resistance up to 50 g and vibration resistance up to 5 g.

Hazardous Locations certification.

Input/output Voltage Protection

Voltage	Minimum	Maximum
Input	-20V	25V
Output	-15V	20V

Maximum Operating Conditions

I_{OL} output low current	8 mA maximum
I_{OH} output high current	-8 mA maximum

DC Input Characteristics

Voltage	Minimum	Maximum
Positive going threshold	1.43V	2.28V
Negative going threshold	0.86V	1.53V
Hysteresis	0.48V	0.83V

DC Output Characteristics

Voltage	Conditions	Minimum	Maximum
High	x	x	5.25V
	Sourcing 100 μ A	4.65V	x
	Sourcing 2 mA	3.60V	x

	Sourcing 3.5 mA	3.44V	x
Low	Sourcing 100 μ A	x	0.10 V
	Sourcing 2 mA	x	0.64 V
	Sourcing 3.5 mA	x	0.80 V



Figure A.1:1. 8-Slot, TSN-Enabled Ethernet Compact DAQ Chassis

2. NI 9211C Series Temperature Input Module

During experiments, the connection between the data logger and the temperature sensors was ensured by the NI 9211C Series Temperature Input Module represented in Figure A.2

Power Requirements

Power consumption from chassis	
Active mode	170 mW max
Sleep mode.....	4 mW max
Thermal dissipation (at 70 °C)	
Active mode	170 mW max Sleep
mode.....	4 mW max



Figure A.2:2. NI 9211C Series Temperature Input Module

3. 400 W FLOOD LIGHT

The solar simulator was composed of the 400W flood light and a single-sided holder, as shown in Figure A.3.

Model: ACDC model: df-250hps-s

Product Description

Product name: Metro 400w metal fitting
material used: Imported reflector of high quality with high tensile iron
power: 400w
Single-sided holder
Waterproof IP65

Technical Details

Manufacturer	Plusrite
Part Number	2406
Product Dimensions	2.54 x 2.54 x 6.86 cm; 90.72 Grams
Item model number	2406
Shape	T15
Wattage	400.00
Item Package Quantity	1
Included Components	Plusrite 02406 - MH400/T15/HOR/10K 2406 400-watt Metal Halide Light Bulb
Batteries Required?	No
Item Weight	90.7 g



Figure A.3 Solar simulator

4. TDGC2 /TSGC2 VOLTAGE REGULATORS

For the variation of voltage on the solar simulator, voltage regulator TDGC2 (shown in Figure A.4) was used.

Specifications

Model	Rated capacity kVA	Phase number	Rated frequency Hz	Rated input(V) voltage	Output voltage scope(V)	Rated output current(A)
TDGC2-0.5	0.5	1	50	220	0-250	2
TDGC -12	1	1	50	220	0-250	4
TDGC -22	2	1	50	220	0-250	8
TDGC -32	3	1	50	240	0-260	12
TDGC -52	5	1	50	220	0-250	20
TDGC -102	10	1	50	220	0-250	40
TDGC -152	15	1	50	220	0-250	60
TDGC -202	20	1	50	220	0-250	80
TDGC -302	30	1	50	220	0-250	120

Service conditions

- Ambient temperature: the maximum temperature is +40°C, the minimum temperature is -5°C.
- Sea level elevation: The sea level elevation of the installation place of the voltage regulator cannot be more than 1000m.
- Air relative humidity: The monthly relative humidity of the wettest month is 90%. Simultaneously the average temperature of the month is 25°C.
- Line-voltage wave form: The line-voltage wave form is sinusoidal wave, or approximates the sinusoidal wave.
- There is no gas, steam, chemical deposition, dust and dirt that can seriously affect the insulation of the voltage regulator and other explosive and erosive medium in the installation location.
- There is no serious vibration in the installation place.
- Use indoors.
- It is not allowed to be used in parallel connection.



Figure A.4: Voltage regulator TDGC2

5. Power meter NanoVIP plus

The power meter represented in Figure A.5 was used for the measurement of voltage, current and power during the experiments.

GENERAL TECHNICAL DATA

- Inputs:

Voltmeter: (L1-N) max 600 Vrms up to 600 Hz.

Ammeter: 1 Volt up to 600 Hz.

- Number of scales:

3 voltage scales; 3 current scales.

- Automatic scale change:

Scale change response time: 1 sec. max

Passage to the scale above takes place at 105% of the scale in use

Passage to the scale below takes place at 20% of the scale in use

Instrument dimensions: 80x175x32.5 mm (without cover)

Instrument weight: 500 g

Kit weight: 1,1Kg. (Without instrument)

SERVICE AND TESTING CONDITIONS

- Ambient operating conditions:

Ambient temperature range: from -10°C to +50°C

Relative humidity range (R.H.): from 20% to 80%

- Storage temperature: from -20°C to +60°C

- Condensation: not permitted

- Reference standards: IEC 348, VDE 411 class 2, for operating

Voltages - 600 VAC RMS, IEC 1010 600 V CAT III,

EMC: EN50081-1, EN 50082-2, EN55022

POWER SUPPLY

4 x 15V batteries (size AA)



Figure A.5: Power meter NanoVIP plus

6. An MT 942 light meter

The light meter shown in Figure A.6 was used to measure the global irradiance from the solar simulator.

Features

- Professional light meter providing quick light readings in Lux
- 4000 Count LCD display with a 41-segment bar graph
- Measures to 400 000 Lux
- 4 Measuring ranges
- Peak Hold
- Relative mode
- Min/Max
- Data Hold
- Short rise and fall time
- Data logging up to 99 readings
- USB interface

GENERAL SPECIFICATIONS

Function	Range
Light Source	Tungsten/Daylight
Selecting	Fluorescent 0-9 select rating
Measuring Range	40, 400, 4000 40000, 400 000 Lux 40, 400, 4000 40 000-foot candle
Accuracy	+/- 3 % (calibrate to standard) incandescent lamp 2856 K and corrected LED day white-light spectrum) +/- 6% other visible light source
Display	4000 count
Battery life	9V Battery
Size (HxWxD)	160 x 58x27mm
Weight	280g



Figure A.6: MT 942 light meter

7. Vacuum pump

The Vacuum in the heat pipe was created using the vacuum pump N 035 AN.18 IP 20-Motor, shown in Figure A.7

Specifications

	N 035 AN.18 IP 20-Motor
Flow (l/min) ¹	30
Ultimate vacuum (mbar abs.)	100
Operating pressure (bar g)	4
Connectors for tube (mm)	ID 9
Gas permissible ambient temperature	+5...+40 °C
Voltage/Frequency	230V/50Hz
Motor protection	IP 20

Power P1	220 W
Current	1 To
Weight	8.2 kg
Dimensions [length x height x width (mm)]	265/254/143



Figure A.7: Vacuum pump N 035 AN.18 IP 20-Motor

APPENDIX B: Data collected during the heat pipe tests for various internal geometries and working fluids

1. Data collected during the heat pipe containing distilled water test

Time [min]	NI		II		VI		TI		SI	
	Amb temp	Water temp	Amb temp	Water temp	Amb temp	Water temp	Amb temp	Water temp	Amb temp	Water temp
0.0	26.5	31.1	25.4	28.1	27.4	28.5	27.4	27.7	28.3	28.7
5.0	26.7	32.6	25.5	29.1	27.3	28.8	27.6	28.3	28.4	29.5
10.0	27.1	32.9	25.7	30.5	27.2	29.5	27.8	29.0	28.6	30.4
15.0	27.2	33.3	26.0	31.8	27.3	30.3	27.9	30.0	28.7	31.1
20.0	27.3	33.6	26.2	32.5	27.5	30.8	28.1	30.8	29.0	31.8
25.0	27.4	34.0	26.3	33.2	27.6	31.1	28.3	31.8	29.4	32.3
30.0	27.5	34.3	26.5	34.2	27.6	31.5	28.5	32.3	29.7	32.6
35.0	27.6	34.7	26.7	34.5	27.7	32.0	28.7	32.9	30.1	33.2
40.0	27.6	35.1	26.8	34.9	28.0	32.5	28.8	33.4	30.3	33.7
45.0	27.6	35.6	27.0	35.4	28.1	33.2	29.0	34.0	30.6	34.3
50.0	27.8	35.9	27.1	35.9	28.1	33.9	29.2	34.7	30.7	34.8
55.0	27.8	36.3	27.2	36.5	28.2	34.5	29.5	35.3	30.8	35.6
60.0	27.9	36.7	27.3	37.2	28.3	35.2	30.0	36.0	30.8	36.4
65.0	27.9	37.2	27.4	37.8	28.4	35.9	30.2	36.8	30.8	37.2
70.0	28.1	37.6	27.5	38.4	28.6	36.6	30.9	37.5	30.9	38.0
75.0	28.1	38.0	27.6	39.0	28.6	37.3	30.7	38.2	30.9	38.9
80.0	28.2	38.5	27.7	39.7	28.7	38.0	30.7	38.9	31.0	39.7
85.0	28.3	39.0	27.8	40.3	28.7	38.7	30.8	39.6	31.0	40.5
90.0	28.3	39.4	27.8	40.9	28.8	39.4	30.9	40.4	31.0	41.4
95.0	28.4	39.9	27.9	41.6	28.9	40.6	31.1	41.1	31.0	42.2
100.0	28.4	40.3	28.0	42.2	28.9	41.5	31.3	41.9	31.1	43.0
105.0	28.4	40.9	28.1	42.8	29.0	42.2	31.6	42.6	31.1	43.8
110.0	28.5	41.4	28.2	43.4	29.0	42.9	31.7	43.3	31.1	44.6
115.0	28.5	42.0	28.2	44.0	29.0	43.6	31.7	44.1	31.1	45.4
120.0	28.5	42.6	28.2	44.6	29.0	44.4	31.7	44.8	31.1	46.2
125.0	28.6	43.3	28.2	45.2	29.1	45.0	31.7	45.5	31.1	46.9
130.0	28.6	43.9	28.3	45.9	29.2	45.8	31.7	46.2	31.1	47.7
135.0	28.6	44.6	28.3	46.5	29.3	46.4	31.6	47.0	31.1	48.5
140.0	28.7	45.6	28.4	47.1	29.3	47.1	31.7	47.7	31.1	49.3
145.0	28.7	46.2	28.4	47.7	29.3	47.8	31.7	48.4	31.1	50.0
150.0	28.8	46.7	28.5	48.3	29.3	48.5	31.7	49.1	31.1	50.8
155.0	28.8	47.3	28.5	48.9	29.2	49.2	31.7	49.8	31.1	51.5
160.0	28.8	47.8	28.5	49.5	29.3	49.9	31.7	50.5	31.1	52.3
165.0	28.8	48.3	28.5	50.1	29.3	50.5	31.6	51.2	31.1	53.0
170.0	28.9	48.9	28.5	50.7	29.3	51.2	31.7	51.9	31.1	53.7
175.0	29.0	49.4	28.5	51.3	29.4	51.8	31.7	52.5	31.1	54.4
180.0	29.0	49.9	28.6	51.9	29.5	52.5	31.7	53.2	31.1	55.1

185.0	29.0	50.5	28.6	52.4	29.4	53.1	31.7	53.9	31.1	55.9
190.0	29.1	51.0	28.7	53.0	29.4	53.7	31.7	54.5	31.1	56.6
195.0	29.2	51.6	28.8	53.6	29.4	54.4	31.7	55.2	31.1	57.3
200.0	29.2	52.2	28.9	54.2	29.4	55.0	31.7	55.8	31.2	58.0
205.0	29.3	52.7	28.9	54.8	29.3	55.6	31.7	56.5	31.2	58.6
210.0	29.4	53.2	29.0	55.3	29.4	56.3	31.8	57.1	31.2	59.3
215.0	29.4	53.8	29.0	55.9	29.4	56.9	31.7	57.7	31.2	60.0
220.0	29.5	54.4	29.0	56.4	29.3	57.5	31.7	58.4	31.2	60.7
225.0	29.5	54.9	29.1	57.0	29.2	58.1	31.6	58.9	31.2	61.3
230.0	29.6	55.4	29.2	57.6	29.3	58.7	31.6	59.6	31.2	62.0
235.0	29.6	56.0	29.3	58.1	29.2	59.3	31.6	60.1	31.3	62.6
240.0	29.6	56.4	29.3	58.7	29.2	59.9	31.6	60.7	31.3	63.2
245.0	29.6	57.0	29.4	59.2	29.3	60.5	31.6	61.3	31.3	63.9
250.0	29.6	57.5	29.4	59.8	29.2	61.1	31.5	61.9	31.3	64.5
255.0	29.6	58.1	29.4	60.3	29.3	61.7	31.6	62.5	31.3	65.2
260.0	29.6	58.5	29.4	60.8	29.2	62.2	31.6	63.0	31.3	65.8
265.0	29.7	59.0	29.4	61.4	29.2	62.8	31.6	63.6	31.3	66.4
270.0	29.6	59.5	29.5	61.9	29.3	63.3	31.5	64.2	31.3	67.0
275.0	29.8	60.0	29.6	62.4	29.3	63.9	31.6	64.7	31.3	67.6
280.0	29.7	60.5	29.6	62.9	29.2	64.4	31.5	65.3	31.3	68.2
285.0	29.8	61.0	29.6	63.4	29.2	65.0	31.5	65.9	31.3	68.8
290.0	29.8	61.4	29.6	64.0	29.1	65.5	31.3	66.4	31.3	69.3
295.0	29.8	62.0	29.6	64.5	29.1	66.1	31.5	67.0	31.3	69.9
300.0	29.8	62.4	29.6	65.0	29.0	66.6	31.4	67.5	31.2	70.5
305.0	29.8	62.9	29.5	65.5	29.2	67.2	31.5	68.1	31.1	71.0
310.0	29.9	63.4	29.5	66.0	29.1	67.7	31.5	68.6	31.3	71.6
315.0	30.0	63.9	29.5	66.5	29.0	68.2	31.4	69.2	31.3	72.1
320.0	30.0	64.3	29.4	67.0	29.1	68.8	31.4	69.7	31.3	72.7
325.0	30.1	64.8	29.4	67.5	29.1	69.3	31.4	70.2	31.2	73.2
330.0	30.1	65.3	29.4	68.0	28.9	69.8	31.5	70.8	31.3	73.8
335.0	30.2	65.7	29.4	68.5	28.9	70.3	31.4	71.3	31.3	74.3
340.0	30.2	66.2	29.3	68.9	29.0	70.9	31.4	71.8	31.3	74.9
345.0	30.2	66.6	29.3	69.4	29.0	71.3	31.4	72.3	31.3	75.4
350.0	30.1	67.1	29.2	69.9	28.8	71.9	31.3	72.9	31.3	75.9
355.0	30.1	67.5	29.3	70.4	29.0	72.4	31.3	73.4	31.2	76.4
360.0	30.1	68.0	29.2	70.8	28.9	72.9	31.3	73.9	31.2	77.0
365.0	30.1	68.3	29.2	71.3	29.0	73.4	31.2	74.4	31.2	77.5
370.0	30.0	68.8	29.1	71.7	28.8	73.8	31.2	74.9	31.2	78.0
375.0	30.1	69.2	28.9	72.2	28.6	74.3	31.2	75.4	31.1	78.5
380.0	30.2	70.1	29.0	72.7	28.5	74.8	31.2	75.9	31.1	79.1
385.0	30.1	70.8	28.9	73.2	28.4	75.3	31.2	76.4	30.9	79.6
390.0	30.1	71.4	28.9	73.6	28.4	75.8	31.1	76.9	30.8	79.9
395.0	30.1	72.1	28.8	74.0	28.4	76.3	31.0	77.4	30.8	80.4
400.0	30.1	72.8	28.8	74.8	28.4	76.7	31.4	77.9	30.6	80.9

405.0	30.1	73.8	28.8	75.5	28.4	77.4	31.4	78.4	30.5	81.6
410.0	30.0	75.0	28.7	76.3	28.7	78.7	31.4	78.9	30.5	82.2
415.0	30.0	75.9	28.7	77.0	28.6	79.3	31.4	79.5	30.4	83.4
420.0	30.0	76.5	28.6	78.4	28.6	80.1	31.5	79.6	30.4	83.5

2. Data collected during the heat pipe containing methanol test

Time [min]	NI		II		VI		TI		SI	
	Amb temp	Water temp	Amb temp	Water temp	Amb temp	Water temp	Amb temp	Water temp	Amb temp	Water temp
0.0	26.4	28.7	26.5	29.6	25.5	28.6	27.1	29.0	27.3	28.7
5.0	26.6	29.1	26.7	29.9	25.6	28.9	27.3	29.3	27.4	28.9
10.0	26.7	29.4	26.6	30.1	25.7	29.1	27.6	29.5	27.5	29.1
15.0	26.9	29.8	26.7	30.8	25.9	29.4	27.8	29.8	27.7	29.5
20.0	27.0	30.1	26.9	31.5	26.0	29.7	27.9	30.1	27.9	29.8
25.0	27.1	30.5	27.0	32.2	26.1	30.0	28.2	30.5	28.1	30.1
30.0	27.3	30.8	27.1	33.2	26.2	30.4	29.7	31.0	28.3	30.4
35.0	27.5	31.2	27.2	33.5	26.3	30.9	30.1	31.6	29.9	31.0
40.0	27.6	31.6	27.3	33.9	26.5	31.4	30.4	32.1	30.1	31.5
45.0	27.8	32.1	27.4	34.4	26.6	32.1	31.2	32.7	30.6	32.1
50.0	27.9	32.4	27.5	34.9	26.8	32.8	30.7	33.4	31.2	32.6
55.0	27.9	32.8	27.6	35.5	26.9	33.4	30.4	34.0	30.8	33.4
60.0	28.1	33.2	27.7	36.2	27.1	34.1	30.4	34.7	30.6	34.2
65.0	28.1	33.7	27.8	36.8	27.3	34.8	30.4	35.5	30.5	35.0
70.0	28.2	34.1	27.9	37.4	27.3	35.5	30.6	36.2	30.5	35.8
75.0	28.2	34.5	27.9	38.0	27.6	36.2	30.8	36.9	30.6	36.7
80.0	28.4	35.0	28.0	38.7	27.6	36.9	31.0	37.6	30.8	37.5
85.0	28.5	35.5	28.0	39.3	27.8	37.6	31.2	38.3	30.9	38.3
90.0	28.6	35.9	28.1	39.9	27.8	38.3	31.4	39.1	31.1	39.2
95.0	28.6	36.4	28.2	40.6	27.9	39.5	31.4	39.8	31.2	40.0
100.0	28.7	36.8	28.2	41.2	28.0	40.4	31.4	40.6	31.1	40.8
105.0	28.8	37.4	28.3	41.8	28.0	41.1	31.5	41.3	31.1	41.6
110.0	28.9	37.9	28.4	42.4	28.0	41.8	31.5	42.0	31.1	42.4
115.0	29.0	38.5	28.5	43.0	28.1	42.5	31.5	42.8	31.1	43.2
120.0	29.0	39.1	28.6	43.6	28.1	43.3	31.6	43.5	31.1	44.0
125.0	29.0	39.8	28.7	44.2	28.2	43.9	31.6	44.2	31.1	44.7
130.0	29.1	40.4	28.8	44.9	28.3	44.7	31.6	44.9	31.1	45.5
135.0	29.2	41.1	28.8	45.5	28.3	45.3	31.7	45.7	31.1	46.3
140.0	29.1	42.1	29.0	46.1	28.3	46.0	31.7	46.4	31.1	47.1
145.0	29.1	42.7	29.1	46.7	28.3	46.7	31.7	47.1	31.1	47.8
150.0	29.1	43.2	29.2	47.3	28.3	47.4	31.7	47.8	31.1	48.6
155.0	29.2	43.8	29.2	47.9	28.3	48.1	31.8	48.5	31.1	49.3
160.0	29.4	44.3	29.3	48.5	28.4	48.8	31.7	49.2	31.0	50.1
165.0	29.3	44.8	29.4	49.1	28.4	49.4	31.8	49.9	31.1	50.8
170.0	29.3	45.4	29.5	49.7	28.4	50.1	31.9	50.6	31.1	51.5
175.0	29.3	45.9	29.5	50.3	28.4	50.7	31.8	51.2	31.1	52.2

180.0	29.5	46.4	29.6	50.9	28.6	51.4	31.8	51.9	31.1	52.9
185.0	29.4	47.0	29.7	51.4	28.6	52.0	31.8	52.6	31.1	53.7
190.0	29.5	47.5	29.8	52.0	28.4	52.6	31.8	53.2	31.2	54.4
195.0	29.5	48.1	29.8	52.6	28.5	53.3	31.9	53.9	31.2	55.1
200.0	29.5	48.7	29.9	53.2	28.5	53.9	31.9	54.5	31.2	55.8
205.0	29.5	49.2	29.9	53.8	28.6	54.5	31.9	55.2	31.1	56.4
210.0	29.5	49.7	29.9	54.3	28.4	55.2	31.9	55.8	31.1	57.1
215.0	29.6	50.3	30.0	54.9	28.5	55.8	31.8	56.4	31.1	57.8
220.0	29.7	50.9	30.0	55.4	28.6	56.4	31.8	57.1	31.1	58.5
225.0	29.7	51.4	30.1	56.0	28.6	57.0	31.8	57.6	31.0	59.1
230.0	29.6	51.9	30.2	56.6	28.6	57.6	31.8	58.3	31.1	59.8
235.0	29.7	52.5	30.2	57.1	28.5	58.2	31.7	58.8	31.0	60.4
240.0	29.7	52.9	30.3	57.7	28.5	58.8	31.6	59.4	31.0	61.0
245.0	29.7	53.5	30.3	58.2	28.5	59.4	31.7	60.0	31.0	61.7
250.0	29.8	54.0	30.3	58.8	28.6	60.0	31.6	60.6	31.0	62.3
255.0	29.8	54.6	30.4	59.3	28.5	60.6	31.7	61.2	31.0	63.0
260.0	29.8	55.0	30.4	59.8	28.5	61.1	31.7	61.7	31.0	63.6
265.0	29.8	55.5	30.4	60.4	28.5	61.7	31.6	62.3	31.1	64.2
270.0	29.8	56.0	30.5	60.9	28.5	62.2	31.7	62.9	31.0	64.8
275.0	29.9	56.5	30.6	61.4	28.5	62.8	31.7	63.4	31.0	65.4
280.0	29.9	57.0	30.6	61.9	28.5	63.3	31.7	64.0	31.1	66.0
285.0	30.0	57.5	30.6	62.4	28.5	63.9	31.6	64.6	31.1	66.6
290.0	29.9	57.9	30.6	63.0	28.6	64.4	31.6	65.1	31.1	67.1
295.0	29.9	58.5	30.6	63.5	28.5	65.0	31.5	65.7	31.1	67.7
300.0	29.9	58.9	30.7	64.0	28.6	65.5	31.5	66.2	31.1	68.3
305.0	30.0	59.4	30.7	64.5	28.6	66.1	31.5	66.8	31.1	68.8
310.0	30.1	59.9	30.7	65.0	28.5	66.6	31.5	67.3	31.1	69.4
315.0	29.9	60.4	30.7	65.5	28.5	67.1	31.4	67.9	31.1	69.9
320.0	29.9	60.8	30.7	66.0	28.5	67.7	31.4	68.4	31.1	70.5
325.0	30.0	61.3	30.8	66.5	28.5	68.2	31.4	68.9	31.1	71.0
330.0	30.0	61.8	30.7	67.0	28.5	68.7	31.3	69.5	31.1	71.6
335.0	30.0	62.2	30.8	67.5	28.4	69.2	31.3	70.0	31.1	72.1
340.0	30.0	62.7	30.8	67.9	28.5	69.8	31.3	70.5	31.2	72.7
345.0	29.9	63.1	30.8	68.4	28.4	70.2	31.3	71.0	31.1	73.2
350.0	29.9	63.6	30.8	68.9	28.5	70.8	31.3	71.6	31.0	73.7
355.0	29.9	64.0	30.8	69.4	28.3	71.3	31.3	72.1	31.1	74.2
360.0	29.9	64.5	30.9	69.8	28.4	71.8	31.3	72.6	31.1	74.8
365.0	29.7	64.8	31.0	70.3	28.5	72.3	31.3	73.1	31.0	75.3
370.0	29.8	65.3	31.0	70.7	28.4	72.7	31.2	73.6	31.0	75.8
375.0	29.8	65.7	31.0	71.2	28.4	73.2	31.1	74.1	31.0	76.3
380.0	29.8	66.6	30.9	71.7	28.4	73.7	31.2	74.6	31.0	76.9
385.0	29.6	67.3	30.8	72.2	28.4	74.2	31.2	75.1	31.0	77.4
390.0	29.8	67.9	30.7	72.6	28.3	74.7	31.1	75.6	31.0	77.9
395.0	29.8	68.6	30.5	73.0	28.5	75.2	31.2	76.1	31.0	78.6

400.0	29.6	69.3	30.4	73.8	28.4	75.6	31.1	76.6	30.9	79.0
405.0	29.6	70.0	30.4	74.5	28.3	76.1	31.0	77.1	31.0	79.6
410.0	29.6	70.7	30.3	75.3	28.3	76.6	31.0	77.6	30.9	80.0
415.0	29.5	71.4	30.2	76.0	28.3	77.0	31.0	78.2	31.0	80.6
420.0	29.5	72.0	30.2	76.3	28.2	77.5	30.9	78.9	30.9	80.8

3. Data collected during the heat pipe containing acetone test

Time [min]	NI		II		VI		TI		SI	
	Amb temp	Water temp	Amb temp	Water temp	Amb temp	Water temp	Amb temp	Water temp	Amb temp	Water temp
0.0	28.4	28.7	27.0	28.2	29.4	28.5	27.6	29.7	27.8	31.0
5.0	28.7	29.0	27.3	28.9	29.4	30.2	28.1	30.0	28.0	31.2
10.0	28.8	29.0	27.6	29.1	29.4	31.3	28.5	30.4	28.3	31.6
15.0	29.1	29.4	27.8	29.8	29.4	31.9	29.0	30.9	28.5	32.1
20.0	29.2	29.7	28.0	30.5	29.5	32.2	29.2	31.5	28.7	32.7
25.0	29.4	30.1	28.0	31.2	29.6	32.7	29.3	32.2	28.9	33.4
30.0	29.5	30.4	28.2	32.2	29.6	33.2	29.4	32.9	29.1	34.1
35.0	29.6	30.8	28.2	32.5	29.6	33.7	29.6	33.6	29.3	34.8
40.0	29.7	31.2	28.3	32.9	29.6	34.1	29.7	34.4	29.5	35.5
45.0	29.8	31.7	28.4	33.4	29.6	34.7	29.9	35.2	29.7	36.3
50.0	29.8	32.0	28.5	33.9	29.6	35.4	30.1	36.0	29.8	37.1
55.0	29.8	32.4	28.6	34.5	29.5	36.0	30.3	36.8	30.0	37.9
60.0	29.9	32.8	28.6	35.2	29.5	36.5	30.6	37.5	30.3	38.6
65.0	30.0	33.3	28.6	35.8	29.5	37.0	30.8	38.3	30.8	39.4
70.0	30.1	33.7	28.7	36.4	29.4	37.5	31.1	39.1	30.9	40.2
75.0	30.1	34.1	28.8	37.0	29.4	38.0	31.2	39.9	31.3	40.9
80.0	30.2	34.6	28.9	37.7	29.4	38.6	31.3	40.6	31.1	41.7
85.0	30.2	35.1	28.9	38.3	30.5	39.9	31.3	41.3	31.4	42.5
90.0	30.3	35.5	29.0	38.9	30.5	40.6	31.4	42.1	31.6	43.2
95.0	30.3	36.0	29.1	39.6	30.7	41.3	31.4	42.8	31.2	44.0
100.0	30.4	36.4	29.1	40.2	30.8	42.1	31.5	43.6	31.4	44.7
105.0	30.5	37.0	29.1	40.8	31.0	42.8	31.3	44.3	31.6	45.4
110.0	30.5	37.5	29.2	41.4	31.1	43.5	31.4	45.0	31.8	46.1
115.0	30.5	38.1	29.3	42.0	31.2	44.3	31.5	45.7	32.0	46.9
120.0	30.6	38.7	29.3	42.6	31.2	45.0	31.5	46.4	32.2	47.7
125.0	30.6	39.4	29.4	43.2	31.2	45.7	31.5	47.1	32.3	48.4
130.0	30.7	40.0	29.4	43.9	31.3	46.4	31.5	47.8	32.4	49.1
135.0	30.7	40.7	29.4	44.5	31.4	47.1	31.5	48.5	32.5	49.8
140.0	30.7	41.7	29.5	45.1	31.5	47.8	31.6	49.2	32.5	50.5
145.0	30.8	42.3	29.5	45.7	31.5	48.5	31.6	49.9	32.5	51.2
150.0	30.8	42.8	29.6	46.3	31.6	49.1	31.6	50.5	32.6	51.9
155.0	30.9	43.4	29.7	46.9	31.6	49.8	31.6	51.2	32.6	52.5
160.0	30.9	43.9	29.7	47.5	31.7	50.5	31.6	51.9	32.7	53.3
165.0	30.9	44.4	29.8	48.1	31.8	51.2	31.6	52.5	32.6	53.9
170.0	30.9	45.0	29.9	48.7	31.8	51.8	31.6	53.2	32.6	54.5

175.0	31.0	45.5	29.9	49.3	31.9	52.5	31.6	53.8	32.7	55.2
180.0	31.0	46.0	30.0	49.9	31.9	53.2	31.6	54.4	32.7	55.9
185.0	31.0	46.6	30.1	50.4	31.9	53.9	31.6	55.1	32.6	56.5
190.0	31.0	47.1	30.2	51.0	32.0	54.5	31.6	55.7	32.7	57.1
195.0	30.9	47.7	30.3	51.6	31.9	55.2	31.6	56.3	32.7	57.8
200.0	31.0	48.3	30.4	52.2	32.0	55.8	31.6	56.9	32.8	58.5
205.0	31.0	48.8	30.4	52.8	32.0	56.4	31.6	57.5	32.7	59.1
210.0	30.9	49.3	30.5	53.3	32.0	57.0	31.6	58.2	32.8	59.8
215.0	30.9	49.9	30.5	53.9	32.0	57.7	31.6	58.8	32.8	60.5
220.0	30.9	50.5	30.7	54.4	32.0	58.3	31.6	59.4	32.8	61.1
225.0	30.9	51.0	30.6	55.0	32.1	58.9	31.6	60.0	32.8	61.7
230.0	30.9	51.5	30.7	55.6	32.1	59.5	31.6	60.6	32.8	62.3
235.0	30.9	52.1	30.7	56.1	32.1	60.1	31.7	61.2	32.8	63.0
240.0	30.8	52.5	30.9	56.7	32.2	60.7	31.7	61.8	32.8	63.6
245.0	30.8	53.1	30.9	57.2	32.2	61.3	31.7	62.4	32.8	64.2
250.0	30.7	53.6	30.9	57.8	32.1	61.9	31.7	62.9	32.8	64.8
255.0	30.8	54.2	30.9	58.3	32.1	62.5	31.7	63.6	32.8	65.5
260.0	30.8	54.6	31.0	58.8	32.1	63.1	31.6	64.1	32.8	66.1
265.0	30.8	55.1	31.0	59.4	32.0	63.6	31.7	64.7	32.8	66.7
270.0	30.7	55.6	31.0	59.9	32.0	64.1	31.7	65.3	32.7	67.3
275.0	30.7	56.1	31.1	60.4	32.1	64.7	31.7	65.8	32.8	67.9
280.0	30.7	56.6	31.1	60.9	32.0	65.2	31.7	66.4	32.8	68.5
285.0	30.6	57.1	31.1	61.4	32.0	65.7	31.6	66.9	32.8	69.1
290.0	30.7	57.5	31.1	62.0	32.1	66.3	31.6	67.5	32.8	69.7
295.0	30.7	58.1	31.2	62.5	32.1	66.8	31.6	68.1	32.8	70.3
300.0	30.7	58.5	31.2	63.0	32.1	67.3	31.6	68.6	32.8	70.8
305.0	30.7	59.0	31.2	63.5	32.1	67.8	31.6	69.1	32.8	71.4
310.0	30.7	59.5	31.2	64.0	32.1	68.3	31.6	69.7	32.8	72.0
315.0	30.6	60.0	31.2	64.5	32.1	68.8	31.6	70.2	32.8	72.5
320.0	30.6	60.4	31.2	65.0	32.1	69.3	31.6	70.7	32.8	73.1
325.0	30.6	60.9	31.2	65.5	32.2	69.8	31.5	71.2	32.8	73.6
330.0	30.6	61.4	31.1	66.0	32.1	70.3	31.5	71.7	32.8	74.2
335.0	30.6	61.8	31.1	66.5	32.1	70.8	31.5	72.3	32.8	74.7
340.0	30.6	62.3	31.0	66.9	32.1	71.2	31.5	72.8	32.8	75.3
345.0	30.6	62.7	31.0	67.4	32.1	71.7	31.5	73.3	32.8	75.8
350.0	30.5	63.2	30.9	67.9	32.1	72.2	31.4	73.8	32.8	76.3
355.0	30.5	63.6	30.9	68.4	32.1	72.7	31.4	74.3	32.8	76.8
360.0	30.5	64.1	30.9	68.8	32.1	73.1	31.4	74.8	32.8	77.4
365.0	30.5	64.4	30.9	69.3	32.1	73.6	31.4	75.3	32.8	77.9
370.0	30.6	64.9	30.9	69.7	32.0	74.1	31.4	75.8	32.7	78.4
375.0	30.5	65.3	30.9	70.2	32.1	74.5	31.4	76.3	32.8	78.9
380.0	30.5	66.2	30.9	70.7	32.0	75.0	31.3	76.8	32.7	79.4
385.0	30.5	66.9	30.9	71.2	32.0	75.4	31.3	77.2	32.7	80.0
390.0	30.4	67.5	30.9	71.6	32.0	75.8	31.3	77.7	32.7	80.5

395.0	30.4	68.2	30.9	72.0	32.0	76.3	31.3	78.2	32.7	81.0
400.0	30.4	68.9	31.0	72.8	32.0	76.7	31.3	78.7	32.7	81.5
405.0	30.4	69.6	30.2	73.5	32.0	77.2	31.2	79.2	32.7	82.0
410.0	30.4	70.3	30.3	74.3	31.9	77.6	31.2	79.6	32.7	82.5
415.0	30.4	71.0	30.4	75.0	31.9	78.1	31.1	80.1	32.6	83.0
420.0	30.4	71.6	30.4	75.3	31.8	78.5	31.2	80.9	32.6	83.5

4. Data collected during the heat pipe containing toluene test

Time [min]	NI		II		VI		TI		SI	
	Amb temp	Water temp	Amb temp	Water temp	Amb temp	Water temp	Amb temp	Water temp	Amb temp	Water temp
0.0	26.7	29.6	27.3	28.3	26.3	30.3	25.2	29.8	25.1	29.8
5.0	26.9	30.2	27.4	29.1	26.5	31.0	25.5	29.9	25.3	29.8
10.0	27.1	30.3	27.6	29.3	26.6	32.1	25.7	30.3	25.6	30.2
15.0	27.3	30.6	27.9	30.0	26.8	32.7	25.9	30.8	25.7	30.7
20.0	27.5	31.0	28.3	30.7	26.9	33.0	26.1	31.4	25.8	31.3
25.0	27.6	31.3	28.5	31.4	27.1	33.5	26.2	32.0	26.0	32.0
30.0	27.9	31.7	28.6	32.4	27.2	34.0	26.3	32.8	26.0	32.7
35.0	28.0	32.1	29.0	32.7	27.3	34.5	26.4	33.5	26.1	33.4
40.0	28.2	32.5	29.2	33.1	27.4	34.9	26.5	34.3	26.2	34.1
45.0	28.3	32.9	29.3	33.6	27.6	35.5	26.6	35.1	26.2	34.9
50.0	28.5	33.3	29.5	34.1	27.7	36.2	26.7	35.9	26.3	35.7
55.0	28.6	33.7	29.6	34.7	27.8	36.8	26.7	36.7	26.3	36.5
60.0	28.7	34.1	29.7	35.4	27.9	37.3	26.8	37.4	26.3	37.2
65.0	28.8	34.5	29.9	36.0	28.0	37.8	26.9	38.2	26.4	38.0
70.0	28.9	35.0	30.1	36.6	28.1	38.3	27.0	39.0	26.4	38.8
75.0	29.0	35.3	30.1	37.2	28.2	38.8	27.1	39.7	26.5	39.5
80.0	29.2	35.8	30.3	37.9	28.3	39.4	27.2	40.5	26.5	40.3
85.0	29.3	36.3	30.4	38.5	28.4	40.7	27.3	41.2	26.5	41.1
90.0	29.4	36.8	30.5	39.1	28.6	41.4	27.5	42.0	26.6	41.8
95.0	29.6	37.2	30.6	39.8	28.7	42.1	27.7	42.7	26.6	42.6
100.0	29.8	37.7	30.7	40.4	28.8	42.9	27.8	43.5	26.6	43.3
105.0	29.8	38.3	30.8	41.0	28.9	43.6	27.9	44.2	26.7	44.0
110.0	30.0	38.8	30.8	41.6	29.0	44.3	28.0	44.9	26.8	44.7
115.0	30.2	39.4	31.0	42.2	29.1	45.1	28.0	45.6	26.8	45.5
120.0	30.4	40.0	31.0	42.8	29.2	45.8	28.1	46.3	26.8	46.3
125.0	30.6	40.6	31.1	43.4	29.4	46.5	28.2	47.0	26.8	47.0
130.0	30.7	41.3	31.1	44.1	29.5	47.2	28.3	47.7	26.8	47.7
135.0	30.8	42.0	31.1	44.7	29.6	47.9	28.3	48.4	26.8	48.4
140.0	30.9	43.0	31.2	45.3	29.7	48.6	28.4	49.1	26.8	49.1
145.0	31.0	43.5	31.3	45.9	29.9	49.3	28.4	49.7	26.8	49.8
150.0	31.1	44.1	31.2	46.5	30.0	49.9	28.4	50.4	26.9	50.5
155.0	31.2	44.6	31.3	47.1	30.2	50.6	28.5	51.1	26.9	51.1
160.0	31.2	45.2	31.3	47.7	30.3	51.3	28.4	51.8	26.9	51.9

165.0	31.3	45.7	31.3	48.3	30.4	52.0	28.4	52.4	27.0	52.5
170.0	31.4	46.2	31.3	48.9	30.5	52.6	28.5	53.1	27.0	53.1
175.0	31.4	46.7	31.3	49.5	30.7	53.3	28.4	53.7	27.0	53.8
180.0	31.4	47.3	31.4	50.1	30.8	54.0	28.4	54.3	27.1	54.5
185.0	31.5	47.8	31.4	50.6	30.9	54.7	28.4	55.0	27.1	55.1
190.0	31.6	48.4	31.4	51.2	30.9	55.3	28.4	55.6	27.1	55.7
195.0	31.6	49.0	31.5	51.8	31.0	56.0	28.5	56.2	27.1	56.4
200.0	31.7	49.5	31.5	52.4	31.1	56.6	28.5	56.8	27.1	57.1
205.0	31.7	50.0	31.5	53.0	31.2	57.2	28.5	57.4	27.2	57.7
210.0	31.7	50.6	31.6	53.5	31.2	57.8	28.4	58.0	27.2	58.4
215.0	31.8	51.1	31.6	54.1	31.2	58.5	28.5	58.7	27.2	59.1
220.0	31.8	51.7	31.6	54.6	31.4	59.1	28.5	59.3	27.3	59.7
225.0	31.9	52.3	31.6	55.2	31.4	59.7	28.5	59.9	27.3	60.3
230.0	31.9	52.7	31.6	55.8	31.4	60.3	28.5	60.5	27.3	60.9
235.0	31.9	53.3	31.7	56.3	31.5	60.9	28.5	61.1	27.4	61.6
240.0	32.0	53.8	31.7	56.9	31.6	61.5	28.5	61.7	27.4	62.2
245.0	31.9	54.3	31.7	57.4	31.7	62.1	28.5	62.2	27.5	62.8
250.0	31.9	54.9	31.7	58.0	31.7	62.7	28.6	62.8	27.5	63.4
255.0	32.0	55.4	31.7	58.5	31.7	63.3	28.5	63.4	27.5	64.1
260.0	32.0	55.9	31.6	59.0	31.8	63.9	28.5	64.0	27.5	64.7
265.0	32.0	56.4	31.6	59.6	31.8	64.4	28.5	64.6	27.6	65.3
270.0	32.0	56.8	31.6	60.1	31.9	64.9	28.5	65.1	27.6	65.9
275.0	32.0	57.3	31.7	60.6	31.9	65.5	28.5	65.7	27.7	66.5
280.0	32.1	57.8	31.7	61.1	31.9	66.0	28.5	66.3	27.7	67.1
285.0	32.0	58.3	31.7	61.6	31.9	66.5	28.4	66.8	27.7	67.7
290.0	32.1	58.8	31.6	62.2	31.9	67.1	28.4	67.4	27.7	68.3
295.0	32.1	59.3	31.6	62.7	32.0	67.6	28.4	67.9	27.8	68.9
300.0	32.1	59.8	31.6	63.2	32.0	68.1	28.4	68.5	27.8	69.4
305.0	32.1	60.2	31.5	63.7	31.9	68.6	28.4	69.0	27.8	70.0
310.0	32.1	60.7	31.5	64.2	32.0	69.1	28.4	69.5	27.8	70.6
315.0	32.2	61.2	31.5	64.7	32.0	69.6	28.3	70.1	27.8	71.1
320.0	32.2	61.6	31.4	65.2	32.0	70.1	28.4	70.6	27.8	71.7
325.0	32.2	62.1	31.4	65.7	32.0	70.6	28.3	71.1	27.8	72.2
330.0	32.1	62.6	31.4	66.2	32.1	71.1	28.3	71.6	27.8	72.8
335.0	32.1	63.1	31.4	66.7	32.1	71.6	28.2	72.1	27.8	73.3
340.0	32.1	63.5	31.4	67.1	32.1	72.0	28.2	72.6	27.8	73.9
345.0	32.0	64.0	31.3	67.6	32.2	72.5	28.3	73.1	27.9	74.4
350.0	32.0	64.4	31.3	68.1	32.2	73.0	28.2	73.7	27.9	74.9
355.0	32.0	64.9	31.1	68.6	32.2	73.5	28.2	74.2	27.9	75.4
360.0	31.9	65.3	31.2	69.0	32.2	73.9	28.2	74.7	27.8	76.0
365.0	31.8	65.7	31.2	69.5	32.2	74.4	28.1	75.1	27.9	76.5
370.0	31.8	66.1	31.1	69.9	32.2	74.9	28.1	75.7	27.8	77.0
375.0	31.8	66.5	31.0	70.4	32.2	75.3	28.2	76.1	27.9	77.5
380.0	31.8	67.4	30.9	70.9	32.2	75.8	28.1	76.6	27.9	78.0

385.0	31.8	68.1	30.9	71.4	32.2	76.2	28.1	77.1	27.9	78.6
390.0	31.8	68.8	30.8	71.8	32.3	76.6	28.1	77.6	27.9	79.1
395.0	31.9	69.5	30.7	72.2	32.3	77.1	28.1	78.1	28.0	79.6
400.0	31.9	70.5	30.8	73.0	32.3	77.5	28.1	78.6	28.1	80.1
405.0	32.0	71.3	30.7	73.7	32.3	78.0	27.8	79.0	28.3	80.6
410.0	31.9	72.1	30.6	74.5	32.3	78.4	28.0	79.5	28.4	81.1
415.0	31.9	72.9	30.6	75.2	32.3	78.9	28.2	79.9	28.0	81.6
420.0	31.9	73.9	30.5	76.0	32.3	79.5	28.3	80.0	28.0	81.6

5. Data collected during the heat pipe containing ethanol test

Time [min]	NI		II		VI		TI		SI	
	Amb temp	Water temp	Amb temp	Water temp	Amb temp	Water temp	Amb temp	Water temp	Amb temp	Water temp
0.0	26.3	29.7	26.9	29.0	27.7	28.6	27.9	29.8	26.2	31.0
5.0	26.7	29.9	27.1	29.2	28.0	28.9	28.1	30.3	26.4	31.3
10.0	27.0	30.2	27.1	29.5	28.2	29.1	28.3	30.7	26.5	31.6
15.0	27.2	30.4	27.3	29.8	28.4	29.3	28.5	31.2	26.7	31.8
20.0	27.4	30.7	27.5	30.1	28.4	29.7	28.7	31.6	26.8	32.1
25.0	27.7	31.0	27.5	30.5	28.5	30.0	28.8	32.1	26.9	32.5
30.0	27.9	31.3	27.5	31.1	28.7	30.4	28.8	32.5	27.0	32.8
35.0	28.1	31.7	27.8	31.7	28.9	30.9	28.9	33.0	27.1	33.2
40.0	28.3	32.0	28.0	32.2	29.1	31.4	29.1	33.5	27.2	33.5
45.0	28.4	32.4	27.9	32.8	29.2	32.0	29.2	33.9	27.3	33.9
50.0	28.6	32.9	28.1	33.3	29.2	32.6	29.5	34.4	27.4	34.3
55.0	28.8	33.3	28.1	34.0	29.5	33.0	29.2	34.8	27.5	34.7
60.0	29.0	33.8	27.9	34.7	29.5	33.6	29.5	35.2	27.6	35.4
65.0	29.1	34.3	28.2	35.3	29.5	34.1	29.6	35.6	27.7	36.0
70.0	29.2	34.3	28.3	35.9	29.5	34.7	29.7	36.0	27.7	36.6
75.0	29.4	34.7	28.3	36.5	29.6	35.2	29.8	36.5	27.8	37.2
80.0	29.5	35.1	28.3	37.2	29.7	35.8	29.9	36.9	27.9	37.9
85.0	29.6	35.6	28.4	37.8	29.7	36.4	30.1	37.5	27.9	38.6
90.0	29.7	36.1	28.4	38.4	29.9	36.9	30.2	38.0	28.0	39.2
95.0	29.8	36.6	28.5	39.0	29.8	37.5	30.3	38.6	28.1	39.9
100.0	29.9	37.2	28.6	39.5	30.0	38.1	30.4	39.2	28.2	40.5
105.0	30.0	37.7	28.7	40.1	30.0	38.7	30.4	39.8	28.2	41.1
110.0	30.1	38.3	28.6	40.7	30.1	39.2	30.5	40.4	28.2	41.7
115.0	30.3	38.8	28.7	41.2	30.3	39.8	30.7	41.0	28.3	42.4
120.0	30.3	39.4	28.6	41.8	30.3	40.3	30.3	41.6	28.3	43.0
125.0	30.4	40.0	28.7	42.3	30.2	40.8	30.4	42.2	28.4	43.5
130.0	30.5	40.5	28.8	42.8	30.4	41.4	30.5	42.8	28.5	44.2
135.0	30.5	41.1	28.7	43.4	30.4	41.9	30.5	43.4	28.5	44.8
140.0	30.6	41.6	28.8	43.9	30.3	42.4	30.7	44.0	28.6	45.3
145.0	30.7	42.2	28.9	44.4	30.4	43.0	30.8	44.6	28.6	45.9
150.0	30.7	42.7	28.5	44.9	30.4	43.5	30.9	45.1	28.6	46.5

155.0	30.8	43.2	28.7	45.4	30.3	44.0	30.9	45.7	28.7	47.0
160.0	30.8	43.7	28.8	45.9	30.4	44.5	30.3	46.2	28.8	47.6
165.0	30.9	44.2	28.7	46.5	30.5	45.0	30.4	46.8	28.8	48.2
170.0	30.9	44.7	28.9	47.0	30.5	45.5	30.5	47.4	28.9	48.7
175.0	31.0	45.2	29.0	47.4	30.4	46.0	30.6	47.9	29.0	49.3
180.0	31.0	45.7	28.8	47.9	30.6	46.5	30.8	48.4	29.1	49.8
185.0	31.0	46.2	29.1	48.4	30.5	47.0	31.0	49.0	29.2	50.4
190.0	31.0	46.7	29.0	48.9	30.5	47.5	31.1	49.5	29.2	50.9
195.0	31.0	47.2	28.9	49.4	30.6	47.9	31.1	50.1	29.2	51.5
200.0	31.1	47.7	29.0	49.8	30.7	48.4	31.2	50.6	29.3	52.1
205.0	31.1	48.2	29.1	50.3	30.5	49.0	31.2	51.2	29.3	52.7
210.0	31.1	48.6	29.2	50.8	30.7	49.4	31.2	51.7	29.3	53.2
215.0	31.1	49.1	28.9	51.2	30.6	49.9	31.2	52.2	29.4	53.8
220.0	31.1	49.5	29.3	51.7	30.8	50.3	31.2	52.8	29.4	54.3
225.0	31.1	49.9	29.0	52.1	30.9	50.8	31.2	53.3	29.4	54.9
230.0	31.2	50.4	29.2	52.6	30.8	51.3	31.1	53.8	29.5	55.4
235.0	31.2	50.8	29.2	53.0	30.8	51.7	31.1	54.3	29.6	56.0
240.0	31.3	51.3	29.2	53.4	30.8	52.2	31.0	54.8	29.5	56.5
245.0	31.3	51.7	29.3	53.9	30.9	52.7	31.0	55.3	29.6	57.1
250.0	31.2	52.2	29.1	54.3	30.9	53.1	31.0	55.8	29.6	57.6
255.0	31.2	52.5	29.2	54.7	30.9	53.6	30.9	56.4	29.6	58.1
260.0	31.3	53.0	28.9	55.2	31.0	54.0	30.9	56.9	29.7	58.7
265.0	31.3	53.4	29.1	55.6	30.9	54.5	30.9	57.4	29.7	59.2
270.0	31.2	53.8	28.7	56.0	31.0	54.9	30.8	57.8	29.7	59.7
275.0	31.3	54.2	28.8	56.4	31.0	55.3	30.8	58.4	29.8	60.2
280.0	31.3	54.7	29.0	56.8	31.0	55.8	30.8	58.9	29.8	60.7
285.0	31.3	55.1	28.7	57.2	31.1	56.3	30.7	59.4	29.9	61.3
290.0	31.2	55.5	28.9	57.6	31.1	56.7	30.7	59.8	30.0	61.8
295.0	31.3	55.9	28.8	57.9	31.0	57.1	30.7	60.4	30.0	62.3
300.0	31.3	56.4	28.8	58.3	31.1	57.5	30.7	60.9	30.1	62.8
305.0	31.4	56.8	29.2	58.7	31.1	57.9	30.7	61.4	30.2	63.3
310.0	31.4	57.2	28.9	59.1	31.1	58.4	30.7	61.8	30.2	63.8
315.0	31.4	57.6	29.0	59.5	31.1	58.7	30.8	62.3	30.3	64.3
320.0	31.4	58.1	29.0	59.9	31.2	59.1	30.8	62.8	30.3	64.8
325.0	31.5	58.5	28.9	60.3	31.1	59.5	30.8	63.3	30.3	65.3
330.0	31.4	58.9	29.0	60.7	31.1	59.9	30.7	63.8	30.3	65.7
335.0	31.4	59.4	29.0	61.0	31.1	60.2	30.8	64.3	30.4	66.2
340.0	31.5	59.8	28.7	61.4	31.0	60.7	30.8	64.8	30.4	66.7
345.0	31.5	60.2	28.8	61.8	30.8	61.0	30.8	65.2	30.4	67.2
350.0	31.5	60.7	28.9	62.2	30.9	61.4	30.8	65.7	30.4	67.6
355.0	31.5	61.1	29.1	62.6	30.9	61.8	30.8	66.2	30.3	68.1
360.0	31.5	61.5	28.9	62.9	30.5	62.1	30.8	66.7	30.4	68.5
365.0	31.6	62.0	28.7	63.3	30.7	62.9	30.8	67.2	30.4	69.0
370.0	31.6	62.4	28.8	63.7	30.5	63.4	30.8	67.7	30.4	69.4

375.0	31.7	62.8	29.0	64.1	30.7	63.9	30.8	68.1	30.4	69.9
380.0	31.6	63.2	28.9	64.4	30.5	64.5	30.8	68.6	30.4	70.3
385.0	31.6	63.7	28.7	64.8	30.8	65.0	30.8	69.1	30.4	70.8
390.0	31.6	64.1	28.1	65.5	30.4	65.6	30.8	69.6	30.4	71.2
395.0	31.4	64.5	28.3	66.0	30.3	66.1	30.7	70.1	30.5	71.7
400.0	31.5	64.9	28.5	66.5	30.3	66.7	30.7	70.5	30.5	72.0
405.0	31.4	65.3	28.7	67.1	30.4	67.2	30.7	71.0	30.4	72.5
410.0	31.4	65.7	28.8	67.6	30.4	67.8	30.7	71.4	30.5	72.9
415.0	31.3	66.1	28.8	68.1	30.3	68.3	30.6	71.9	30.5	73.3
420.0	31.4	66.4	28.8	68.7	30.3	69.9	30.7	72.3	30.5	73.7

6. Data collected during the heat pipe containing ethyl acetate test

Time [min]	NI		II		VI		TI		SI	
	Amb temp	Water temp	Amb temp	Water temp	Amb temp	Water temp	Amb temp	Water temp	Amb temp	Water temp
0.0	25.5	29.7	26.2	30.8	25.7	29.3	26.5	30.2	25.5	28.4
5.0	25.5	30.0	26.2	31.0	25.9	29.9	26.7	31.0	25.7	28.7
10.0	25.7	30.3	26.3	31.0	26.1	30.3	26.9	31.9	25.9	29.0
15.0	25.8	30.6	26.3	31.4	26.2	31.4	27.1	32.3	26.1	29.2
20.0	25.8	30.9	26.3	31.4	26.4	32.0	27.2	32.8	26.3	29.5
25.0	25.9	31.2	26.3	31.8	26.5	32.5	27.4	33.2	26.5	29.9
30.0	26.0	31.5	26.4	32.3	26.6	33.1	27.6	33.7	26.6	30.2
35.0	26.1	31.8	26.4	32.9	26.8	34.1	27.6	34.1	26.8	30.6
40.0	26.2	32.0	26.4	32.7	26.8	34.8	27.8	34.6	27.1	30.9
45.0	26.3	32.3	26.4	33.2	27.0	35.5	27.9	35.1	27.5	31.3
50.0	26.4	32.6	26.5	33.4	27.0	36.0	28.0	35.5	27.6	31.7
55.0	26.5	33.4	26.5	34.1	27.1	36.4	28.2	36.0	27.7	32.1
60.0	26.6	34.1	26.5	34.8	27.2	36.9	28.3	36.6	27.7	32.8
65.0	26.7	34.7	26.5	35.4	27.2	37.4	28.4	37.2	27.9	33.4
70.0	26.8	35.3	26.6	36.0	27.3	37.9	28.6	37.9	28.1	34.0
75.0	26.8	35.8	26.6	36.6	27.4	38.4	28.7	38.4	28.3	34.6
80.0	26.9	36.4	26.6	37.3	27.3	38.9	29.1	39.1	28.5	35.3
85.0	27.0	36.9	26.6	37.9	27.4	39.4	29.2	39.7	28.7	36.0
90.0	27.0	37.5	26.7	38.5	27.5	39.9	29.2	40.3	28.8	36.6
95.0	27.0	38.0	26.7	39.1	27.4	40.4	29.3	40.9	29.1	37.3
100.0	27.1	38.5	26.7	39.6	27.5	40.9	29.4	41.4	29.4	37.9
105.0	27.2	39.1	26.7	40.2	27.5	41.5	29.6	42.1	29.7	38.5
110.0	27.2	39.6	26.8	40.8	27.5	42.0	29.7	42.6	29.7	39.1
115.0	27.2	40.1	26.8	41.3	27.6	42.5	29.8	43.2	29.7	39.8
120.0	27.3	40.6	26.8	41.9	27.6	43.0	30.0	43.7	29.8	40.4
125.0	27.3	41.1	26.8	42.4	27.7	43.6	30.2	44.3	29.9	40.9
130.0	27.3	41.5	26.9	42.9	27.6	44.0	30.4	44.8	30.0	41.6
135.0	27.3	42.0	26.9	43.5	27.7	44.5	30.6	45.3	30.0	42.2
140.0	27.4	42.6	26.9	44.0	27.7	45.0	30.8	45.8	30.1	42.7

145.0	27.5	43.0	26.9	44.5	27.8	45.5	30.9	46.3	30.2	43.3
150.0	27.6	43.6	27.0	45.0	27.7	46.0	30.9	46.9	30.2	43.9
155.0	27.6	44.1	27.0	45.5	27.8	46.5	30.9	47.4	30.2	44.4
160.0	27.7	44.5	27.0	46.0	27.8	47.0	30.9	47.9	30.2	45.0
165.0	27.7	44.9	27.0	46.6	27.9	47.5	30.9	48.4	30.2	45.6
170.0	27.7	45.4	27.1	47.1	28.0	47.9	31.0	49.0	30.3	46.1
175.0	27.8	45.9	27.1	47.5	28.0	48.4	30.9	49.5	30.3	46.7
180.0	27.8	46.3	27.1	48.0	28.1	48.8	30.9	50.0	30.3	47.2
185.0	27.8	46.8	27.1	48.5	28.1	49.3	30.9	50.5	30.4	47.8
190.0	27.8	47.3	27.2	49.0	28.1	49.7	31.0	51.0	30.4	48.3
195.0	27.8	47.7	27.2	49.5	28.2	50.1	31.0	51.5	30.4	48.9
200.0	27.8	48.2	27.2	49.9	28.3	50.6	31.0	52.0	30.4	49.5
205.0	27.7	48.7	27.2	50.4	28.4	51.1	31.0	52.5	30.4	50.1
210.0	27.7	49.1	27.3	50.9	28.4	51.5	31.0	53.0	30.4	50.6
215.0	27.7	49.7	27.3	51.3	28.5	52.0	31.0	53.6	30.4	51.2
220.0	27.8	50.1	27.3	51.8	28.5	52.4	31.0	54.1	30.4	51.7
225.0	27.7	50.5	27.3	52.2	28.6	52.9	31.1	54.6	30.4	52.3
230.0	27.7	50.9	27.4	52.7	28.6	53.2	31.1	55.1	30.4	52.8
235.0	27.8	51.3	27.4	53.1	28.7	53.7	31.1	55.5	30.4	53.4
240.0	27.8	51.8	27.4	53.5	28.7	54.2	31.0	56.0	30.4	53.9
245.0	27.8	52.2	27.4	54.0	28.8	54.7	31.0	56.5	30.4	54.5
250.0	27.9	52.7	27.5	54.4	28.8	55.1	31.1	57.0	30.4	55.0
255.0	27.9	53.1	27.5	54.8	28.8	55.5	31.1	57.4	30.4	55.5
260.0	28.0	53.5	27.5	55.3	28.9	55.9	31.0	57.8	30.4	56.1
265.0	28.1	54.0	27.6	55.7	28.8	56.3	31.0	58.3	30.4	56.6
270.0	28.2	54.4	27.6	56.1	28.9	56.7	31.0	58.8	30.4	57.1
275.0	28.3	54.8	27.4	56.5	28.9	57.1	31.0	59.2	30.4	57.6
280.0	28.3	55.2	27.4	56.9	28.9	57.6	31.0	59.7	30.3	58.1
285.0	28.4	55.7	27.4	57.3	28.9	57.9	31.1	60.1	30.3	58.7
290.0	28.4	56.1	27.4	57.7	29.0	58.3	31.0	60.6	30.3	59.2
295.0	28.4	56.5	27.4	58.0	29.0	58.7	31.0	61.0	30.3	59.7
300.0	28.4	56.9	27.4	58.4	29.1	59.2	31.0	61.5	30.3	60.2
305.0	28.5	57.3	27.4	58.8	29.1	59.6	31.0	61.9	30.3	60.7
310.0	28.5	57.7	27.4	59.2	29.1	59.9	31.0	62.4	30.3	61.2
315.0	28.5	58.1	27.4	59.6	29.1	60.3	31.0	62.9	30.2	61.7
320.0	28.6	58.5	27.4	60.0	29.2	60.7	31.0	63.3	30.2	62.2
325.0	28.6	58.9	27.4	60.4	29.2	61.2	31.0	63.7	30.2	62.7
330.0	28.7	59.3	27.4	60.8	29.2	61.5	31.0	64.1	30.2	63.1
335.0	28.6	59.7	27.4	61.1	29.3	61.8	31.0	64.6	30.1	63.6
340.0	28.7	60.1	27.4	61.5	29.2	62.2	30.9	65.0	30.1	64.1
345.0	28.8	60.5	27.4	61.9	29.3	62.6	31.0	65.4	30.1	64.6
350.0	28.8	60.8	27.4	62.3	29.3	63.0	30.9	65.8	30.1	65.0
355.0	28.9	61.2	27.4	62.7	29.3	63.3	31.0	66.2	30.0	65.5
360.0	28.9	61.6	27.4	63.0	29.3	63.7	31.0	66.6	30.1	65.9

365.0	28.9	62.0	27.4	63.4	29.4	64.1	30.9	67.0	30.0	66.4
370.0	28.9	62.4	27.4	63.8	29.4	64.4	30.9	67.4	30.0	66.8
375.0	28.9	62.7	27.3	64.2	29.4	64.9	30.9	67.8	30.0	67.3
380.0	28.9	63.0	27.3	64.5	29.4	65.2	30.9	68.2	30.0	67.7
385.0	28.9	63.4	27.3	64.9	29.4	65.5	30.9	68.6	30.0	68.2
390.0	28.9	63.7	27.3	65.6	29.5	65.8	30.9	69.0	30.1	68.6
395.0	28.9	64.2	27.3	66.1	29.5	66.2	30.9	69.4	30.2	69.1
400.0	28.9	64.5	27.3	66.6	29.5	66.9	30.8	69.8	30.3	69.4
405.0	28.9	64.9	27.3	67.2	29.6	67.7	30.9	70.2	30.4	69.9
410.0	28.8	65.3	27.3	67.7	29.5	68.4	30.8	70.6	30.4	70.3
415.0	28.8	65.7	27.3	68.2	29.4	69.1	30.9	71.0	30.5	70.7
420.0	28.9	66.1	27.3	68.9	29.4	69.8	30.8	71.4	30.7	70.8
420.0		66.1		68.9		69.8		71.4		70.8

APPENDIX C: Properties of working fluids

1. Thermophysical properties of working fluid

1. Distilled water

Temperature [K]	Latent heat [kJ/kg]	Liquid density [kg/m ³]	Liquid surface tension [N/m] x 10 ²	Liquid viscosity: [Pa.s] x 10 ³	Merit number [W/m ²]
293.15	2248	998.2	7.28	1	1.6336E+11
313.15	2402	992.3	6.96	0.65	2.55218E+11
333.15	2359	983	6.62	0.47	3.26619E+11
353.15	2309	972	6.26	0.36	3.90267E+11
373.15	2258	958	5.89	0.28	4.55037E+11
393.15	2200	945	5.5	0.23	4.97152E+11
413.15	2139	928	5.06	0.2	5.02203E+11
433.15	2074	909	4.66	0.17	5.16785E+11
453.15	2003	888	4.29	0.15	5.08698E+11
473.15	1967	865	3.89	0.14	4.72761E+11

2. Methanol

Temperature [K]	Latent heat [kJ/kg]	Liquid density [kg/m ³]	Liquid surface tension [N/m] x 10 ²	Liquid viscosity: [Pa.s] x 10 ³	Merit number [W/m ²]
223.15	1194	843.5	3.26	1.7	1.9E+10
243.15	1187	833.5	2.95	1.3	2.2E+10
263.15	1182	818.7	2.63	0.945	2.7E+10
283.15	1175	800.5	2.36	0.701	3.2E+10
303.15	1155	782	2.18	0.521	3.8E+10
323.15	1125	764.1	2.01	0.399	4.3E+10
343.15	1085	746.2	1.85	0.314	4.8E+10
363.15	1035	724.4	1.66	0.259	4.8E+10
383.15	980	703.6	1.46	0.211	4.8E+10
403.15	920	685.2	1.25	0.166	4.7E+10
423.15	850	653.2	1.04	0.138	4.2E+10

3. Acetone

Temperature [K]	Latent heat [kJ/kg]	Liquid density [kg/m ³]	Liquid surface tension [N/m] x 10 ²	Liquid viscosity: [Pa.s] x 10 ³	Merit number [W/m ²]
233.15	660	860	3.1	0.8	2.2E+10
253.15	615.6	845	2.76	0.5	2.9E+10
273.15	564	812	2.62	0.395	3.0E+10
293.15	552	790	2.37	0.323	3.2E+10
313.15	536	768	2.12	0.269	3.2E+10
333.15	517	744	1.86	0.226	3.2E+10
353.15	495	719	1.62	0.192	3.0E+10
373.15	472	689.6	1.34	0.17	2.6E+10
393.15	426.1	660.3	1.07	0.148	2.0E+10
413.15	394.4	631.8	0.81	0.132	1.5E+10

4. Toluene

Temperature [K]	Latent heat [kJ/kg]	Liquid density [kg/m ³]	Liquid surface tension [N/m] x 10 ²	Liquid viscosity: [Pa.s] x 10 ³	Merit number [W/m ²]
230	1880	920.4	6.3	2.93	3.72E+10
250	1765	914.6	6.1	2.9	3.40E+10
270	1730	900.4	5.81	2.87	3.15E+10
290	1645	894.2	5.5	2.84	2.85E+10
310	1589	887.3	5.1	2.82	2.55E+10
330	1511	878.7	4.9	2.76	2.36E+10
350	1439	869.6	4.65	2.51	2.32E+10
370	1372	860.6	4.2	2.41	2.06E+10
390	1309	851.1	4.1	2.38	1.92E+10
410	1249	841.8	3.9	2.34	1.75E+10
430	1194	832.6	3.8	1.93	1.96E+10

5. Ethanol

Temperature [K]	Latent heat [kJ/kg]	Liquid density [kg/m ³]	Liquid surface tension [N/m] x 10 ²	Liquid viscosity: [Pa.s] x 10 ³	Merit number [W/m ²]
243.15	939.4	825	2.76	3.4	6.3E+09
263.15	928.7	813	2.66	2.2	9.1E+09
283.15	904.8	798	2.57	1.5	1.2E+10
303.15	888.6	781	2.44	1.02	1.7E+10
323.15	872.3	762.2	2.31	0.72	2.1E+10
343.15	858.3	743.1	2.17	0.51	2.7E+10
363.15	832.1	725.3	2.04	0.37	3.3E+10
383.15	786.6	704.1	1.89	0.28	3.7E+10
403.15	734.4	678.7	1.75	0.21	4.2E+10

6. Ethyl acetate

Temperature [K]	Latent heat [kJ/kg]	Liquid density [kg/m ³]	Liquid surface tension [N/m] x 10 ²	Liquid viscosity: [Pa.s] x 10 ³	Merit number [W/m ²]
303.15	920.4	880.0	22.2	0.453	4.0E+09
313.15	910	871.0	20.7	0.421	3.9E+09
323.15	906.4	857.1	19.6	0.399	3.8E+09
333.15	886.6	850.2	18.6	0.381	3.7E+09
343.15	871.2	837.9	17.4	0.363	3.5E+09
353.15	853.6	822.5	16.3	0.346	3.3E+09
363.15	833.8	808.2	20.1	0.332	4.1E+09
373.15	815.1	843.1	19.9	0.325	4.2E+09
383.15	812.3	825.3	19.2	0.317	4.1E+09
393.15	793.4	804.1	19.1	0.298	4.1E+09
403.15	762.5	778.7	18.5	0.281	3.9E+09

2. Constants for Vapor Pressure Calculation Using Antoine Equation

Substance	Range (K)	A	B	C
Acetic acid	290 – 430	16.8080	3405.57	- 56.34
Acetone	241 – 350	16,0051	3342,46	- 51,93
Ammonia	179 – 261	16.9481	2132.50	- 32.98
Benzene	280 – 377	15.9008	2788.51	- 52.36
Carbon Disulfide	288 – 342	15.9844	2690.85	- 31.62
Carbon Tetrachloride	253 – 374	15.8742	2808.19	- 45.99
Chloroform	260 – 370	15.9731	2696.79	- 46.16
Cyclohexane	280 – 380	15.7527	2766.63	- 50.50
Ethyl Acetate	240 – 385	16,4672	2695,01	-56,81
Ethanol	244 – 369	18,3852	3478,91	-51,00
Ethyl Bromide	226 – 333	15.9338	2511.68	- 41.44
n-Heptane	270 – 400	15.8737	2911.32	- 56.51
n-Hexane	245 – 370	15.8366	2697.55	- 48.78
Methanol	257 – 364	16,4187	3728,55	-37,17
n-Pentane	220 – 330	15.8333	2477.07	- 39.94
Sulfur Dioxide	195 – 280	16.7680	2302.35	- 35.97
Toluene	280 – 410	16,0137	3313.52	-54,97
Water	280 – 441	17,3030	3915,44	-58,07

APPENDIX D: Sample calculations

1. Working fluid inventory

If V_{wick} is the space volume of the wick:

$$V_{wick} = \pi(r_o^2 - r_i^2) \times L_{eff} \times \varepsilon$$

With

r_o : outer radius of the heat pipe

r_i : inner radius of the heat pipe

L_{eff} : effective length of the heat pipe

ε : Porosity of the weak structure

The total volume V_{tot} of the heat pipe is given by:

$$V_{tot} = \pi R_i^2 \chi L_{eff} + V_{wick}$$

According to Lin *et al.* (2011), in practical conditions, the volume corresponding to the desirable amount of working fluid V_f in the heat pipe should be greater than V_{wick} and less than the total volume of the heat pipe.

$$V_{wick} < V_f < V_{tot}$$

According to Banovčan *et al.* (2018), the maximum amount of the working fluid in the heat pipe should be 25% of the total volume V_{tot} .

After calculation, it appears that the total amount of working fluid in this study should be 17.11 ml of distilled water, which was used for its good thermophysical properties. But Mozumder *et al.* (2010) demonstrated in their study that for 55% fill ratio, values of thermal resistances decrease for methanol, ethanol and acetone and water. These working fluids were also selected for this study. A filling ratio of 55% was selected, which gave an amount of 10 ml for each test.

2. Sample calculation of efficiency of the evacuated tube heat pipe solar collector

The efficiency is calculated as the ratio of the output power based on mass of water in the tank and its temperature difference, as well as the input power depending on the direct radiation on the absorber area and the test duration.

$$\eta = \frac{m_w c_p (t_{max} - t_{min})}{I_R A_a t}$$

- η : efficiency
- m_w : amount of water in the tank
- c_p : water specific heat capacity at constant pressure
- t_{max} : water tank final temperature for heat pipe containing distilled water and S insert
- t_{min} : water tank initial temperature for heat pipe containing distilled water and S insert
- I_R : direct radiation from the solar simulator was set to 700 W/m² corresponding to the annual average radiation in KwaZulu-Natal
- A_a : absorber area is given by the product of the effective length and the diameter of the inner glass of the evacuated tube

- t : test duration, which was set to 7 hours.

$m_w [kg]$	4
$c_p \left[\frac{kJ}{kg \cdot K} \right]$	4.187
$t_{max} [^{\circ}C]$	83.5
$t_{min} [^{\circ}C]$	28.7
$I_R \left[\frac{W}{m^2} \right]$	700
$A_a [m^2]$	1.72 m x 0.047 = 0.08084
$t [s]$	25200 (=7hours)

$$\eta = \frac{4 \times 4.187 \times 1000 \times (83.5 - 28.7)}{700 \times 0.08084 \times 25200} \times 100 = 64$$

3. Example of the calculation of the boiling point for water using the Antoine equation

$$T = \frac{-B}{\log P - A} - C$$

P= 2.3 KPa

A=17.3030

B= 3915.44

C= - 58.07

$$T = \frac{-3915.44}{\log 2.3 - 17.3030} - (-58.07)$$

T= 289.2 K

APPENDIX E: Regression analysis model

1. Multivariate polynomial regression analysis for the prediction of the efficiency of the evacuated heat pipe as a function surface area of the insert

x	y
0	53.3
0.0224	59.1
0.0426	60.6
0.0577	61.0
0.0632	64.3

SUMMARY OUTPUT

<i>Regression Statistics</i>	
Multiple R	0.94463766
R Square	0.892340308
Adjusted R Square	0.856453744
Standard Error	1.521992033
Observations	5

ANOVA

	<i>df</i>	<i>SS</i>	<i>MS</i>	<i>F</i>	<i>Significance F</i>
Regression	1	57.60012	57.60012	24.86558	0.015507
Residual	3	6.949379	2.31646		
Total	4	64.5495			

	<i>Coefficients</i>	<i>Standard Error</i>	<i>t Stat</i>	<i>P-value</i>	<i>Lower 95%</i>	<i>Upper 95%</i>	<i>Lower 95.0%</i>	<i>Upper 95.0%</i>
Intercept	54.27083493	1.279446	42.41745	2.88E-05	50.19907	58.3426	50.19907	58.3426
X Variable 1	145.3003261	29.13851	4.98654	0.015507	52.5686	238.0321	52.5686	238.0321

2. Multivariate polynomial regression analysis for the prediction of the efficiency of the evacuated heat pipe as a function of the merit number

ln x	y	
2.21E+01	49.3	3.83E+09
2.40E+01	50.2	2.71E+10
2.37E+01	60.9	2.00E+10
2.41E+01	61.7	3.04E+10
2.45E+01	62.3	4.27E+10
2.66E+01	64.3	3.48E+11

SUMMARY OUTPUT

<i>Regression Statistics</i>	
Multiple R	0.721524
R Square	0.520597
Adjusted R Square	0.400746
Standard Error	5.105286
Observations	6

ANOVA

	<i>df</i>	<i>SS</i>	<i>MS</i>	<i>F</i>	<i>Significance F</i>
Regression	1	113.2142	113.2142	4.343709	0.105526
Residual	4	104.2558	26.06394		
Total	5	217.47			

	<i>Coefficients</i>	<i>Standard Error</i>	<i>t Stat</i>	<i>P-value</i>	<i>Lower 95%</i>	<i>Upper 95%</i>	<i>Lower 95.0%</i>	<i>Upper 95.0%</i>
Intercept	-21.1166	38.07201	-0.55465	0.608685	-126.821	84.58824	-126.821	84.5882388
ln x	3.278476	1.573047	2.084157	0.105526	-1.089	7.645954	-1.089	7.645954

3. Multivariate polynomial regression analysis for the prediction of the efficiency of the evacuated heat pipe as a function of both the merit number and surface area of the insert

Surface area	Merit Number	Efficiency	
	x2		
x1	ln x2	Y	x2
0.0224	2.21E+01	44.8	3.83E+09
0.0224	2.40E+01	46.6	2.71E+10
0.0224	2.37E+01	54.9	2.00E+10
0.0224	2.41E+01	55.3	3.04E+10
0.0224	2.45E+01	56.1	4.27E+10
0.0224	2.66E+01	59.1	3.48E+11
0.0426	2.21E+01	47.6	3.83E+09
0.0426	2.40E+01	48.4	2.71E+10
0.0426	2.37E+01	57.4	2.00E+10
0.0426	2.41E+01	57.8	3.04E+10
0.0426	2.45E+01	58.7	4.27E+10
0.0426	2.66E+01	60.6	3.48E+11
0.0577	2.21E+01	48.3	3.83E+09
0.0577	2.40E+01	49.9	2.71E+10
0.0577	2.37E+01	58.6	2.00E+10
0.0577	2.41E+01	58.9	3.04E+10
0.0577	2.45E+01	60.1	4.27E+10
0.0577	2.66E+01	61.0	3.48E+11
0.0632	2.21E+01	49.3	3.83E+09
0.0632	2.40E+01	50.2	2.71E+10
0.0632	2.37E+01	60.9	2.00E+10

SUMMARY OUTPUT

<i>Regression Statistics</i>	
Multiple R	0.770620242
R Square	0.593855557
Adjusted R Square	0.555175134
Standard Error	3.885757294
Observations	24

ANOVA

	<i>df</i>	<i>SS</i>	<i>MS</i>	<i>F</i>	<i>Significance F</i>
Regression	2	463.629377	231.8147	15.35287	7.78E-05
Residual	21	317.081305	15.09911		
Total	23	780.710682			

	<i>Coefficients</i>	<i>Standard Error</i>	<i>t Stat</i>	<i>P-value</i>	<i>Lower 95%</i>	<i>Upper 95%</i>	<i>Lower 95.0%</i>	<i>Upper 95.0%</i>
Intercept	-22.5805261	14.6750815	-1.5387	0.138811	-53.099	7.937976	-53.099	7.937976
x1	117.4585401	50.1561971	2.341855	0.029124	13.15302	221.7641	13.15302	221.7641
ln x2	3.006438634	0.59864209	5.022097	0.569321	1.761494	4.251383	1.761494	4.251383

0.0632	2.41E+01	61.7	3.04E+10
0.0632	2.45E+01	62.3	4.27E+10
0.0632	2.66E+01	64.3	3.48E+11

RESIDUAL OUTPUT

<i>Observation</i>	<i>Predicted Y</i>	<i>Residuals</i>
1	46.39101284	-1.63340878
2	52.27361789	-5.69645432
3	51.36025747	3.53974253
4	52.61908439	2.70362329
5	53.64054089	2.45945911
6	59.94805984	-0.80393798
7	48.76367535	-1.19864134
8	54.6462804	-6.21396632
9	53.73291999	3.66708001
10	54.9917469	2.8082531
11	56.0132034	2.6867966
12	62.32072236	-1.73637309
13	50.53729931	-2.19004511
14	56.41990436	-6.5353661
15	55.50654394	3.09345606
16	56.76537085	2.13462915
17	57.78682736	2.31317264
18	64.09434631	-3.08621782
19	51.18332128	-1.89594456
20	57.06592633	-6.89257189
21	56.15256591	4.74950141
22	57.41139283	4.30043102
23	58.43284933	3.86715067
24	64.74036828	-0.44036828

4. Multivariate polynomial regression analysis for the prediction of the efficiency of the evacuated heat pipe as a function of the boiling point of the working fluid

x	x ²	x ³	y
289,2	83630,7	24185136,2	64,3
269,4	72563,7	19546963,8	62,3
264,3	69863,6	18466168,1	61,7
266,4	70983,2	18911807,9	60,9
244,0	59546,1	14530468,4	50,2
224,1	50238,8	11260532,4	49,3

SUMMARY OUTPUT

<i>Regression Statistics</i>	
Multiple R	0,995197
R Square	0,990416
Adjusted R Square	0,976041
Standard Error	1,020816
Observations	6

ANOVA

	<i>df</i>	<i>SS</i>	<i>MS</i>	<i>F</i>	<i>Significance F</i>
Regression	3	215,38583	71,79528	68,89707	0,014341
Residual	2	2,0841315	1,042066		
Total	5	217,46996			

	<i>Coefficients</i>	<i>Standard Error</i>	<i>t Stat</i>	<i>P-value</i>	<i>Lower 95%</i>	<i>Upper 95%</i>	<i>Lower 95,0%</i>	<i>Upper 95,0%</i>
Intercept	4822,601	1044,8428	4,615624	0,043874	327,0056	9318,197	327,0056	9318,197
x	-56,7272	12,248149	-4,63149	0,043593	-109,427	-4,02767	-109,427	-4,02767
x ²	0,222898	0,0476452	4,678299	0,04278	0,017898	0,427899	0,017898	0,427899

5. Multivariate polynomial regression analysis for the prediction of the efficiency of the evacuated heat pipe as a function of both the surface area of the insert and the boiling point of the working fluid

surface area	Boiling temp				
x1	x2	X2^2	x2^3	Y	
0,0224	224,1	50238,80302	11260532,4	44,8	
0,0224	244,0	59546,06627	14530468,4	46,6	
0,0224	266,4	70983,16597	18911807,9	54,9	
0,0224	264,3	69863,63682	18466168,1	55,3	
0,0224	269,4	72563,7201	19546963,8	56,1	
0,0224	289,2	83630,69226	24185136,2	59,1	
0,0426	224,1	50238,80302	11260532,4	47,6	
0,0426	244,0	59546,06627	14530468,4	48,4	
0,0426	266,4	70983,16597	18911807,9	57,4	
0,0426	264,3	69863,63682	18466168,1	57,8	
0,0426	269,4	72563,7201	19546963,8	58,7	
0,0426	289,2	83630,69226	24185136,2	60,6	
0,0577	224,1	50238,80302	11260532,4	48,3	
0,0577	244,0	59546,06627	14530468,4	49,9	
0,0577	266,4	70983,16597	18911807,9	58,6	
0,0577	264,3	69863,63682	18466168,1	58,9	
0,0577	269,4	72563,7201	19546963,8	60,1	
0,0577	289,2	83630,69226	24185136,2	61,0	
0,0632	224,1	50238,80302	11260532,4	49,3	
0,0632	244,0	59546,06627	14530468,4	50,2	
0,0632	266,4	70983,16597	18911807,9	60,9	

0,0632	264,3	69863,63682	18466168,1	61,7	
0,0632	269,4	72563,7201	19546963,8	62,3	
0,0632	289,2	83630,69226	24185136,2	64,3	

SUMMARY OUTPUT

Regression Statistics

Multiple R	0,990230459
R Square	0,980556363
Adjusted R Square	0,976462965
Standard Error	0,8938343
Observations	24

ANOVA

	<i>df</i>	<i>SS</i>	<i>MS</i>	<i>F</i>	<i>Significance F</i>
Regression	4	765,5308265	191,3827	239,5458546	0
Residual	19	15,17985536	0,79894		
Total	23	780,7106818			

	<i>Coefficients</i>	<i>Standard Error</i>	<i>t Stat</i>	<i>P-value</i>	<i>Lower 95%</i>	<i>Upper 95%</i>	<i>Lower 95,0%</i>	<i>Upper 95,0%</i>
Intercept	3886,584452	457,436382	8,496448	6,77589E-08	2929	4844	2929,159	4844,009803
x1	117,4585401	11,53734676	10,18072	3,9409E-09	93,3	142	93,3106	141,6064844
x2	-45,7370856	5,362285206	-8,5294	6,38778E-08	-57	-35	-56,9605	-34,5136937
X2^2	0,17983545	0,020859247	8,621378	5,42214E-08	0,14	0,22	0,136177	0,223494357
x2^3	-0,00023336	2,69331E-05	-8,6645	5,02295E-08	-0	-0	-0,00029	-0,00017699

RESIDUAL OUTPUT

<i>Observation</i>	<i>Predicted Y</i>	<i>Residuals</i>	<i>Error %</i>	
1	44,6	0,1	0,3	
2	46,1	0,5	1,1	
3	55,6	-0,7	-1,3	
4	54,8	0,6	1,0	
5	56,7	-0,6	-1,1	
6	58,4	0,7	1,3	
7	47,0	0,6	1,2	
8	48,4	0,0	0,0	
9	58,0	-0,6	-1,0	
10	57,1	0,7	1,1	
11	59,1	-0,4	-0,7	
12	60,8	-0,2	-0,3	
13	48,8	-0,4	-0,9	
14	50,2	-0,3	-0,6	
15	59,8	-1,2	-2,0	
16	58,9	0,0	0,0	
17	60,9	-0,8	-1,3	
18	62,5	-1,5	-2,5	
19	49,4	-0,1	-0,3	
20	50,9	-0,7	-1,3	
21	60,4	0,5	0,8	
22	59,6	2,1	3,6	
23	61,5	0,8	1,3	
24	63,2	1,1	1,8	